WAVE-INDUCED OSCILLATIONS OF SMALL MOORED VESSELS

by

Fredric Raichlen

W. M. Keck Laboratory of Hydraulics and Water Resources
Division of Engineering and Applied Science
CALIFORNIA INSTITUTE OF TECHNOLOGY
Pasadena, California

Report No. KH-R-10 October 1965

FILE COPY

WAVE-INDUCED OSCILLATIONS OF SMALL MOORED VESSELS

by

Fredric Raichlen
Assistant Professor of Civil Engineering

Report to:

U. S. Army Engineer Waterways Experiment Station
Corps of Engineers
Office of the Director
Vicksburg, Mississippi
Contract DA-22-079-CIVENG-64-11

W. M. Keck Laboratory of Hydraulics and Water Resources
Division of Engineering and Applied Science
California Institute of Technology
Pasadena, California

Report KH-R-10

October 1965

TABLE OF CONTENTS

LIST OF FIGURES

LIST OF TABLES

ABSTRACT

The general objective of this research is to investigate the motion of small boats moored to fixed or floating platforms in a standing wave environment. The study is directed toward an understanding of the problems of mooring small craft in marinas and toward providing information that will assist in the planning and operation of marinas.

This report deals with the first phase of the experimental study concerning the surge motions of a simply moored body in a standing wave system. The body is a rectangular parallelpiped moored to a fixed support by means of a linear spring.

In general it can be stated that the inviscid theory proposed by Wilson (5) and Kilner (7) adequately describes the surge motion of this body for standing waves ranging from shallow-water to deep-water waves and for ratios of body length to wave length from 0.1 to 1.5. Agreement between the experimental data and the theoretical response curves is better for certain ranges of the ratio of the natural period of the body to the wave period than for others. This is attributed to the effect of wave generation by the body on its motion. The response curves become more selective with respect to frequency as the distance of the body from a reflecting surface increases. Therefore, coupling this with viscous effects it is possible to reduce the effect of resonance considerably simply by choosing the proper body location in its standing wave environment for a particular natural frequency.

The coefficient of virtual mass of the body in surge (ratio of width to length, 1:4) determined from simple free oscillations was found to correlate best with the ratio of draft to beam. For a variation of draft to beam from 0.25 to 0.95 the coefficient of virtual mass varied from approximately 1.1 to 1.25.

This study emphasizes the need for more field information on the characteristics of small craft, such as the elastic characteristics of the mooring system, natural frequencies of moored boats, and the relative importance of viscous effects upon boat motions.

Wave-Induced Oscillations of Small Moored Vessels

by

Fredric Raichlen

1. Introduction

1.1 General Considerations

The problem of the mooring of small craft has become increasingly important in recent years with the increase in the number and size of small boat marinas in both coastal and inland areas. Small craft harbors have ceased being simply harbors of refuge; some marinas now exist which are multi-million dollar investments providing valuable real estate which can be developed in addition to berthing facilities for pleasure craft. An example of one of these large projects is the Marina del Rey located near Los Angeles, California. The total investment for this marina (including federal government, local government, and private investments) exceeds $150,000,000 (see Lee (1)). When a harbor of this size is not usable due to excessive motions of the moored boats and the attendant damage a great deal of attention is directed to the project and methods of correcting the problem. There are many other coastal and inland marinas throughout the United States which are smaller in size or in the total funds invested, but to the owner of the moored boat excessive boat motions are as important to him as they are to the managers of a complex the size of Marina del Rey.

According to Dunham (2) in the period from 1950 to 1959 the number of recreational boats in use throughout the United States more than doubled. In 1950 there were less than 3,000,000 small craft being used in the United States whereas this number grew to approximately 7,800,000 in 1959. The incremental yearly growth itself increased during the period by roughly 100,000 boats per year. Of course all of these boats are not moored in marina facilities; however, from these numbers it is apparent that the problems of the adequate design of mooring facilities and of the overall marina design are of increasing importance.

These two problem areas are very much related. The small boat and its mooring arrangement in effect form a system having certain response characteristics analogous to a mechanical system restrained by linear or non-linear springs. The wave system within the marina can also be thought of as having a mechanical analogue. Therefore, the response characteristics of the moored body intimately depend upon the response of the harbor to certain wave systems incident upon the harbor entrance, since the latter provides the forcing function for the small boat. Hence, a general study of the problems related to the oscillation of small moored vessels must really deal with two phases: the investigation of the wave induced oscillations of arbitrary shaped basins, and the response of moored small boats in this wave environment.

A study was initiated at the W. M. Keck Laboratory of Hydraulics and Water Resources at the California Institute of Technology, Pasadena, California late in 1963 to study the general problem of the wave induced

oscillations of small moored vessels. In a broad sense this study has three major objectives:

1. The investigation of the motions of simple bodies elastically moored to a fixed support and subjected to standing waves having depth to wave length ratios which range from the limits of deep water to shallow water waves.

2. The study of the motion of simple bodies elastically moored to floating platforms which are in turn moored to fixed supports. This mooring arrangement has some of the features of a typical marina mooring system.

3. The investigation of the wave induced oscillations in basins of arbitrary shape.

This report deals primarily with the first of these three objectives. Specifically, it was considered important to first investigate experimentally the behavior of simple bodies, simply moored, to compare these results to certain theoretical approaches that have been proposed by others. The theoretical considerations will be treated in some detail in Section 2.1.

The problem of the mooring of small craft is considered to be somewhat different from the large ship mooring problem. In the large ship problem usually waves of relatively long periods are important as far as motions are concerned. This more or less limits the problem to a shallow water wave system. In the case of pleasure craft the wave system which is important for vessel motions may vary from shallow water to deep water waves depending upon the characteristics of the vessel and its mooring system. In addition there is a question as to

the relative importance of inertial forces and viscous forces in the two cases. For large craft, inertial forces are usually much greater than viscous forces and the latter can be neglected. However, this question has not been satisfactorily answered for small craft.

1.2 Literature Survey - Moored Bodies

Wilson in Reference 3 begins a series of papers on the motions of moored ships in standing wave systems. In this paper Wilson presents the concept of a ship and its mooring system responding in surge motion to a long period standing wave system in a manner which is analogous to a spring-suspended mass. Surge motion is defined as the motion of the ship in the horizontal plane in the direction of the horizontal water particle velocities. He treats in some detail the mooring line system which, due to the nature of mooring arrangement, is best represented by a non-linear spring system. The general non-linear equation of motion of a body moored in a standing wave system with non-linear constraints is presented. A functional relationship for the natural period in terms of parameters of the system is determined from dimensional analysis. The problem of interest is the variation of the resonant period (in the longitudinal direction) of a ship-mooring system as a function of wave amplitude and mooring line constraint. It is shown that the more non-linear the restraining force, the more dependent the natural frequency is upon the wave height (and hence the maximum water particle excursions). The natural period of a moored vessel is also shown to be a function of the displacement tonnage and the draft for a given depth of water. For a given ship and mooring system as the wave amplitude increases the natural period decreases. As the

ship tonnage decreases for a given mooring system and wave environment the natural period also decreases. Some experimental studies were conducted in conjunction with this work, but only for the case where a ship model is moored at the nodal point of a uninodal seiche (a long period standing wave). Although model results are not presented, it is stated that the tests showed that the theory developed is reliable in predicting the effect of non-linear constraints in such a system.

Abramson and Wilson (4) obtain solutions to the undamped equation of motion developed in Reference 3 to determine the amplitude response of a moored body as a function of both the wave period and the type of non-linear constraint. The surge motion of the vessel is of primary interest here. This more rigorous approach confirms to some extent the results presented in Reference 3.

Wilson (5) presents a comprehensive summary of his work on the mooring force problem. In addition to the question of the response of a moored body in the three coordinate directions, the problem of an unmoored ship is treated. Information is presented on the predicted response characteristics of various ships along with summaries of more general information such as virtual mass coefficients of rectangular bodies in surge and heave. The effect of a beam sea on an idealized ship-form is considered from the point of view of the berthing of ships.

In Reference 6, Wilson applies the approach presented in his previous papers to the case where an oil tanker parted its lines while moored in a rectangular basin. In this publication Wilson shows that

the cause of the accident was probably the response characteristics of the tanker and its mooring system when exposed to the fundamental and higher harmonic modes of oscillation of the basin. The non-linear characteristics of the mooring system were taken into account, and the case was treated as an undamped oscillation.

Kilner (7) analyzes the case of a ship restrained in a non-linear fashion after the manner of Wilson (5). Kilner obtains an approximate solution to the non-linear problem assuming no damping. Of primary interest here are his experimental studies of the cases of a linearly and a non-linearly moored body. In order to show some limitations of the experimental study, the experimental equipment will be described in some detail. The tests were conducted in a flume 29 ft long, 5 ft wide, with a maximum water depth of 10 inches. Wave filters were placed at either end of a 15 ft working section. A uninodal seiche was created by pumping water from one end of the flume to another through a discharge line controlled by a programmed butterfly valve. The range of periods was from 2.7 sec to 25 sec. The ship model (80 inches long, a beam of 10 inches, a draft of 6 inches, and a weight of 135 lbs) was moored at the center of the flume so that the node of the standing wave coincided with the center of the body for all wave lengths. The results of these tests tend to confirm the theoretical solution for the linear spring system; however, the testing is limited to the somewhat unrealistic case of the ship remaining at the node of a standing wave for the full range of wave periods. Using the maximum depth of water given, the depth to wave length ratios would then range from 0.06 to 0.006 which are essentially within the limits of the shallow water wave criterion. Thus,

in summary, the experiments were conducted with the vessel moored at the node of a shallow water standing wave system where reflections of waves generated by the oscillating body were minimized by the wave filters placed at either ends of the test section. The case of the motion of vessels with non-linear restraints was also investigated experimentally, and the results agree with the trend predicted theoretically. In addition to these experiments a mechanical analogy to the problem is presented. This consists of a tilting platform whose frequency of motion can be varied and a plank moored with linear springs to the platform and separated from it by roller bearings. Therefore, as the platform tilts, the plank representing a moored ship, oscillates to and fro in a manner similar to a ship. This analogy is satisfactory again for a case of a vessel in shallow water waves; however, it will be shown later that this representation becomes inaccurate as the wave environment approaches a deep water wave system.

Russell (8) has experimentally studied the mooring problem to find a means of reducing the impact between ships and docks. His experiments take two forms: the study of the motion of a model tanker moored alongside jetties in a wave system, and the study of the lateral motions of a more idealized body which was restrained to motion in one direction by a stiff spring and in the other by a soft spring. These springs were meant to represent flexible fenders and mooring lines. In the idealized body study the model was moored at the node of a standing wave of a 3 sec period in 10 inches of water. The variation of the model motion and the mooring force as a function of both the stiffness of the fenders and the stiffness of the springs which represent the mooring

lines were investigated. The study showed that for a given stiffness of the fenders, as the stiffness of the mooring lines increased the amplitude of the motion of the vessel was a function of the initial fender stiffness. This is not surprising, since by changing the characteristics of the mooring lines one is altering the natural frequency of the moored body. However, the natural frequency of the body is also a function of the initial stiffness of the fenders. These two effects combine in such a way that, depending upon the fender stiffness, the change in the elastic characteristics of the mooring lines changes the response of the vessel for a given wave period. Therefore, the amplitude of the motion of the vessel can either increase or decrease as the mooring line characteristics are altered depending upon where the operating point is located on the response curve.

There have been a number of model and prototype studies of mooring forces and ship motions for particular ships. Investigations such as those of Knapp (9), O'Brien and Kuchenreuther (10), O'Brien and Muga (11), and Wiegel et al (12), all add to the fund of general knowledge on the subject of motions of large moored vessels. However, from the point of view of the motion of small craft and the more specific nature of these studies, they will not be discussed here.

1.3 Literature Survey - Virtual Mass

The forces acting on any accelerating or decelerating body include an additional force, not present in the steady state system, which is associated with the inertia of the system and an effect due to the presence of the fluid. This latter effect is due to the kinetic energy which is imparted to the surrounding fluid as the body moves unsteadily

relative to the fluid. It is compensated for in the equations of motion by considering the body to have an added mass which moves with the body such that the resulting kinetic energy of body and fluid is correct. The combination of the mass of the body and the added mass is usually called the virtual mass. The magnitude of this term is important in defining the motions of a moored body.

The major work on measuring the virtual mass of floating bodies has been done for motions of ship forms in heave and pitch. These vertical motions are the more important ones for the case of a ship moving (or dead in the water) in an open-sea wave system. However, for the case of a moored body one of the important motions is the surge motion, i.e., motion in the direction of the longitudinal axis of the ship.

A good general review of the virtual mass problem is given by Korvin-Kroukovsky (13). Some detailed considerations of the virtual mass in surge are presented by Wendel (14). In this treatment little attention is given to the effect of body dimensions on the added mass. Mention is made of the experiments performed by Koch (15), which were electrical analogue experiments, in which he found that for a square face moving in the direction of the free surface the ratio of the added mass in this case to that in an unbounded fluid was 0.286.

Perhaps the information which is of greatest interest in the present study is that given by Wilson in Reference 5. A graph is presented by Wilson showing for surge motion the variation of an inertia coefficient, which is proportional to the added mass, with beam to length ratio. The results of a number of different investigations are shown; however, to the knowledge of this writer the data presented at least from one source

are for the case where the body oscillated vertically instead of in a horizontal direction (which is implicit in the surge problem). Nevertheless a comparison of Wilson's results with the results of the present study will be presented in Section 4.1.

2. Theoretical Considerations

The theoretical approach used in this study to obtain the equation of motion of a single moored body in surge is essentially the same as that proposed by Wilson (5) and Kilner (7). It is presented here in its entirety for the sake of completeness and to describe the importance of various terms in the solution. In addition this method is extended to describe the surge of coupled bodies.

2.1 Single Body Motion in Surge

Since the primary objective of this study is to investigate the fundamental behavior of moored systems, only bodies of simple geometry are considered. The body which is treated here is a simple rectangular parallelpiped of length 2L, draft D, and beam B moored such that the only allowable motions are those in surge. A sketch of the body in its wave environment is shown in Fig. 1. The wave system considered is a standing wave system in a rectangular basin of constant depth d in which the body is moored some distance b from a perfectly reflecting wall. The coordinate x is measured from the center of the body when it is at rest. Using small amplitude wave theory the standing wave is described by the following three expressions for the wave amplitude η, velocity potential Φ, and the water particle velocity u:

$$\eta = A \cos k\,(b+x) \cos \sigma t \tag{1}$$

$$\Phi = \frac{Ag}{\sigma} \frac{\cosh k\,(d+z)}{\cosh kd} \cos k\,(b+x) \sin \sigma t \tag{2}$$

$$u = \frac{Agk}{\sigma} \frac{\cosh k\,(d+z)}{\cosh kd} \sin k\,(b+x) \sin \sigma t \tag{3}$$

where A is the standing wave amplitude, k is the wave number (2π/wave length, λ), σ is the circular wave frequency (2π/wave period, T), g is

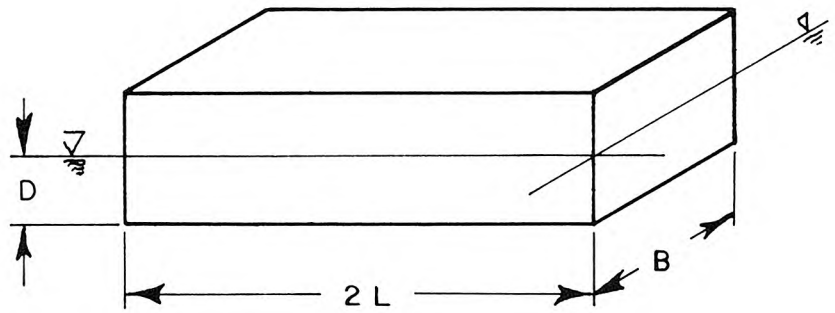

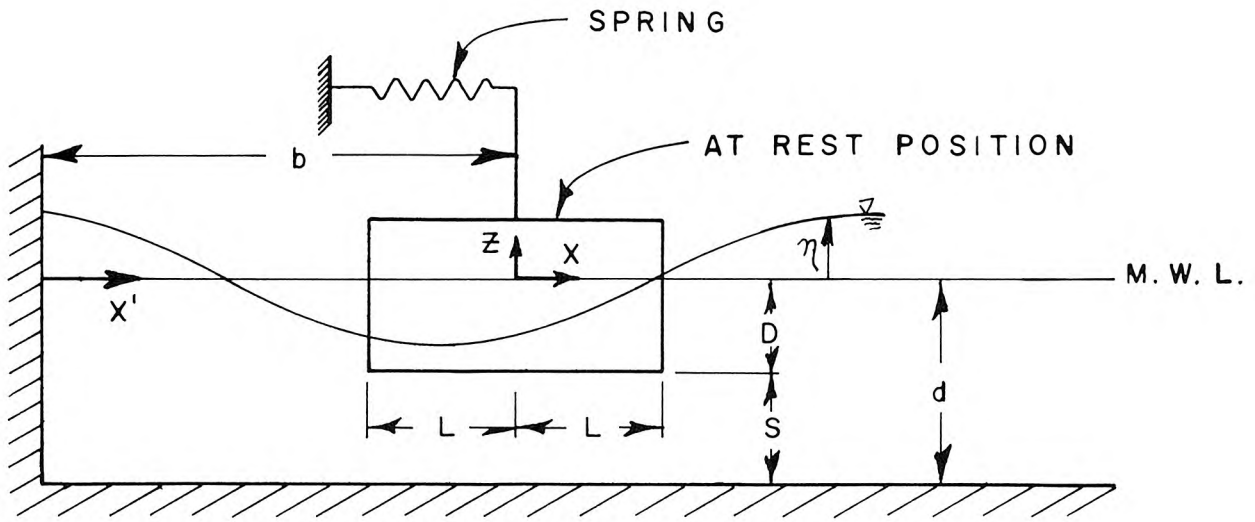

Fig. 1. Definition Sketch of Single Moored Body

the acceleration of gravity, and the other parameters are described in the definition sketch, Fig. 1.

The equation of motion of the moored body in surge is:

$$M\ddot{x} = \sum \text{(External Forces)}$$
$$M\ddot{x} = F_p + F_i + F_d + F_r \tag{4}$$

where $\ddot{x} = \frac{d^2x}{dt^2}$ and M is the mass of the moored body. The first term on the right in Eq. 4 is the net pressure force acting on the ends of the body and is a driving force in the x-direction. It is defined as:

$$F_p = B\int_{-D}^{\eta} p(-L, z)dz - B\int_{-D}^{\eta} p(+L, z)dz \tag{5}$$

where $p(-L, z)$ and $p(L, z)$ are the pressures on the ends of the body at $x = -L$ and $x = +L$ respectively. The general form of the depthwise pressure distribution under a small amplitude standing wave is:

$$p = \gamma\eta \frac{\cosh k(z+d)}{\cosh kd} - \gamma z \tag{6}$$

After substituting Eq. 6 into Eq. 5 and integrating over the immersed height of the body, the net pressure force per unit width of the body is obtained:

$$\frac{F_p}{B} = (\eta_{-L} - \eta_{+L})\frac{\gamma}{k}\left[\frac{\sinh kd - \sinh ks}{\cosh kd}\right] - \frac{\gamma}{2}(\eta^2_{-L} - \eta^2_{+L}) \tag{7}$$

where

$$\eta_{-L} = A \cos k(b-L) \cos \sigma t$$
$$\eta_{+L} = A \cos k(b+L) \cos \sigma t$$

After substituting these definitions of the wave amplitude at the ends of the body into Eq. 7, the net pressure force is given by:

$$F_p = \frac{2AB\gamma}{k}\left[\frac{\sinh kd - \sinh ks}{\cosh kd}\right] \sin kL \sin kb \cos \sigma t$$

$$- \frac{A^2 B\gamma}{2} \sin 2kL \sin 2kb \cos^2 \sigma t \qquad (8)$$

It can be shown that the ratio of the second term in Eq. 8 to the first term, at worse, goes as the wave steepness $\frac{A}{\lambda}$. Therefore for small amplitude waves the net pressure force reduces to:

$$F_p = \frac{2AB\gamma}{k}\left[\frac{\sinh kd - \sinh ks}{\cosh kd}\right] \sin kL \sin kb \cos \sigma t \qquad (9)$$

It is convenient now to define an average water particle velocity and an average water particle acceleration as being the average of the total velocity and acceleration over the wetted surface, i.e.,:

$$U = \frac{1}{2LD}\int_{-L}^{L}\int_{-D}^{\eta} u \, dx \, dz \qquad (10a)$$

$$\dot{U} = \frac{1}{2LD}\int_{-L}^{L}\int_{-D}^{\eta} \dot{u} \, dx \, dz \qquad (10b)$$

After substituting Eq. 3 and its derivative into Eqs. 10a and 10b respectively the average water particle velocity and acceleration become:

$$U = \frac{Ag}{kLD\sigma}\left[\frac{\sinh kd - \sinh ks}{\cosh kd}\right] \sin kL \sin kb \sin \sigma t \qquad (11a)$$

$$\dot{U} = \frac{Ag}{kLD}\left[\frac{\sinh kd - \sinh ks}{\cosh kd}\right] \sin kL \sin kb \cos \sigma t \qquad (11b)$$

After substituting Eq. 11b into Eq. 9, the latter reduces to the simple expression:

$$F_p = M\dot{U} \qquad (12)$$

wherein $M = 2\rho LBD$, the mass of the fluid displaced by the floating body.

This same result could have been obtained in a much simpler way from classical hydrodynamic theory, since the net pressure force is the force exerted on the body by the pressure gradient which exists in the absence of the body. The pressure gradient in the horizontal direction resulting from the local acceleration (neglecting convective accelerations which is compatible with small amplitude wave assumptions) is given by the equation of motion:

$$-\frac{dp}{dx} = \rho\frac{du}{dt} \tag{13}$$

The net pressure force is then:

$$F_p = \int_x \int_A -\frac{dp}{dx}\, d\,x\, d\,A = \int_{\forall} \rho \dot{u} d\,\forall$$

Since this integral is the average of the water particle acceleration over the volume, it reduces to:

$$F_p = M\dot{U}$$

which is identical to Eq. 12. It is interesting at this point to reduce Eq. 9 to the case of shallow water waves ($\frac{d}{\lambda} < \frac{1}{20}$). In this case the net pressure force reduces to:

$$F_p \cong \left[2LBD\gamma\right] Ak^2b = W_f\, A\, k^2 b \tag{14}$$

The maximum wave slope with respect to time, from Eq. 1, for shallow water waves is:

$$\frac{d\eta}{dx} \cong -Ak\,(kb + kx) \tag{15}$$

or at the center of the body (x=0) the slope is:

$$\frac{d\eta}{dx} \cong -Ak^2b \equiv S \tag{16}$$

Therefore, for the case of shallow water waves the net pressure force becomes:

$$F_p \cong -W_f\, S \tag{17}$$

or the component of the body weight causing the body to "slide" down the wave face. Hence, the moored system analogy proposed by Kilner (7) consisting of the tilting plank described in Section 1.2 is valid only for a shallow water wave system.

The term F_i in Eq. 4 is an inertial force which comes about due to the unsteady nature of the problem and the acceleration or deceleration of some mass of fluid in addition to the body. It is the product of the added mass or hydrodynamic mass of the floating body in the x-direction, M'_x, and the relative body acceleration. This term, similar to the drag term F_d, is both a driving force and a restoring force and is expressed as:

$$F_i = M'_x (\dot{U} - \ddot{x}) \tag{18}$$

It is assumed that the water particle acceleration which would be associated with the hydrodynamic mass in surge, M'_x, is an average acceleration given by Eqs. 10b and 11b.

In a similar way the viscous drag term F_d in Eq. 4 is expressed in terms of the relative body velocity. This is given by:

$$F_d = \frac{\rho}{2} C_{D_x} BD (U-\dot{x}) | U-\dot{x} | \tag{19}$$

where C_{D_x} is a drag coefficient for the body in surge. The absolute value of $(U-\dot{x})$ allows the drag force to periodically reverse direction.

The restoring force F_r can take on various forms depending on the type of mooring system used. Wilson (3) has suggested that for ship mooring systems this force is of the form:

$$F_r = -C x^n \tag{20}$$

where C is a constant and the minus sign indicates that the mooring force acts in a direction opposite to the direction of motion.

After substituting Eqs. 12, 18, 19 and 20 into Eq. 4, the equation of motion of the body in surge becomes:

$$M\ddot{x} = M\dot{U} + M'_x (\dot{U}-\ddot{x}) + \frac{\rho}{2} C_{D_x} BD (U-x) \left| U-\dot{x} \right| - C x^n \qquad (21)$$

After defining the virtual mass coefficient C_M as:

$$C_M = 1 + \frac{M'_x}{M}$$

Eq. 21 reduces to:

$$C_M M (\ddot{x}-\dot{U}) + \frac{\rho}{2} C_{D_x} BD (\dot{x}-U) \left| \dot{x}-U \right| + C x^n = 0 \qquad (22)$$

Eq. 22 is non-linear by virtue of the drag force and the restoring force terms. In order to obtain solutions for the case of a non-linear mooring line force Wilson (4) and Kilner (7) have neglected the viscous drag relative to the inertia terms and have then obtained a solution to the reduced expression.

Our interests in the initial phases of this study were directed more toward determining the applicability of this general approach to the small-craft problem where viscous forces may be important and where a full range of depth to wave length and body length to wave length ratios are encountered. Therefore, it was considered reasonable in the experimental phases to limit ourselves initially to the case of a linear restoring force (n = 1), and the following discussion of Eq. 22 is then limited to the simple linear mooring force problem where C is the spring constant.

To simplify the problem further the drag term is linearized by incorporating an effect of the relative velocity in a drag coefficient redefined now as C_{d_x}. Eq. 22 now becomes:

$$C_m M (\ddot{x}-\dot{U}) + \frac{\rho}{2} C_{d_x} BD (\dot{x}-U) + Cx = 0 \tag{23}$$

or $$\ddot{x} + \beta_x \dot{x} + \omega^2 x = \dot{U} + \beta_x U \tag{24a}$$

where: $$\beta_x = \frac{C_{d_x}}{4C_m L} \tag{24b}$$

$$\omega^2 = \frac{C}{C_m M} \tag{24c}$$

The solution to Eq. 24a is obtained in a straightforward manner by assuming a solution of the form:

$$x = X \cos (\sigma t - \varphi) \tag{25}$$

with the average velocity and acceleration defined by Eqs. 11a and 11b or in simplified notation by,

$$U = \frac{\delta}{\sigma} \sin \sigma t \tag{26a}$$

$$\dot{U} = \delta \cos \sigma t \tag{26b}$$

$$\text{where: } \delta \equiv \frac{Ag}{kLD} \frac{\sinh kd - \sinh ks}{\cosh kd} \sin kL \sin kb \tag{26c}$$

The general solution to Eq. 24a in the form of the ratio of the surge amplitude x to the wave amplitude A is then given as:

$$\frac{x}{A} = \frac{\delta}{A\sigma^2} \left\{ \sqrt{\frac{\left[1 - \frac{\sigma^2}{\omega^2} - \frac{\beta_x^2}{\omega^2}\right]^2 + \frac{\beta_x^2}{\sigma^2}}{\frac{\omega^2}{\sigma^2}\left(1 - \frac{\sigma^2}{\omega^2}\right)^2 + \frac{\beta_x^2}{\omega^2}}} \right\} \cos (\sigma t - \varphi) \tag{27}$$

where the phase angle φ is defined by:

$$\tan \varphi = \frac{\beta_x / \sigma}{1 - \frac{\sigma^2}{\omega^2} - \frac{\beta_x^2}{\omega^2}} \tag{28}$$

The solution for the response of the body in surge (Eq. 27) can in effect be divided into two parts. The first part is the wave function coefficient ($\delta/A\sigma^2$) which is representative of the forcing function as embodied in the average water particle acceleration and the average water particle velocity, i.e. the right side of Eq. 24a. The other portion of the solution is the response function of the body, i.e., the second bracketed term in Eq. 27.

It is interesting at this point to look in detail at the wave function coefficient and the overall response and to investigate the variation of these quantities with small and large ratios of depth to wave length, i.e., for shallow water and deep water waves respectively. It can be shown that as the wave length becomes large relative to depth and the dimensions of the system, the wave function coefficient $\delta/A\sigma^2$ tends to b/d (the ratio of the distance in the x-direction of the center of the body from the reflecting surface to the depth) and for the case of zero damping, the response X/A as given by Eq. 27 tends to:

$$\frac{X}{A} \rightarrow \frac{b}{d} \frac{\sigma^2/\omega^2}{1 - \sigma^2/\omega^2}$$

Hence, as the ratio σ/ω (or τ/T where τ is the natural period of the body and T is the wave period) goes to zero, i.e., the wave period becomes very large, the body displacement goes to zero. Physically this can be explained by referring to Eqs. 24, and 26b. For the undamped case, as the wave length becomes long compared to the system dimensions the average water particle acceleration U tends to $A\sigma^2 b/d$ or $\frac{A}{\lambda} \frac{b}{\lambda} (2\pi)^2 g$. Therefore, $\dot{U}$ tends to zero for shallow water waves which have a large wave length compared to the amplitude A and/or the distance b, and the

driving force goes to zero. This may be seen in another way. Since the $\dot{U}$ term in Eq. 24 arises from the net pressure force, for very long waves, from Eq. 17, the wave slope and hence the driving force tends to zero.

For the case with damping, the viscous drag associated with the water particle velocities is a driving force and its magnitude therefore is dependent upon the average water particle velocity U. It can be shown that for shallow water waves:

$$U \rightarrow \frac{A}{\lambda} \frac{b}{d}\sqrt{gd} \quad (2\pi)^2$$

Therefore, as τ / T goes to zero for a given mooring system, U also tends to zero along with $\dot{U}$ and again there is no forcing function to act on the body and the response $\frac{X}{A}$ tends to zero. Physically this is the case of a wave length approaching infinity and simply a rising of the water level associated with infinitesimal horizontal velocities.

For deep water waves it can be shown that the wave function tends to

$$\frac{\delta}{A\sigma^2} \rightarrow \frac{g^2 \tau^4}{LD(2\pi)^4} \left[\frac{1}{\tau / T}\right]^4 \sin kL \sin kb$$

Since this limit depends on the value of τ / T (which in turn depends on the value of T alone for a given value of τ), when the waves become deep water waves, the magnitude of the wave function may or may not be small. Hence, one cannot predict the value of the response function for deep water waves. This will be seen more clearly in the section describing the experimental results.

The general shape of the wave function coefficient ($\delta/A\sigma^2$) may be seen by observing the variation of a quantity α defined as,

$$\alpha \equiv \frac{\delta}{A\sigma^2} \quad \frac{kL}{\sin kL \sin kb} = \frac{1}{kD}\left[1 - \frac{\sinh ks}{\sinh kd}\right] \tag{29}$$

For a given wave number, Eq. 29 shows how the modified wave function changes with increasing draft. The variation of this quantity α with kd and kD is shown in Fig. 2. The curves are shown only for values of $kd \geq kD$ which, of course, is the practical situation. These curves show what at first appears to be a surprising variation, i.e., the value of α decreases with increasing draft for a particular depth to wave length ratio. Upon reflection, however, this is not really that surprising since the variation of α with draft for a given wave number is directly proportional to the variation of average velocity U and average acceleration $\dot{U}$ with draft. From Eq. 29 it is seen that for shallow water waves α is independent of draft since the actual water particle velocities and accelerations are uniform over the depth. For depth to wave length ratios different from shallow water the velocities and accelerations decrease with depth, and for a given wave number the average velocities and accelerations defined by Eqs. 10a and 10b would then have to decrease with increasing draft. For deep water waves and for a given draft this quantity is essentially constant for small draft to depth ratios. This also is to be expected, since an increase in depth will not significantly effect either the variation of the water particle velocity or acceleration with depth.

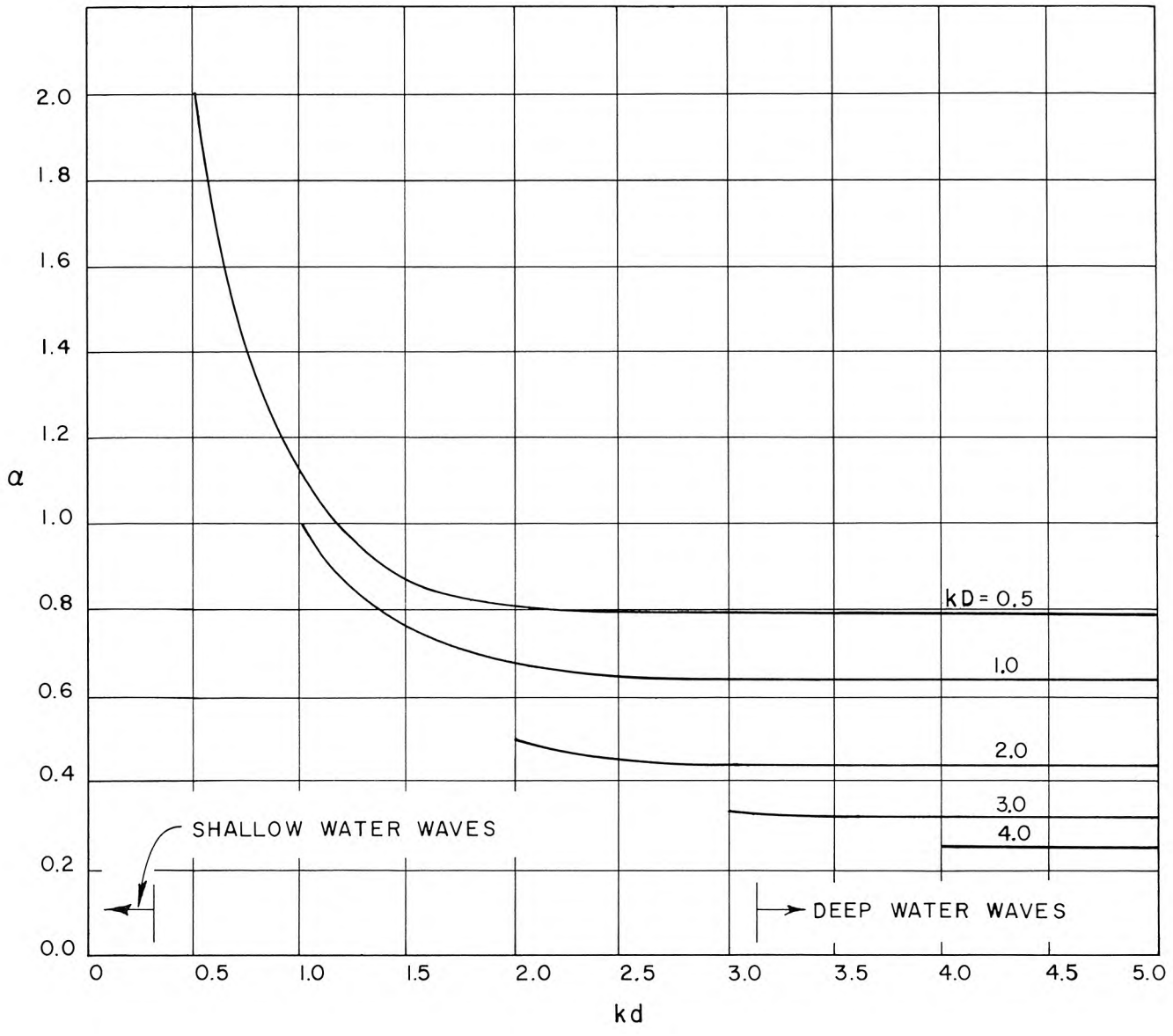

Fig. 2. Variation of Modified Wave Function, α, with Wave Number, Draft, and Depth

The variation of the wave function $\delta/A\sigma^2$ with relative period τ/T is shown in Fig. 3 for the system dimensions and body characteristics indicated. As described previously this quantity approaches b/d (in this case 3.0) as τ/T tends to zero. The function goes to zero at values of τ/T of 1.36, 2.19, and 2.72 for the range shown. These are the first three zeros of sin kb and the last figure is also the first zero of sin kL, and indicate values of τ/T where for a particular configuration there is no net pressure force or viscous drag on the body. In other words an antinode of the standing wave occurs at the center of the moored body due to its location with respect to the reflecting wall of the basin and the body length.

A set of theoretical response curves plotted as X/A vs τ/T (ratio of the maximum surge amplitude to the maximum wave amplitude as a function of the ratio of body period to wave period) for constant damping ratios β_x/ω, are presented in Fig. 4 for the same system dimensions and body characteristics as used in Fig. 3. These curves are given in this section only to show the general shape of the response curves and the effect of friction on the body response. It is seen that where the wave function goes to zero the body response in surge becomes zero and the location of these zeros is not affected by energy dissipation. The "oscillations" in the response curve are caused by the trigonometric terms in Eq. 26c and tend to approach zero as τ/T increases. This effect is a combination of both the variation of the wave function and the dynamic portion of Eq. 27 with τ/T. In addition it is seen that as the dissipation function β_x/ω increases the relative resonant period of the body, τ/T, becomes smaller. Since the normalizing period τ is the

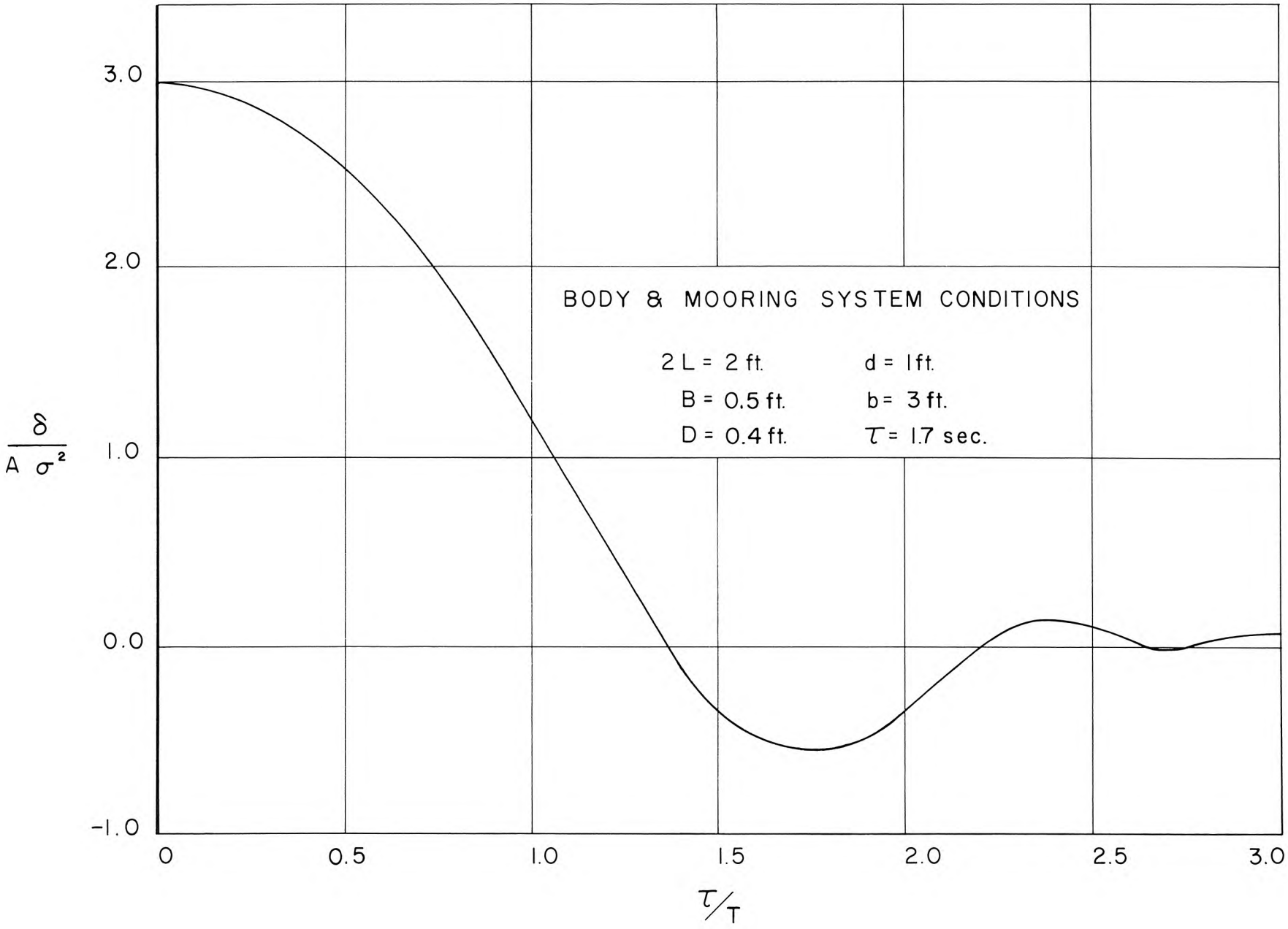

Fig. 3. Variation of Wave Function with Relative Period, τ/T

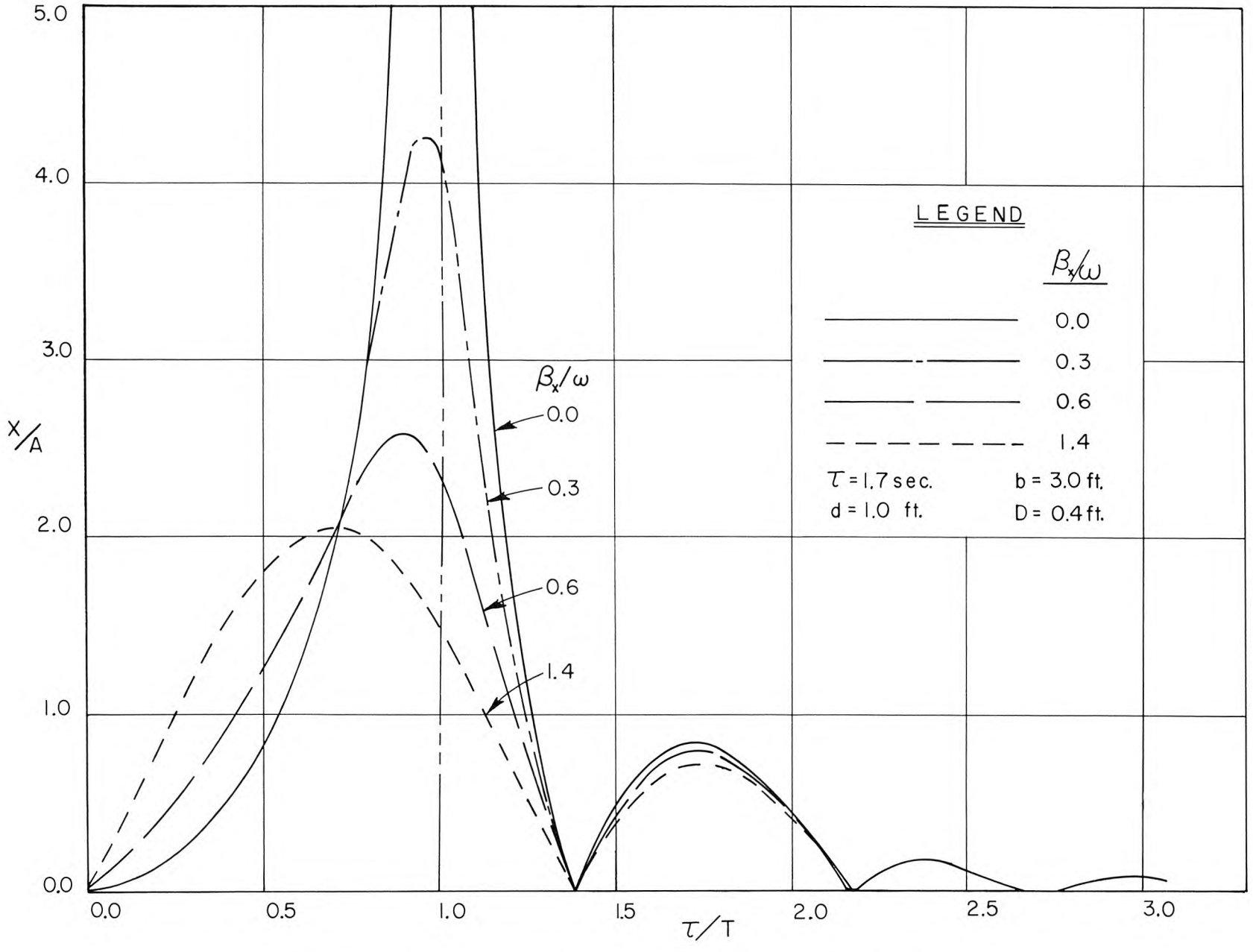

Fig. 4. Theoretical Response Curve Single Moored Body

undamped natural period, this means that the resonant period of the body is increased with increased damping; the same as with its mechanical analogue, the single degree of freedom oscillator. Near resonance, the response of the system decreases as the damping increases. However near $\tau/T = 0$ the response actually increases with increasing damping. In this region the viscous effects become important as a driving force as seen in Eq. 24. Actually for very large values of β_x/ω the response increases at resonance with increased damping. The general characteristics of the response curves and a more physical description of the coefficient β_x/ω will be discussed more fully in Sections 4.3.3 and 4.1 respectively.

2.2 Coupled Body Motion in Surge

In order to investigate a mooring arrangement that is somewhat closer to the marina problem than the single moored body, the problem of the surge motions of coupled bodies was studied analytically. In this system the small craft is moored to a floating platform which is in turn moored to a fixed support. Admittedly this is a highly idealized mooring system; however, it was felt that some of the problems associated with coupled mooring systems could be effectively investigated in this way.

A schematic representation of this coupled body system is shown in Fig. 5. Subscripts 1 refer to the body moored to a fixed support and subscript 2 refer to the body which is moored to Body 1. In this analysis it is assumed that both bodies are neutrally buoyant, only movement in the direction of wave propagation is possible, and that the mooring system consists of linear springs. In addition it is assumed that there is no interference between the two bodies. In other

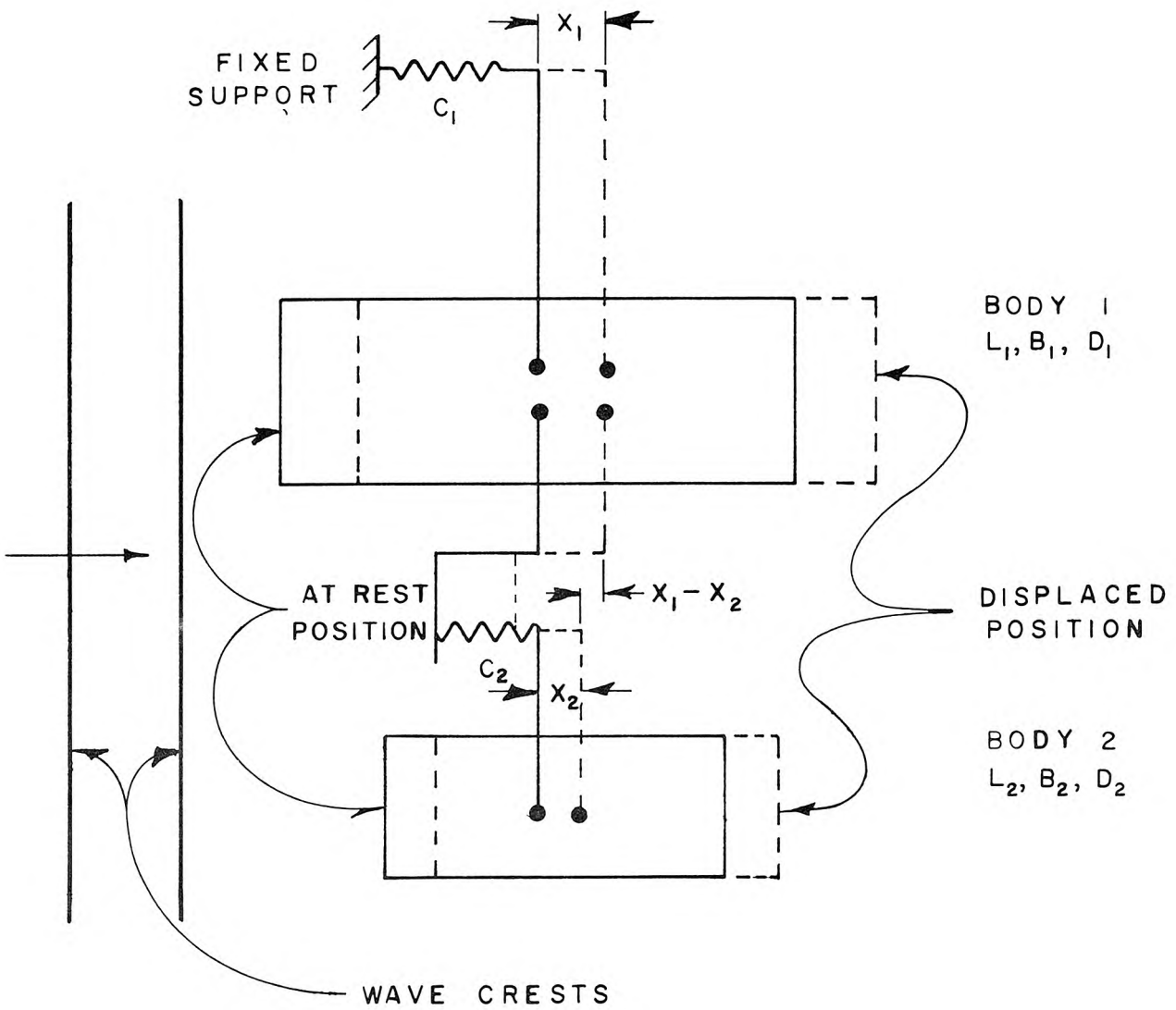

Fig. 5. Definition Sketch of Coupled Body System

words hydrodynamic quantities such as the drag coefficient and the added mass of one body are not affected by the other body. The equations of motion can then be written directly from Eq. 22.

Body 1

$$M_1 \ddot{x}_1 = M_1 \dot{U}_1 + M'_{x_1} (\dot{U}_1 - \ddot{x}_1) + \frac{\rho}{2} C_{D_{x_1}} B_1 D_1 (U_1 - x_1) |U_1 - x_1| - C_1 x_1 - C_2 (x_1 - x_2) \tag{30}$$

Body 2

$$M_2 \ddot{x}_2 = M_2 \dot{U}_2 + M'_{x_2} (\dot{U}_2 - \ddot{x}_2) + \frac{\rho}{2} C_{D_{x_2}} B_2 D_2 (U_2 - x_2) | U_2 - x_2 | + C_2 (x_1 - x_2) \tag{31}$$

After linearizing the drag terms, using the notation of Eq. 22 for the average water particle velocity and the average water particle acceleration, Eqs. 30 and 31 become:

$$\ddot{x}_1 + \beta_1 \dot{x}_1 + (\omega_1^2 + m\omega_2^2) x_1 - m\omega_2^2 x_2 = \dot{U}_1 + \beta_1 U_1 \tag{32}$$

and

$$\ddot{x}_2 + \beta_2 \dot{x}_2 - \omega_2^2 x_1 + \omega_2^2 x_2 = \dot{U}_2 + \beta_2 U_2 \tag{33}$$

where: $\beta_1 \equiv \dfrac{\frac{1}{2} C_{d_{x_1}}}{C_{M_1} (2L_1)}$, $\beta_2 \equiv \dfrac{\frac{1}{2} C_{d_{x_2}}}{C_{M_2} (2L_2)}$

$$\omega_1^2 = \frac{C_1}{C_{M_1} M_1} \quad , \quad \omega_2^2 = \frac{C_2}{C_{M_2} M_2}$$

$$M = \frac{C_{M_2} M_2}{C_{M_1} M_1}$$

From Eq. 33 an expression for x_1 can be obtained in terms of x_2 and U_2 and their derivatives and then this can be differentiated to get $\dot{x}_1$ and $\ddot{x}_1$. Substituting these expressions into Eq. 32 gives a fourth order

linear differential equation in x_2 in terms of known parameters.

Assuming solutions for x_1 and x_2 of the form

$$x_1 = X_1 \cos(\sigma t - \varphi_1) \tag{34}$$

where $X_1 = (L^2 + J^2)^{1/2}$

$$\tan \varphi_1 = J/L$$

and

$$x_2 = X_2 \cos(\sigma t - \varphi_2) \tag{35}$$

where $X_2 = (E^2 + F^2)^{1/2}$

$$\tan \varphi_2 = F/E$$

The following expressions are obtained for the coefficients E, F, L, and J using the notation:

$$a \equiv \frac{\beta_1}{\omega_1} \qquad p \equiv \frac{\beta_2}{\omega_2} \qquad c \equiv \frac{\omega_1}{\omega_2} \qquad \mu \equiv \frac{\sigma}{\omega_2} = \frac{T_2}{T}$$

$$f \equiv \frac{L_2 D_2}{L_1 D_1} \quad \frac{\sin kL_1}{\sin kL_2} \quad \frac{\sinh kd - \sinh ks_1}{\sinh kd - \sinh ks_2}$$

$$\frac{\delta_2}{\sigma_2} = \frac{A}{k^2 L_2 D_2}\left\{1 - \frac{\sinh ks_2}{\sinh kd}\right\} \sin kb \sin kL_2$$

For simplicity the subscript x has not been used in the damping coefficients above; however, it is evident from Eqs. 30 and 31 that only motions in the x-directions are being considered.

$$E = \frac{\delta_2}{\sigma_2}\left\{\frac{f + apc + c^2 + m - \mu^2}{\mu^2 - 1 - apc - c^2 - m + \frac{c^2}{\mu^2}} - \frac{p^2}{\mu^2}\,\frac{\left(\frac{ac}{p} + c^2 + m - \mu^2 - \frac{a\mu^2}{pc}\right)\left(\frac{fac}{p} + c^2 + m - \mu^2 - \frac{a\mu^2}{pc}\right)}{\left(\mu^2 - 1 - apc - c^2 - m + \frac{c^2}{\mu^2}\right)^2}\right\}$$

$$\div \left\{1 + \frac{p^2}{\mu^2}\left[\frac{\frac{ac}{p} + c^2 + m - \mu^2 - \frac{a\mu^2}{pc}}{\mu^2 - 1 - apc - c^2 - m + \frac{c^2}{\mu^2}}\right]\right\} \tag{36a}$$

$$F = \frac{\delta_2}{\sigma^2}\frac{p}{\mu}\left[\frac{\frac{fac}{p} + c^2 + m - \mu^2 - \frac{a\mu^2}{pc}}{\mu^2 - 1 - apc - c^2 - m + \frac{c^2}{\mu^2}}\right]$$

$$+ \frac{p}{\mu}\left[\frac{\frac{ac}{p} + c^2 + m - \mu^2 - \frac{a\mu^2}{pc}}{\mu^2 - 1 - apc - c^2 - m + \frac{c^2}{\mu^2}}\right]E \tag{36b}$$

$$L = (1 - \mu^2)\,E + p\mu\,F - \frac{\delta_2}{\sigma^2}\,\mu^2 \tag{36c}$$

$$J = (1 - \mu^2)\,F + p\mu\,E - p\,\frac{\delta_2}{\sigma^2}\,\mu \tag{36d}$$

The form of the amplification factors $\frac{X_1}{A}$ and $\frac{X_2}{A}$ cannot be viewed as simply as for the single body system discussed previously. Therefore, for this case some general comments will be made and examples of the response curves will be presented for a specific configuration.

To simplify Eqs. 36 the case of zero damping is considered first. For this case, $a = p = 0$, the condition for resonance is that the coefficient E must become infinite since $F = J = 0$ and L is directly proportional to E. This can occur if:

$$\mu^2 - 1 - c^2 - m + \frac{c^2}{\mu^2} = 0 \tag{37}$$

Hence the criterion for resonance is:

$$\mu^2 = \frac{\tau_2^2}{T^2} = \frac{(1 + c^2 + m) \pm \sqrt{(1 + c^2 + m)^2 - 4c^2}}{2} \tag{38}$$

which leads to two non-negative roots. For the case of two identical bodies moored in an identical fashion $c = m = 1$, one obtains $\frac{\tau_2}{T} = 1.62$ and 0.618 for the first and second mode of oscillation respectively.

These values of the relative resonant periods are shown in the theoretical response curve for the undamped system presented in Fig. 6a. Two curves are presented, one for the variation of the surge of Body 1 relative to the wave amplitude (X_1/A) as a function of τ_2/T and a similar curve for Body 2. These curves are for identical bodies and mooring systems and the particular conditions chosen are indicated on the figure. The two resonant spikes are seen for the response of each body, but for the same bodies and the same forcing function the response at particular wave periods can differ by more than a factor of two. It appears that the first resonant peak is strongest for the outboard body (Body 2) and the second spike is strongest for the inboard body (Body 1). These differences are to be expected since for the same springs the restraining forces on the two bodies are different. In Fig. 6b the wave characteristics are shown as a function of the relative period (τ_2/T). For the case chosen the response curve of Fig. 6a is essentially for the region between shallow water and deep water waves. These curves are presented simply to help the reader relate some important wave length characteristics to the relative period parameter, τ_2/T.

Response curves for the same body characteristics are presented in Figs. 7a and 7b for different degrees of damping ($\frac{\beta_1}{\omega_1} = \frac{\beta_2}{\omega_2} = 0.1,\ 0.5$). The same shift of the resonant wave period to larger periods with increasing damping is seen as was observed for the single moored body. In these figures the difference in the response of the two bodies for the same forcing function is even more apparent. Again it is seen that viscous forces are present as a driving force in the system as well as a dissipative force.

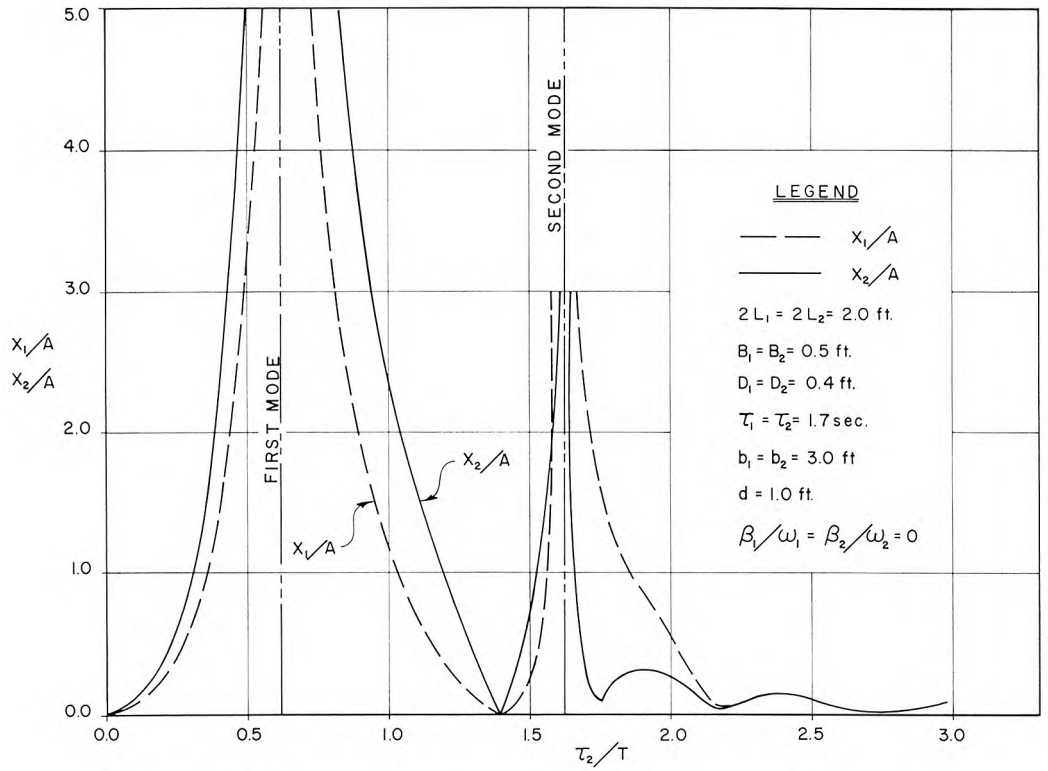

Fig. 6a. Undamped Response Curve Coupled Body System

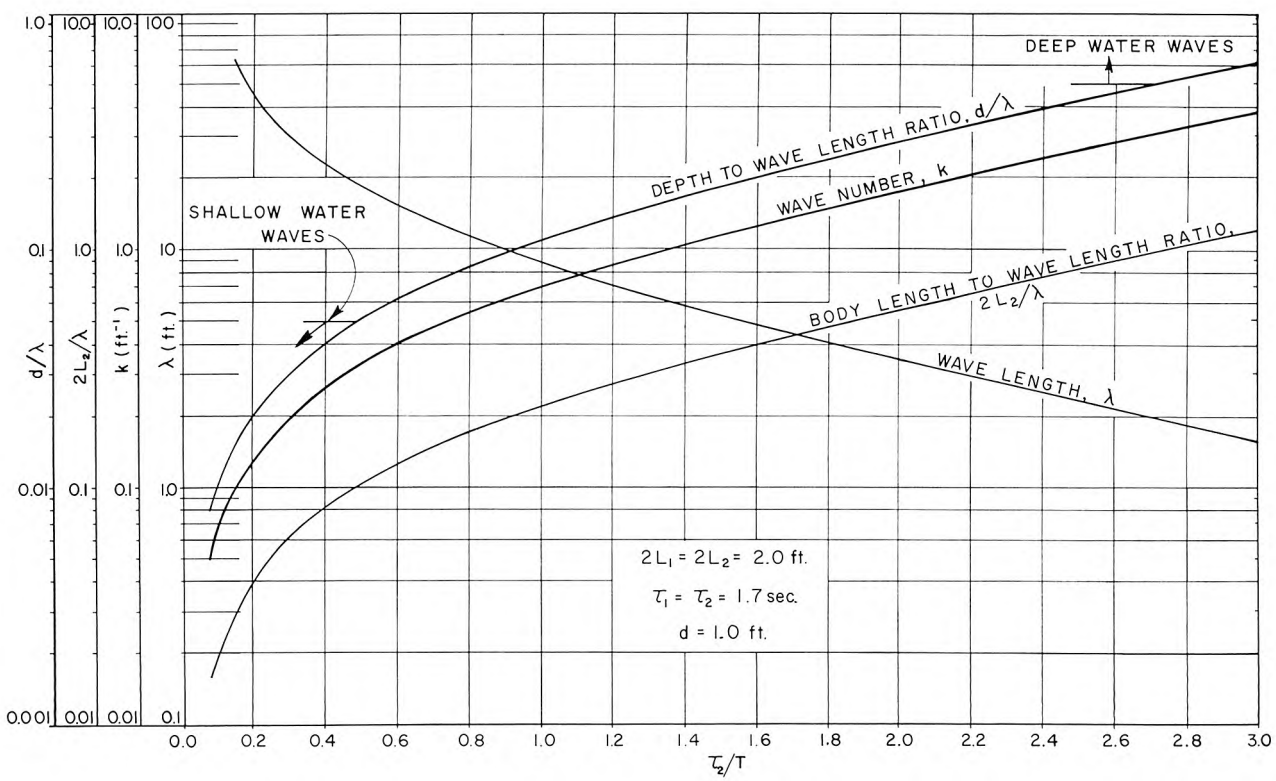

Fig. 6b. General Characteristics of Wave System

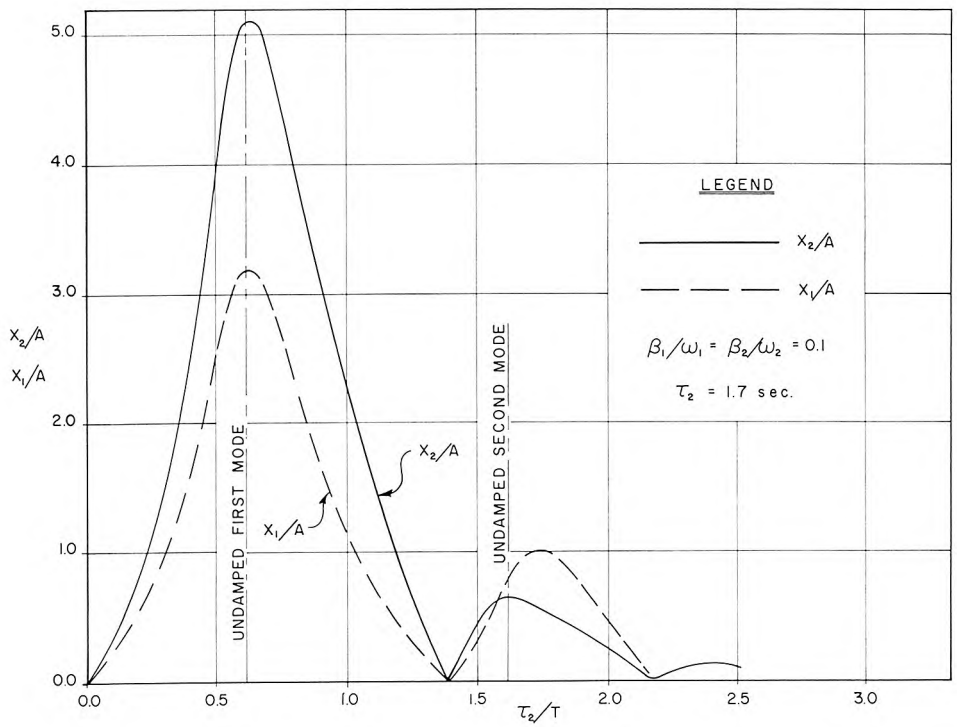

Fig. 7a. Theoretical Response Curve of Coupled Body System $\frac{\beta_1}{\omega} = \frac{\beta_2}{\omega} = 0.1$

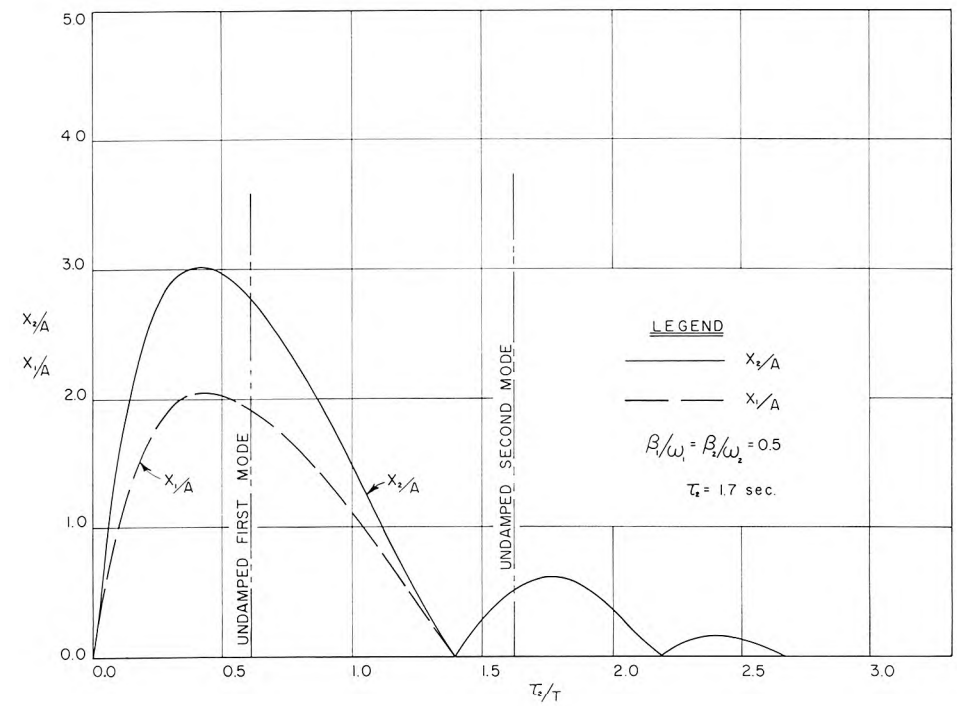

Fig. 7b. Theoretical Response Curve of Coupled Body System $\frac{\beta_1}{\omega} = \frac{\beta_2}{\omega} = 0.5$

The variation of the relative response of the two bodies for the same forcing function (X_1/X_2) as a function of relative period τ_2/T) is shown in Fig. 8 for various values of the damping coefficient. It is seen that independent of the damping the motions of the bodies are the same at $\tau_2/T = 1.585$. For wave periods greater than this the motions of the outboard body are greater than those of the inboard body and the reverse is true for wave periods less than this value. It appears that no simple physical significance can be attached to the value of τ_2/T where $X_1/X_2 = 1$, other than to say that this is the wave period when for the particular body and mooring system characteristics the magnitude of the surge is the same for both bodies. However it is apparent from Eqs. 34, 35, and 36 at least for the inviscid case that independent of the body dimensions and characteristics of the mooring system there is one value of τ_2/T where this will occur. As the dissipative forces increase relative to inertial forces the amplitude of the body motions tends to become the same.

The theoretical effect of damping for this coupled body system and for the single moored body is evident when the value of the relative surge amplitude X/A at resonance is plotted as a function of the relative dissipation β_x/ω. This has been plotted in Fig. 9 for the coupled body case as the value of X_2/A and X_1/A for the fundamental mode of oscillation as a function of the damping coefficient $\beta_2/\omega_2 = \beta_1/\omega_1 = \beta_x/\omega$. As would be expected the response at resonance is reduced significantly with small damping. However, as the damping increases the response at resonance actually tends to increase, since for high damping the damping force drives the body. In this coupled body system for relative damping greater than about 0.1 the ratio of X_1/X_2 at resonance appears to be relatively

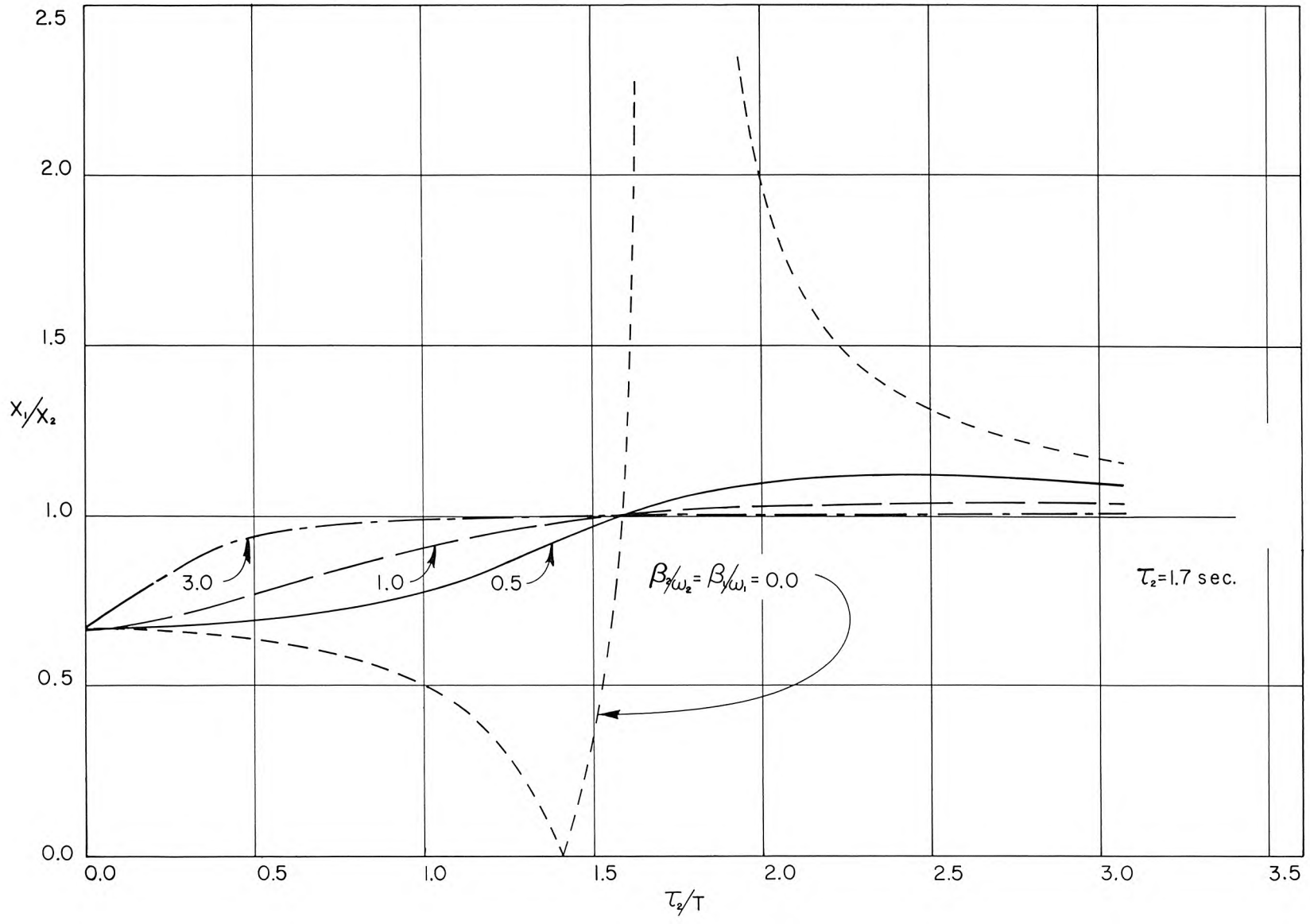

Fig. 8. Variation of Relative Body Motion, X_1/X_2, with Normalized Period τ_2/T

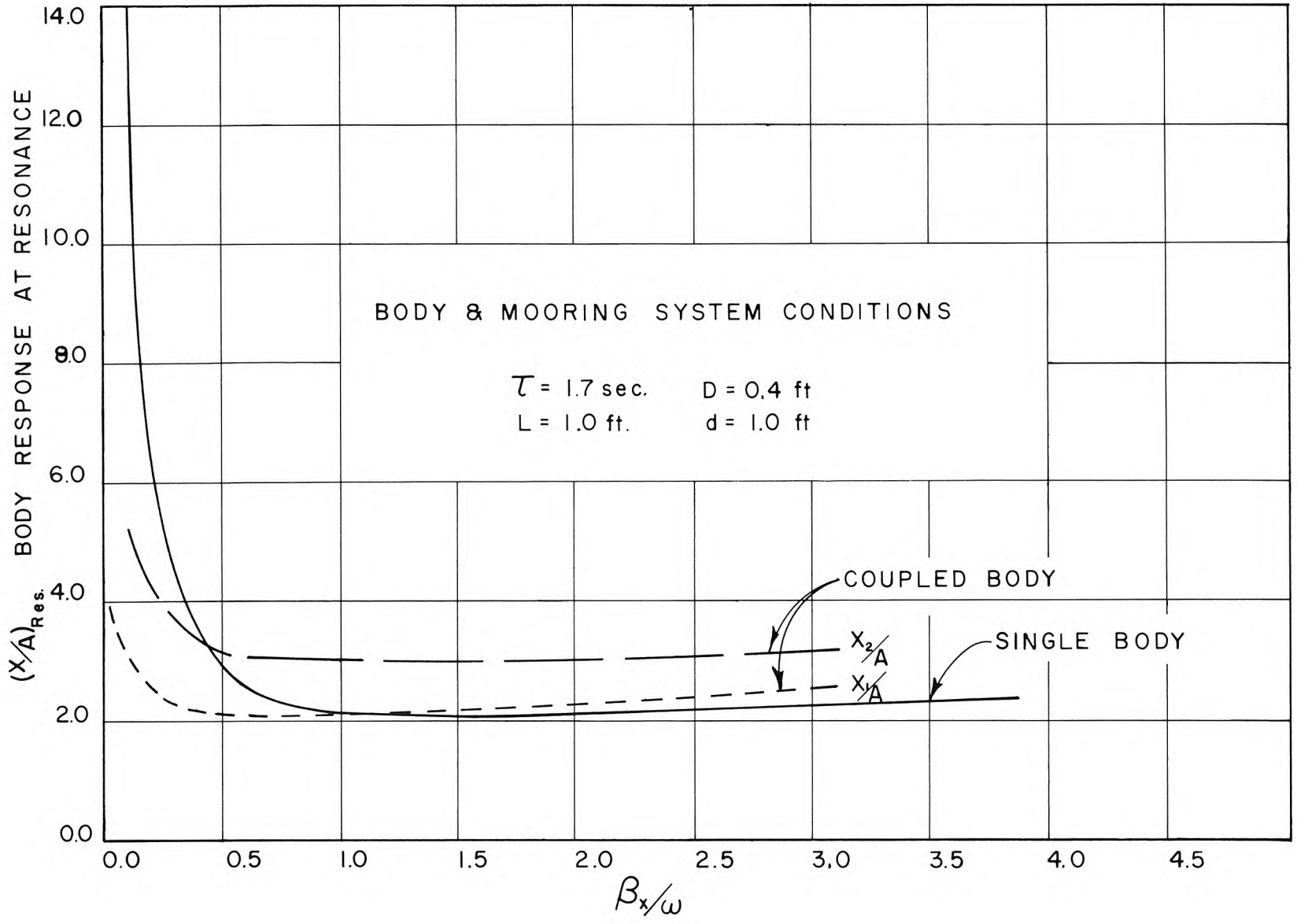

Fig. 9. Variation of Response Function, X/A, at Resonance with Damping Coefficient, β_x/ω for First Mode of Oscillation

constant at a value of approximately 2/3. The case of a single moored body is also shown in this figure. It is seen that for a value of $\beta_x/\omega > 1$ the response X/A for this body and for this particular mooring system is approximately equal to 2.0.

3. Experimental Equipment and Procedures

An overall view of the wave basin and wave generator located in the W. M. Keck Laboratory of Hydraulics and Water Resources, California Institute of Technology, is shown in the drawing and photograph of Fig. 10.

3.1 Wave Basin

The wave basin is 21 in. deep with a working area approximately 30 ft long by 12 ft wide. The actual overall inside dimensions of the basin are 31 ft-5in. long by 15 ft-5 in. wide. The basin is constructed throughout of 3/4-in. and 1-in. marine plywood, the former for all vertical walls and the latter for the floor. The basin floor is located 9-1/2 in. above the laboratory floor. This was done for two reasons: to bring the system up to a more comfortable working level and to provide a means for leveling the basin floor. To properly level the floor seven 1 5/8 in. by 3 5/8 in. wood sills were fastened to the floor, with the short dimension vertical, 32 in. on center running the length of the basin. Perpendicular to these a system of 1 5/8 in. by 7 5/8 in. joists were fastened on 16-in. centers. At the intersection of each sill with a joist, shim material was placed between the two so that the upper face of the joists were reasonably level (within ± 1/32 in.). This substructure can be seen in the drawing and photograph of Fig. 10.

This initial leveling was important since once the floor had been attached to the substructure it was impossible to make adjustments. Before placing the basin floor the complete supporting framework was waterproofed with "Thompson Water Seal". The one-inch plywood floor was then glued and screwed to the joists which had been braced with

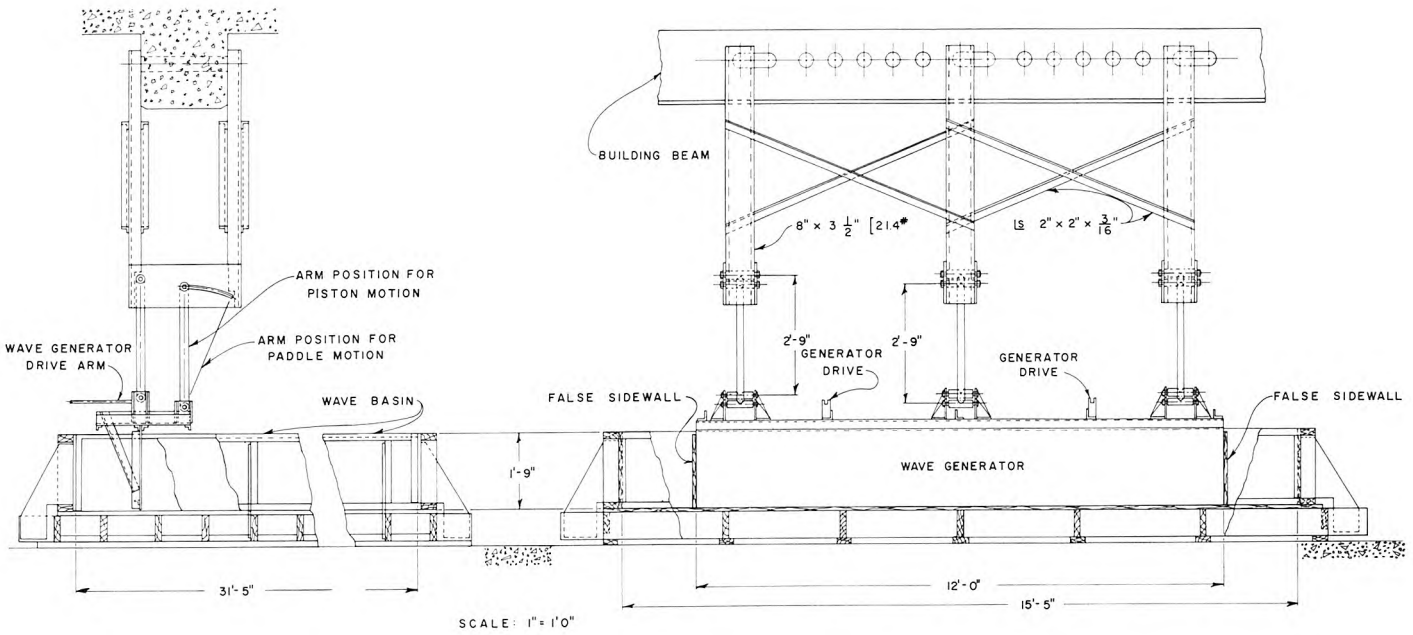

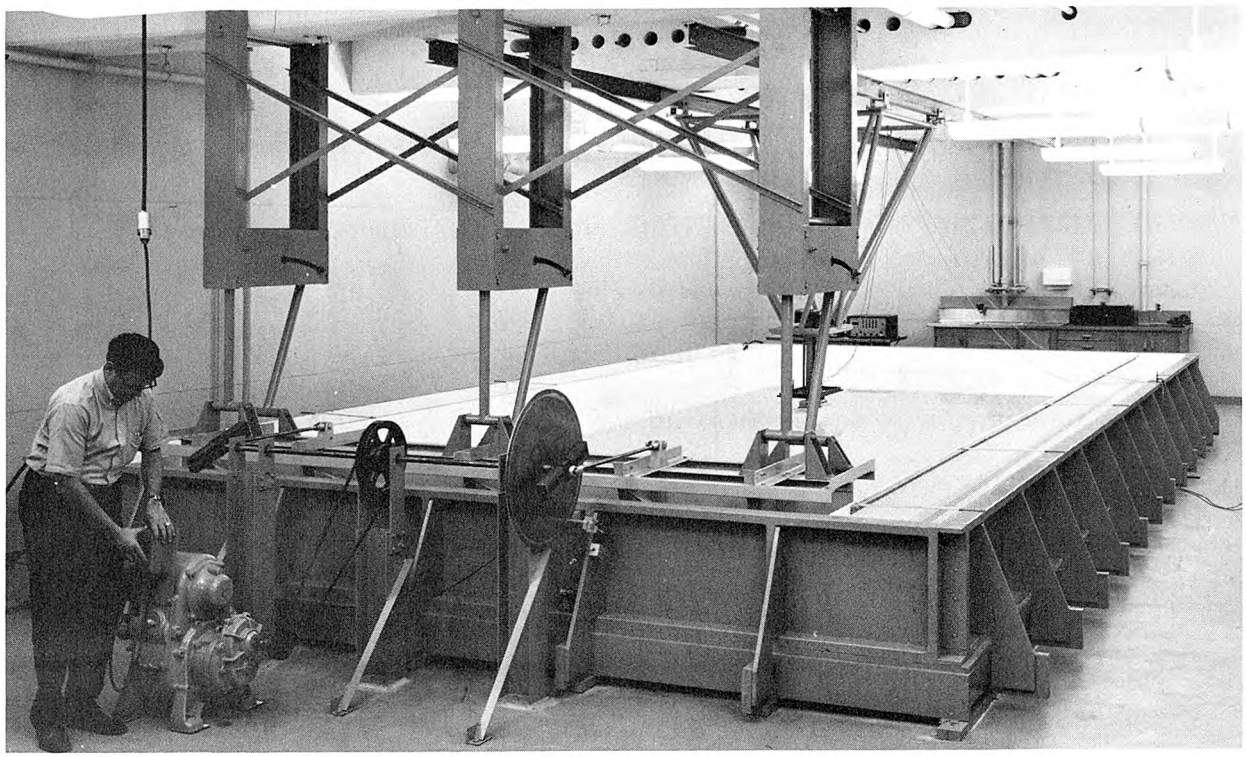

Fig. 10 Detailed Drawing and Overall View of Wave Basin and Wave Generator

solid bridging at 32 in. intervals, making the maximum unsupported area of the floor 16 in. by 32 in. and minimizing deflections. The 3/4 in. vertical outer walls were then placed with their supporting gussets with a caulking compound and a silicone rubber seal between the walls and the floor. The complete interior of the basin was then treated with "Pittsburgh Aquapon", a modified epoxy enamel, to insure watertightness. It was found that this method minimized leaks, although it was necessary at a later date to seal one of the floor joints with waterproof tape to affect better sealing.

False sidewalls of 3/4 in. plywood were installed inside the basin 12 ft apart and perpendicular to the wave generator. This provides a 20 in. space on each side of the basin. At some future date, if desired, these walls can be removed and the space between the false and true walls filled with a damping material to dissipate incident wave energy. These walls are seen in Fig. 10.

Not shown in these figures is a wave filter consisting of a basket of aluminum wool 3 ft wide and 12 ft long located directly in front of the wave generator. The transmission characteristics of this wave filter will be discussed later. It was added to the system simply to add some energy dissipation to the basin which originally had low dissipative characteristics.

3.2 Wave Generator

The wave generator used is a pendulum type similar to one proposed by Ransford (16) and is shown in the drawing and photographs, Figs. 10 and 11a. It is designed to operate as either a paddle or piston type wave machine. This versatility was considered necessary due to the relative

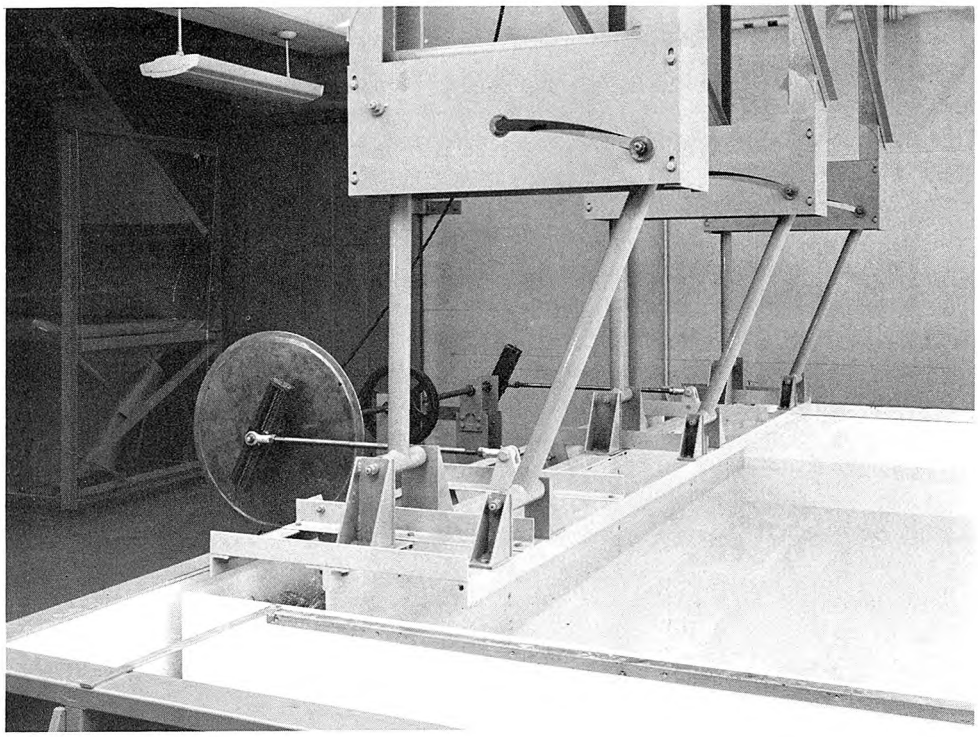

Fig. 11a. View of Wave Generator and Overhead Support

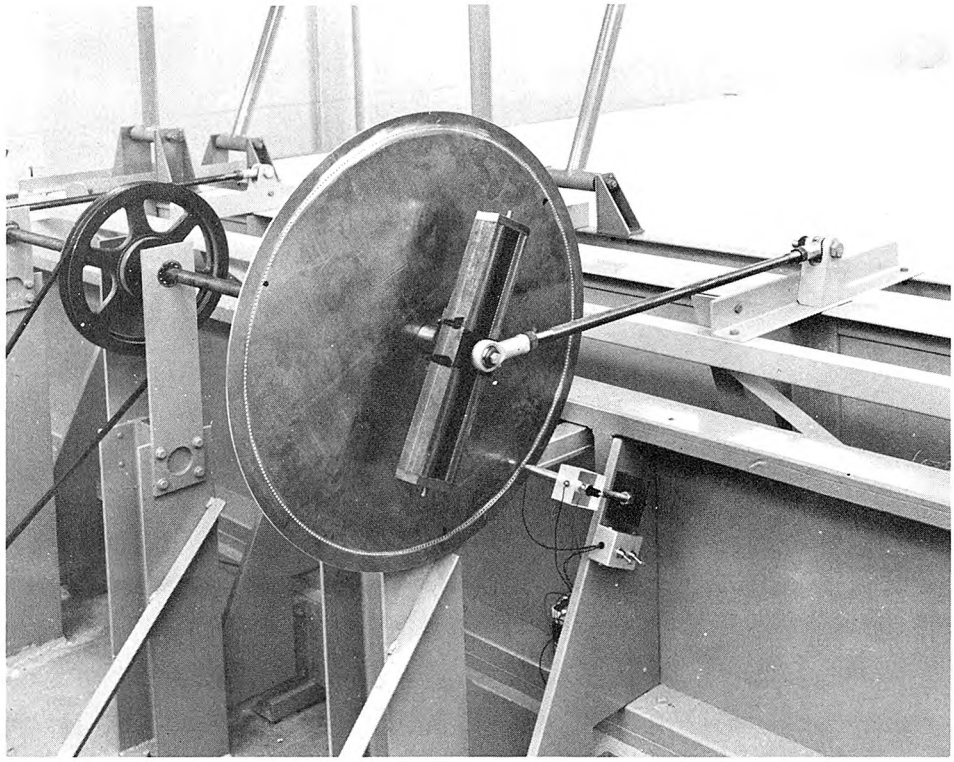

Fig. 11b. View of Skotch Yoke, Wave Period Light Source, and Perforated Disc

shortness of the basin and the range of wave periods required. In order to generate shallow-water waves having a wave length comparable to the basin length a piston generator was desired, whereas for deep-water waves a paddle or flap generator is best. In addition to the wave length considerations, in order to produce a two-dimensional small amplitude wave system the wave-machine strokes must be accurately adjusted; therefore, large strokes were desired. For deep water waves this is best accomplished by the paddle mode of generation.

The generating surface is an aluminum plate 12 ft long, 2 ft high and 1/4 in. thick. To reduce the possibility of the wave machine producing higher order harmonics due to vibration of the plate, the plate is attached to a structural frame of aluminum angle. As seen in Fig. 10 this unit is supported from an overhead structure at three points with two arms at each support point. The structure itself is fastened to a reinforced concrete ceiling beam. The support arms are 33 in. long and have an axle at either end which is free to rotate in a ball bearing retainer. The upper end of the forward arm at each support point can be moved in a slot of 33 in. radius so that the arm moves from a vertical to an inclined position.

When both arms are vertical the generating plate moves horizontally as a piston. When the upper end of the forward arms are at the furthermost forward position the generating plate moves as a paddle with the bottom of the plate acting as an imaginary hinge point. The linkage lengths were designed so that, for the paddle mode of operation, movement of the hinge point was minimized. After a number of trials the best choice of linkage lengths in keeping with the space available was 31 in. from the

bottom of the plate to the centerline of the lower end of the rear support arm and, as mentioned previously, a 33 in. long support arm. This design gave a movement of the bottom of the plate of approximately 1% of the forward and backward movement of the lower end of the support arms when the wave machine was operating as a paddle.

The wave machine is driven by two arms connected to independent Scotch yokes which are in turn driven through a pulley system by a variable speed motor. The drive mechanism and the yokes can be seen in Fig. 10, 11a and 11b. A maximum stroke of ±6 in. can be obtained with this arrangement and measured to within ±. 0005 in. by means of dial gages, one at either end of the paddle. The motor drive is a 1-1/2 hp U. S. Varidrive motor with a 10:1 speed range. Wave periods ranging from 0. 34 sec. to 3. 8 sec. can be obtained with this system. The motor has a greater power output than is actually needed in order to insure a constant speed operation. The speed measuring technique will be described in some detail later; however, it is found that the wave period remains constant to within ±. 05%.

3. 3 Model Support Structure and Model

The model is supported from overhead by the structure shown in Fig. 12 (see also Fig. 10). This structure is a welded tube frame with trolley wheels at the upper end which roll on two aluminum "I" beams which run the full length of the basin and are fastened to the structural frame of the building. Thus the support structure can be moved longitudinally along the basin and the rails are positioned so that the model moves along the basin centerline.

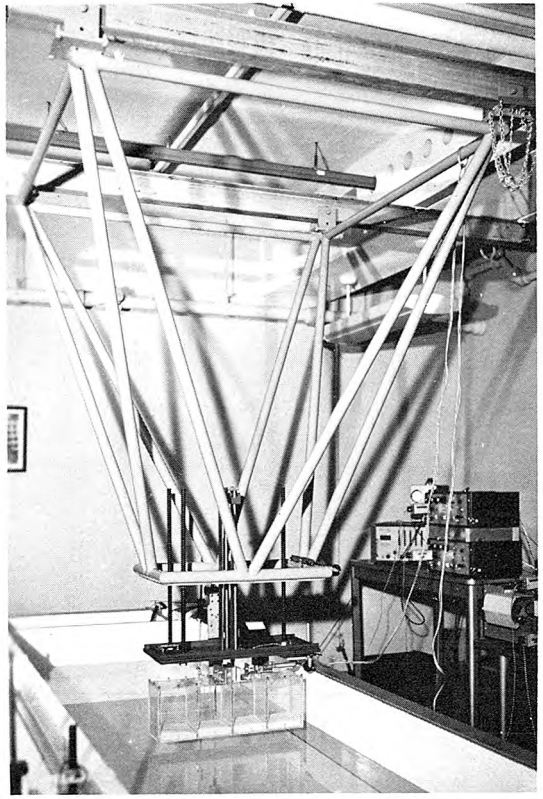

Fig. 12. View of Model Support Structure

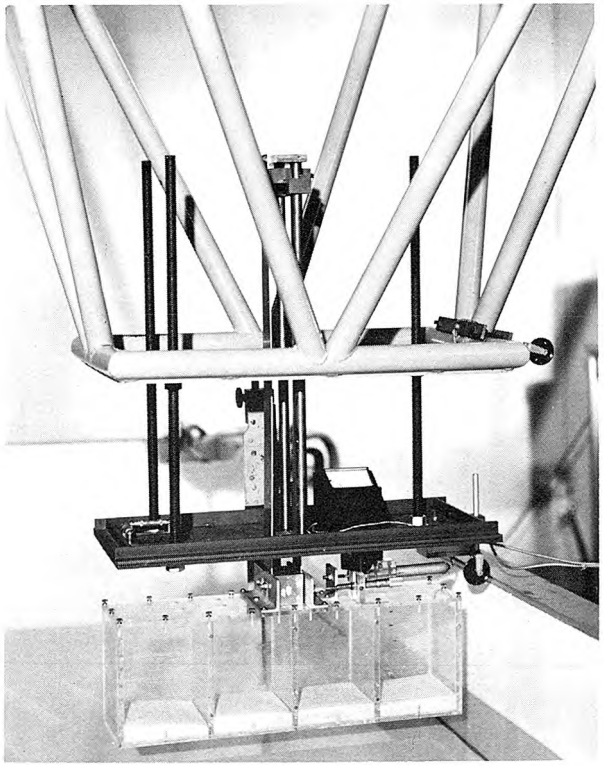

Fig. 13. View of Model and Model Support Structure

A plate is welded to the lower end of the tubing frame which serves as the basic support for the model. Three 3/4 in. diameter lead screws are free to move through this plate and can be locked in position by means of nuts on either side of the upper plate. These screws are firmly attached to a lower plate which forms a rigid frame for the model mooring system. These features are seen clearly in Fig. 13.

Two 3/4-in. diameter rods are attached to the lower plate and are free to move up through the upper plate. The mooring system and hence the model are attached to these rods. Therefore, the lead screws and the rods form a unit that can be adjusted so that the model is immersed to any draft and adjusted so that it is level. This lower system can also be rotated through approximately $\pm 10^{\circ}$ so that the axis of the model can be aligned perpendicular to the standing wave crests.

For the linearally moored model two aluminum leaf springs (.09 in. thick and 2 in. wide) are used to represent the mooring system (see Fig. 13). These springs are 2 inches apart and are attached to the model as a unit. This arrangement eliminates all motions except the surge motion in the model. The length of the springs can be varied by moving the upper spring clamp along the lower plate support rods while maintaining a constant model draft. In this way the spring constant of the mooring system can be varied over a wide range.

The moored body used in this phase of the study was a rectangular parallelpiped 24 in. long, 6 in. wide, and 8 in. high. It was made of 1/4 in. lucite and divided into 4 compartments. The top is removable so that the box can be loaded with sand ballast to make it neutrally buoyant for a particular depth of immersion. This can be seen in detail

in Fig. 13. The transducer and recording system used to give a time-displacement history of the body will be discussed in Section 3.4.3.

3.4 Instrumentation

3.4.1 Measurement of Wave Period

The wave period is determined by a pulse counting technique. The pulse is generated by interrupting a light beam which is directed at a photocell by a disc with 360 evenly spaced holes arranged in a circle near its outer edge. This disc can be seen in Fig. 11b. The output from the photo-cell (photo-multiplier power transistor type PPT-1), whose circuit is shown in Fig. 14, actuates a Beckman/Berkeley Division Industrial Counter Model 7361 which then counts the number of voltage pulses (or the number of holes passing the photocell) in a period of 10 sec. It may be of interest to note that the voltage output of this simple system, using as a light source a 1.5 volt flashlight bulb without an optical system, is approximately 2.5 volts (more than sufficient to drive the counter). Thus the wave period obtained is a 10 sec. average and, as mentioned previously, throughout an experiment this period varied at most by ±.05%.

3.4.2 Measurement of Wave Amplitude

Resistance wave gages were used in conjunction with Sanborn (150 Series) direct-writing recording systems to obtain time histories of the wave amplitude. Sanborn Carrier Preamplifiers (Model 150-1100AS) supply the 2400 cps, 4.5 volt excitation voltage for the gages, and in turn receive the outputs from the wave gages which after de-modulation and amplification, are displayed on the recording unit.

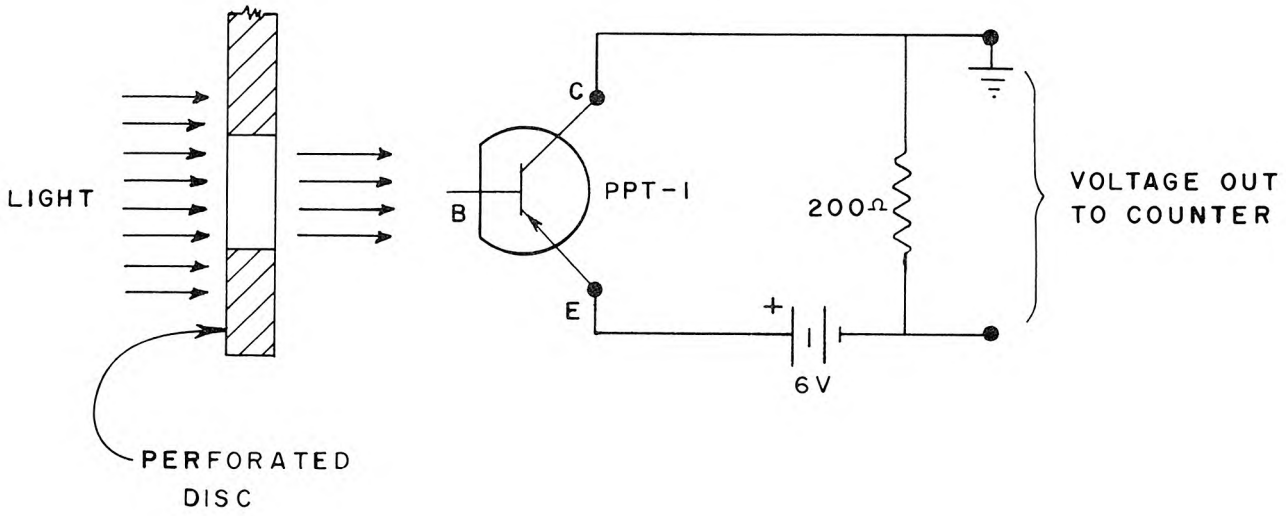

Fig. 14. Schematic Diagram and Circuit of Photo-Cell Device

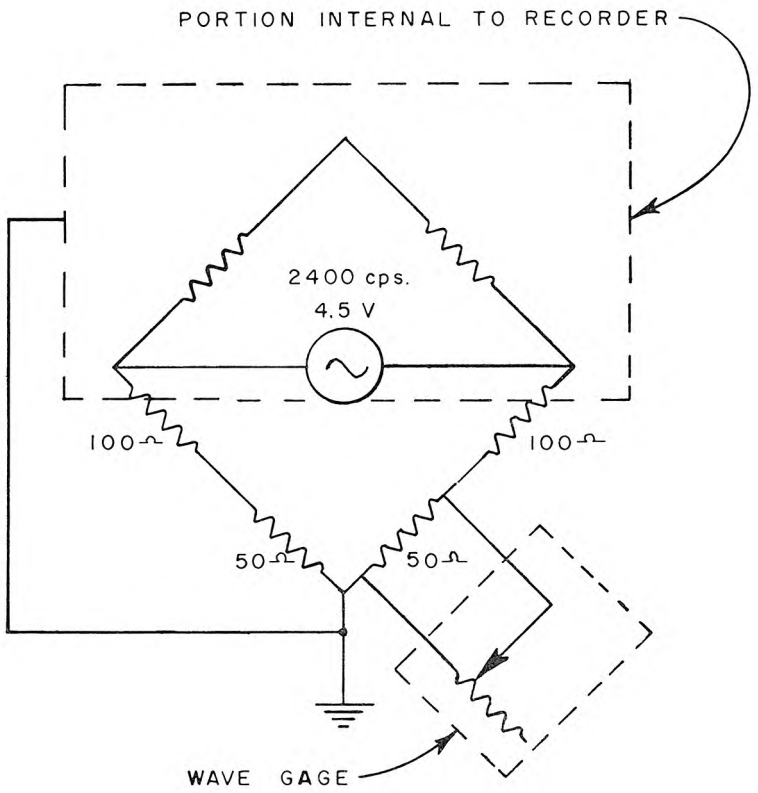

Fig. 15. Circuit Diagram for Wave Gage

The wave gages consist of two wire elements, parallel to and insulated from each other, upon which the excitation voltage is impressed. As the immersion of the wires in a conducting solution is varied their resistance changes proportionately, causing an imbalance in the full bridge circuit shown in Fig. 15 (the portion of the circuit internal to the recorder is shown dotted). This imbalance causes more or less voltage drop across the gage and is recorded by the Sanborn unit as a change from the zero or balanced position. Depending upon the length of the gage and the wire material, the 50 ohm resistance in parallel with the wave gage may have to be changed in order to affect a balance with the Sanborn equipment. This can easily be accomplished by inserting a precision variable resistor in series with the 50 ohm resistor.

Different types of wave gages were used in this study, however, only the type finally decided upon will be described in detail. This gage consists of two stainless steel wires 0.01 in. in diameter approximately 3-1/2 in. long spaced 1/8 in. apart. They are insulated from each other and stretched taut in a 1/8-in. diameter stainless steel frame which becomes an integral part of a point gage used for calibration. A sketch of the wave gage is presented in Fig. 16. The wire elements of this gage can be oriented so that the plane of the wires is at any angle to the plane of the clamp. This feature is important when one is interested in measuring the standing wave amplitude in the vicinity of a reflecting wall. By rotating the two wires into the plane of the clamp and by placing this plane parallel to the reflecting surface the measurements are not affected by the supporting arrangement. As in any resistance type wave gage it is important that the wire elements be kept clean and free from contaminants.

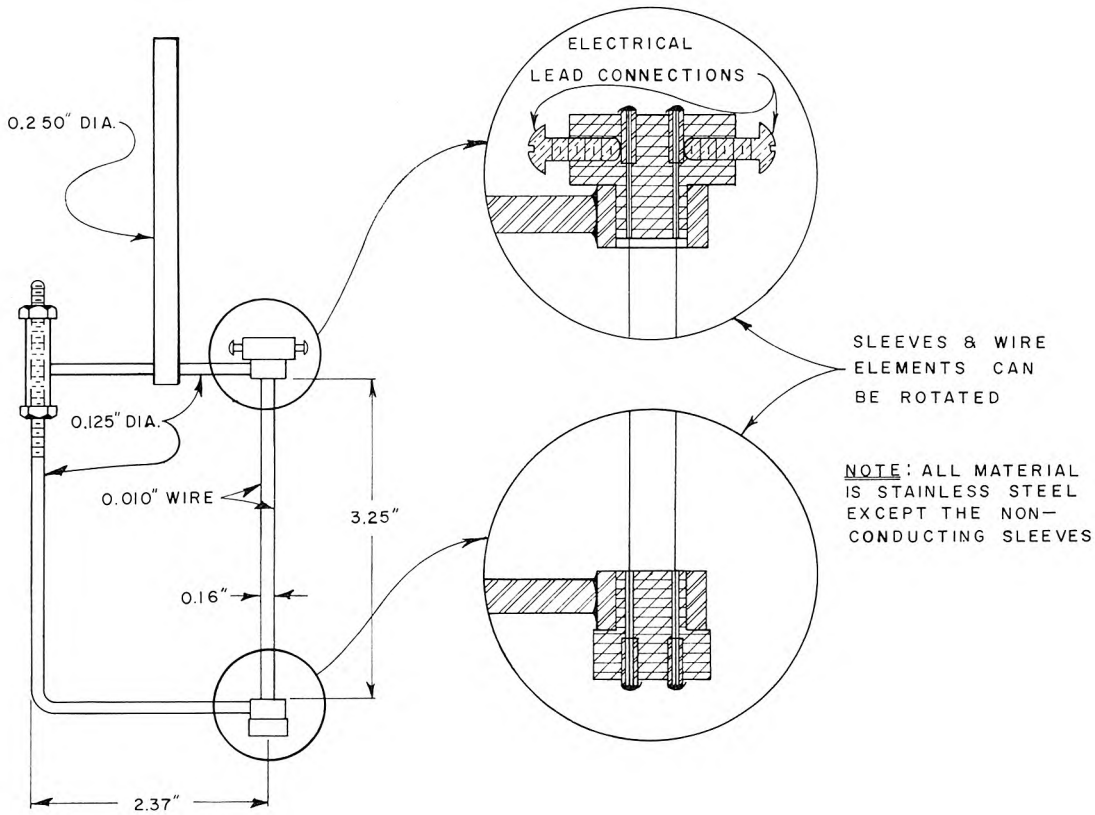

Fig. 16. Drawing of Typical Wave Gage

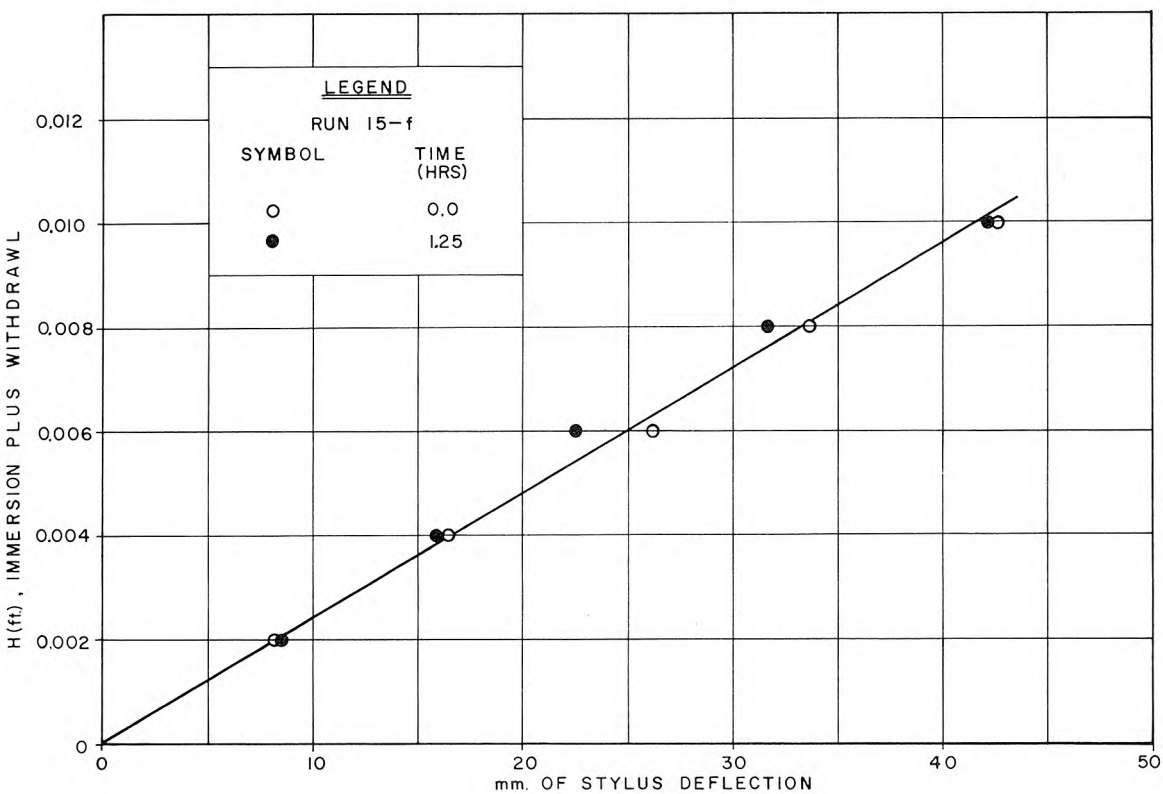

Fig. 17. Typical Calibration Curve for Wave Gage

Since there is an inherent electronic drift associated with these gages, it is unrealistic to speak of wave amplitudes where an unchanging zero line is important. For this reason only wave heights are measured. A typical calibration curve for one of the wave gages is presented in Fig. 17.

The gage is calibrated by first increasing its immersion 0.001 ft, using a point gage, then returning to the original immersion and finally withdrawing it 0.001 ft. This procedure is repeated increasing the immersion and withdrawal increment by 0.001 ft each cycle. This method tends to compensate, to some extent, for dynamic effects. In Fig. 17 the total movement for each calibration step, i.e. immersion plus withdrawal, is plotted as the ordinate and the deflection of the stylus in millimeters as the abscissa. The points shown are for calibrations before and after an experiment that lasted approximately 1.25 hrs. Most calibrations were essentially linear and showed little change through an experiment so that an average of these data was used in reducing the recorded wave amplitude. Throughout an experiment the drift mentioned previously was compensated for to some extent by changing the internal Sanborn resistance so that the signal was always centered on the scale. This procedure is reasonable since one reason for the drift is the change in resistance of the wave gage wires associated with wire contamination. It has been found from dynamic calibrations, see Ippen and Raichlen (17) and Goda and Ippen (18), that the difference between static calibrations and the dynamic use of such a gage introduces an error of at most 5% for wave heights of the order of 0.1 in.

A problem that is usually encountered in wave measurements using more than one wave gage in conjunction with Sanborn equipment is the interference between channels when operating at low attenuation. This has been essentially eliminated here by making certain internal modifications to the Model 150-1100 AS preamplifiers recommended by the manufacturer. In effect this reduces the interference by locking the preamplifier oscillators to one common frequency.

3.4.3 Measurement of Body Amplitude

The time history of body motion in surge is obtained using a linear variable differential transformer (LVDT). This is an electromechanical transducer which produces an electrical output proportional to the displacement of a separate movable core.

Three coils are equally spaced on a cylindrical coil form, and a rod-shaped magnetic core positioned axially inside the coil assembly provides a path for magnetic flux linking the coils. The voltage induced in the secondary coils by movements of the core is displayed on the Sanborn as a stylus displacement from a balanced position. The circuit diagram for connecting the LVDT to the transducer input of the Sanborn Model 150-1100 AS is shown in Fig. 18. The letters refer to the pin connections of the Sanborn input and the colors to the electrical leads of the LVDT.

The core of the LVDT (Schaevitz Model 1000SS-L) is mounted on the model and the coils are mounted to the fixed platform directly above the model as shown in Fig. 13. Therefore, when the model moves in surge a voltage is induced in the secondary coils. The system is calibrated by deflecting the model and reading the deflection by means of a micrometer mounted to the fixed plates and recording the stylus

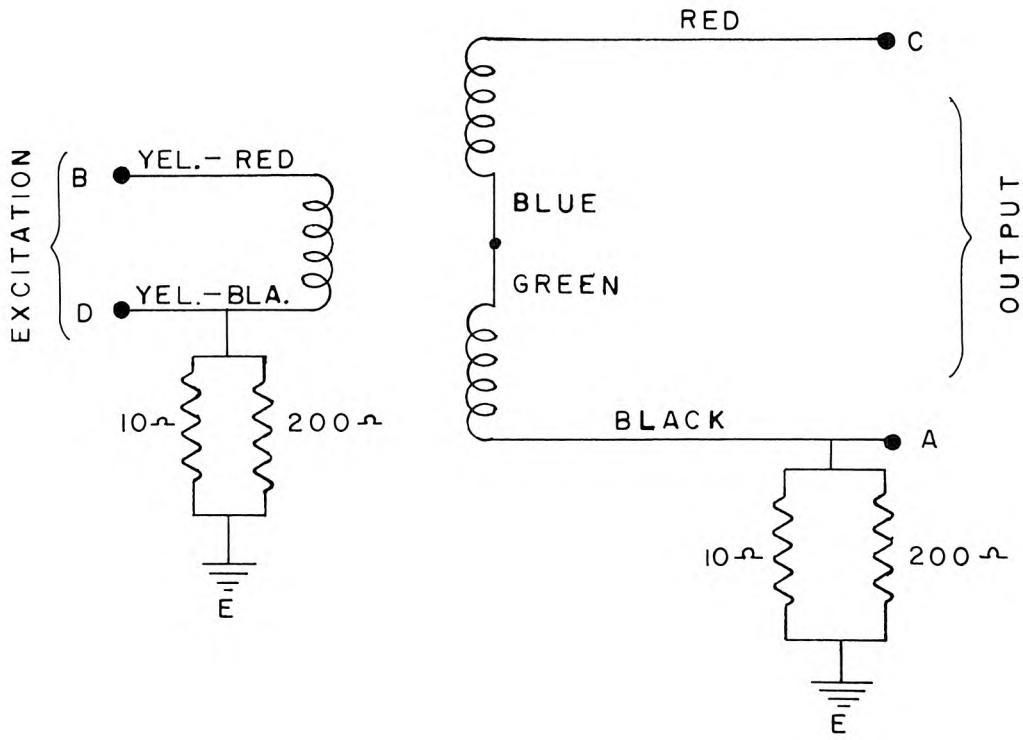

Fig. 18. Circuit Diagram for Linear Variable Differential Transformer used in Recording Body Motion

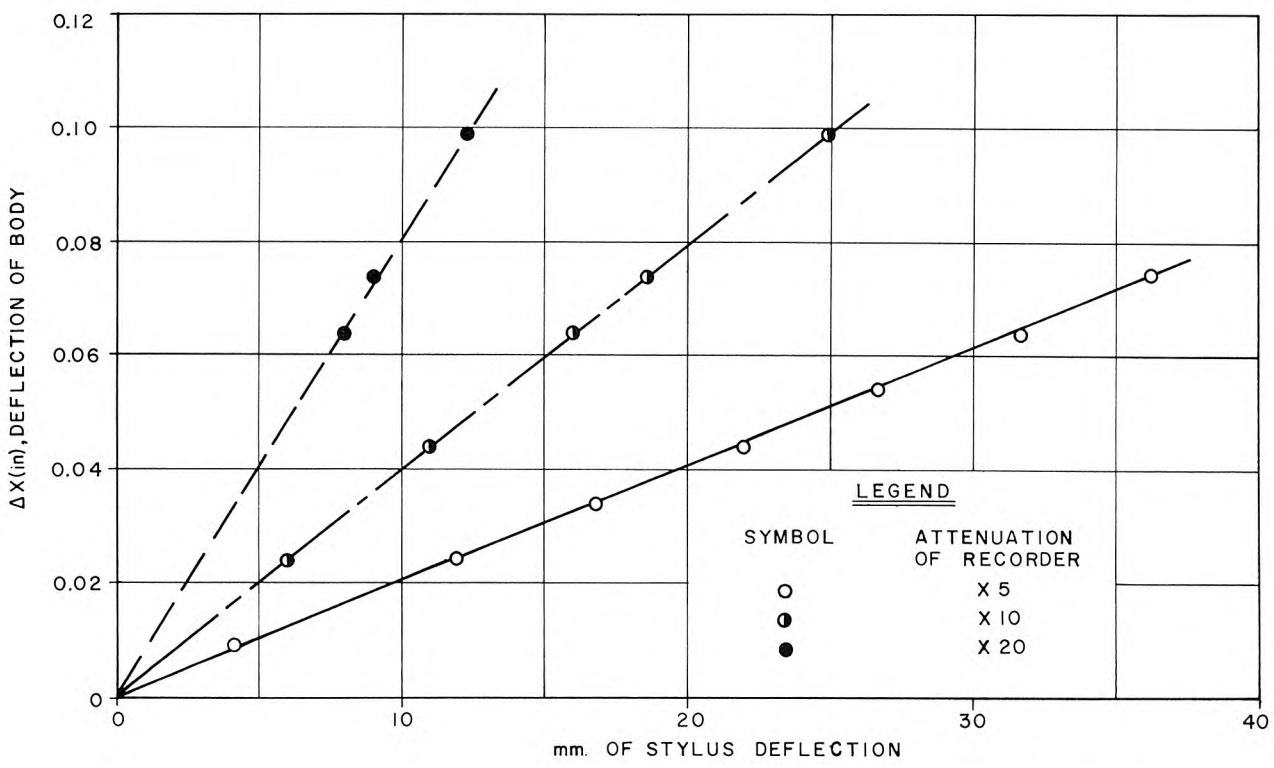

Fig. 19. Typical Calibration Curve for Linear Variable Differential Transformer

deflection. A typical LVDT calibration is presented in Fig. 19 where the deflection of the body in inches is plotted as the ordinate and the stylus deflection in millimeters as the abscissa. This calibration is for three different Sanborn attenuations showing the linearity of the transducer and associated electronics.

Figure 20 is a sample record showing the wave amplitude as a function of time at three locations along the backwall and the motion of the body at the same time. The three locations used are each 1/2 in. from the backwall of the basin with one gage on the centerline of the basin, one 7 1/2 in. in from the East basin falsewall, and one 7 1/2 in. in from the West basin falsewall. (The locations are shown in the upper portion of the figure.) It should be noted that since the wave gage calibrations are different for each gage the wave profiles shown in Fig. 20 for the three locations cannot be directly compared.

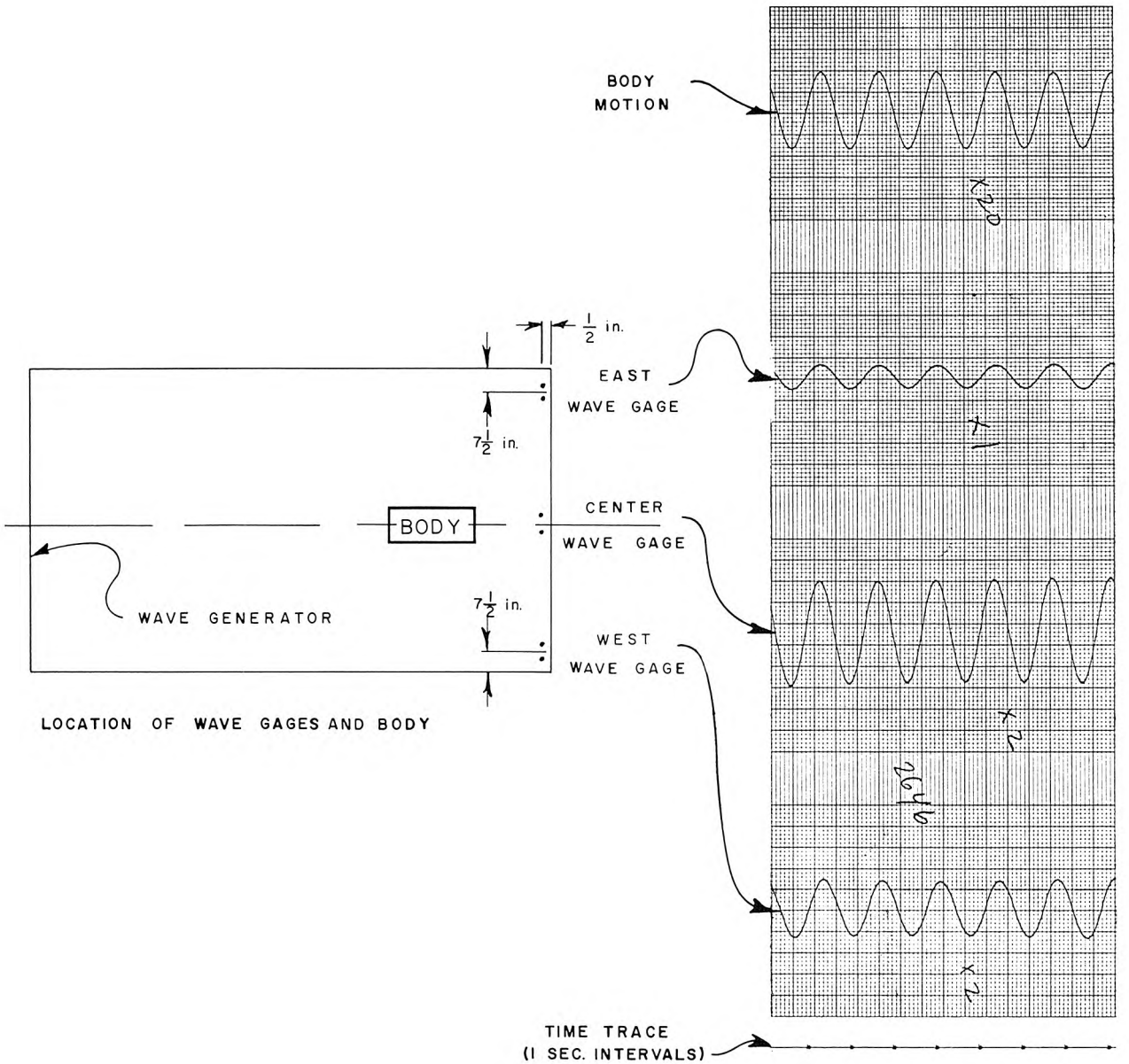

Fig. 20. Wave Gage Locations and Sample Record of Variation of Water Surface and Body Position with Time

4. Presentation and Discussion of Results

This section is devoted to the presentation and discussion of the experimental results obtained in the phase of the study dealing with the surge motions of a single idealized body moored by a linear spring system to a fixed support. Essentially it is divided into two parts, one dealing with the characteristics of the free oscillation of the simple moored body and the other dealing with the forced oscillation of the body by a standing wave system.

4.1 Characteristics of Moored Body in Free Oscillation

To gain a better understanding of the basic nature of the forced motions in surge of a simple body it was considered important to first investigate the free oscillations of the body to evaluate the inertial characteristics of the body motion and the energy dissipation associated with these motions. Eq. 24 reduced to the case of free oscillations becomes:

$$\ddot{x} + \beta_x \dot{x} + \omega^2 x = 0 \tag{39}$$

which has the simple solution:

$$x = X e^{-\frac{\beta_x}{2} t} \sin \left[\sqrt{\omega^2 - \left(\frac{\beta_x}{2}\right)^2}\ t + \varphi \right] \tag{40}$$

It is obvious from Eq. 40 that the investigation of the damped free oscillations of the body would yield information on both the damping coefficient β_x through the decay of the oscillation and the virtual mass coefficient C_M through the natural frequency of the body.

The virtual mass coefficient C_M can be determined by measuring the natural frequency and the spring constant of the body in air and in water and then by calculating the apparent body masses from Eq. 24c. The difference between the two is the added mass. The virtual mass coefficient then follows from the definition used in Eq. 22 where M is the mass of fluid displaced.

The spring constant is evaluated by measuring the static deflection of the body for a known applied force. The results for four experiments with the same spring length and the same body weight in air but different depths of immersion are shown in Fig. 21. It is evident that the spring is linear, but at first glance it is surprising that the spring constant changes as the depth of immersion changes. However, this effect of decreasing apparent spring constant with increasing depth can be ascribed to a "pendulum effect" which arises due to the method of calibration. Referring to the small figure inset in Fig. 21, the force which causes the deflection Δ is not the applied force F alone but some force which is greater or less than F depending upon the depth of immersion. Assuming small deflections (where $\sin\theta \cong \theta = \Delta / \ell$) a spring constant can be derived, C_{act}, which eliminates this effect. Denoting the measured spring constant, i.e., the spring constant obtained from Fig. 21, as C, the actual body weight as W, the weight of the displaced fluid as W_f, and the "pendulum" length as ℓ, one obtains the following expression for C_{act}:

$$C_{act} = C - \frac{W - W_f}{\ell} \tag{41}$$

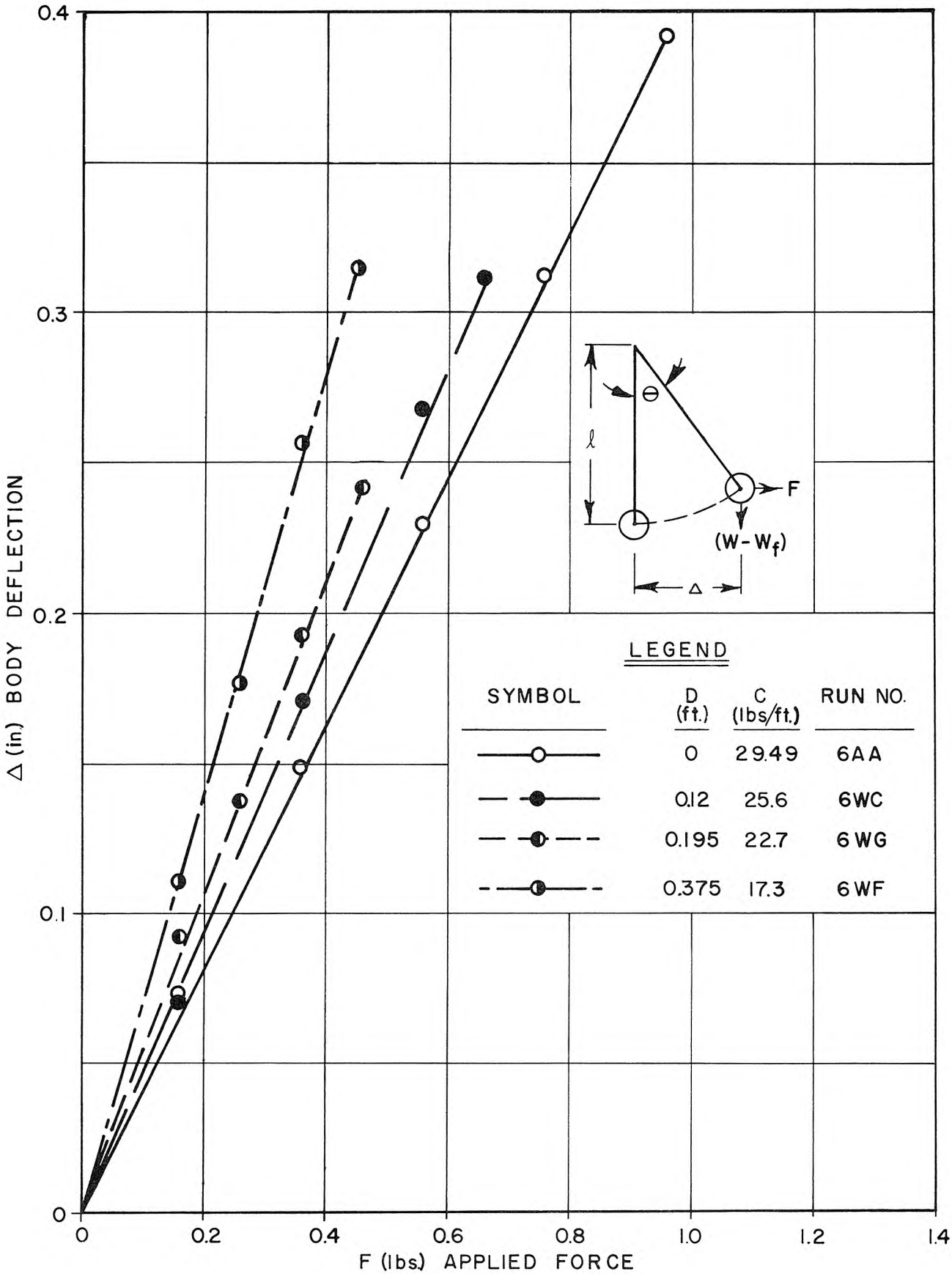

Fig. 21. Variation of Body Displacement with Applied Force

The measured and actual values of the spring constant for three different depths of immersion and in air are given in Table 1. It is seen that after applying this correction the spring constants are within 7%.

Table 1. Comparison of Apparent and Actual Spring Constants for Various Drafts of the Body

Draft D (ft)	C (lb/ft)	C_{act} (lb/ft)
0	29.49	22.1 (Body in air)
0.12	25.6	20.74
0.195	22.7	21.1
0.375	17.3	20.98

For the forced oscillation studies the body was made neutrally buoyant; however, for the majority of the free oscillation experiments only one body weight in air was used for a number of different spring lengths (or natural frequencies) and depths of immersion. The fact that the body may not be neutrally buoyant does not affect the evaluation of the virtual mass coefficient as long as the measured spring constant is used.

The variation of the virtual mass coefficient C_M as a function of the ratio of the draft of the body to the width of the body, D/B, is shown in Fig. 22. The data shown are for a number of experiments having different depths of water, body weights, and natural frequencies. (The interested reader is directed to the Appendix, Table A-1, which presents the physical conditions for the data of Fig. 22.) There appears

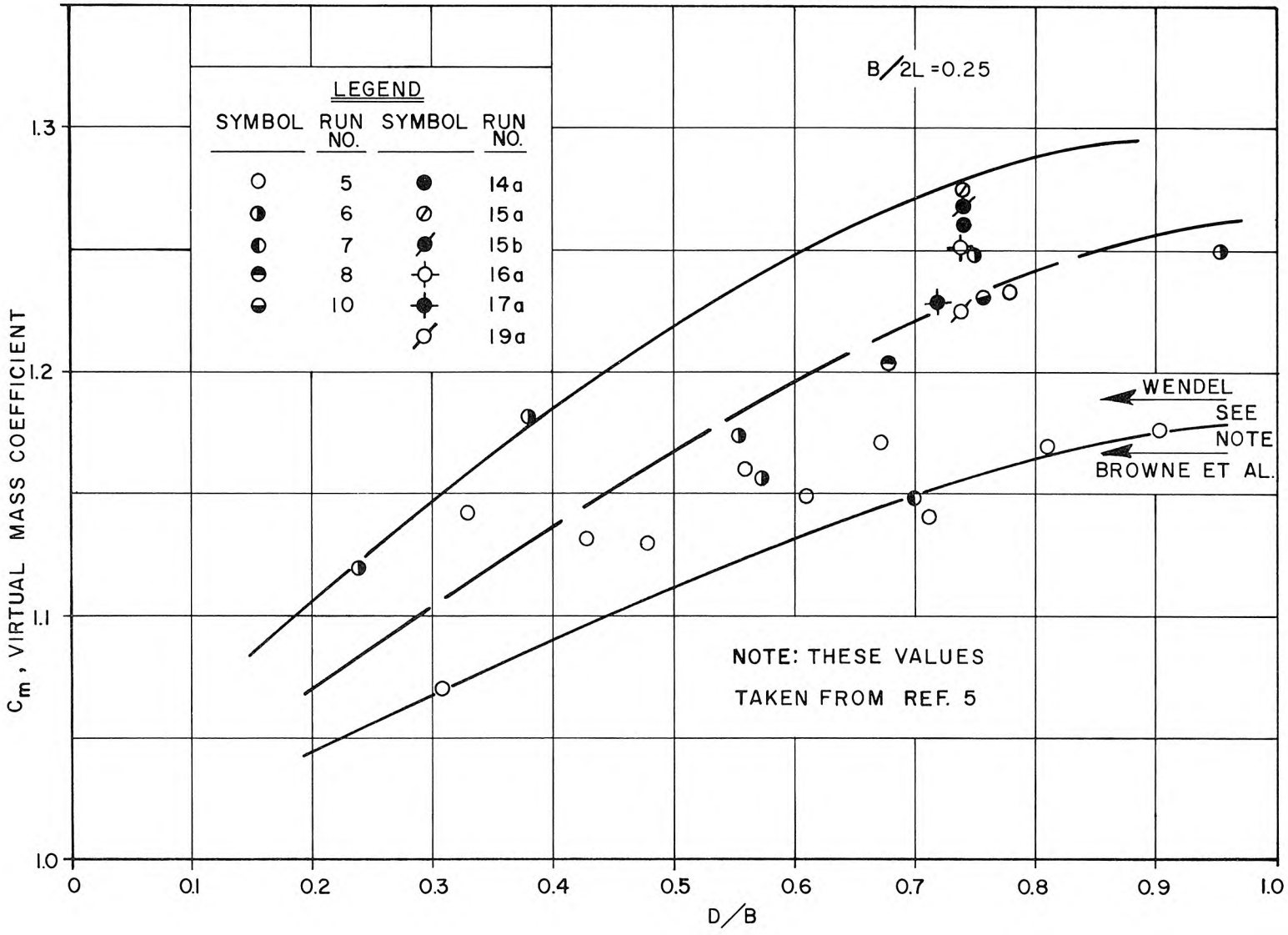

Fig. 22. Variation of Virtual Mass Coefficient, C_M, with Ratio of Draft of Body to Beam of Body, D/B

to be a significant scatter in these data which may be attributable in part to experimental error. If the spring constant and the natural frequency of the body were in error by 2%, this could lead to an error in the analytically determined mass of the body of at most 6%. Assuming the evaluation of the mass in water and in air to be in error the same amount, an error of approximately 10% would occur in the virtual mass coefficient C_M.

Two of the three curves shown in Fig. 22 are upper and lower bounds on the experimental data obtained and the dashed curve is essentially an average curve. The upper and lower curves at most show a deviation of ±5% from the average curve, indicating that the observed scatter could be due to experimental errors involved in determining C and ω. Nevertheless there is a definite trend in the value of C_M with draft showing an increase of approximately 15% as the draft increases from 0.2 of the width to nearly the full body width. This is interesting, since Wilson (5) shows the variation of the virtual mass coefficient only to be a function of the body aspect ratio (B/2L).

Due to the error which is inherent in a method such as this it is difficult to detect other factors which may be important. Some possible factors are waves generated by the body combined with the location of the body with respect to a reflecting surface, the natural frequency of the body, the distance from the bottom of the body to the bottom of the basin, and the depth of water.

The first factor, i.e., the effect of reflected waves on the added mass, does not appear to be serious when one considers the results from Runs 14, 15, and 16. The distance of the center of the body from

the nearest reflecting surface in these three cases was 2 ft, 4 ft, and 6 ft respectively yet at most there is a 2% variation in C_M. However, since a certain amount of energy is imparted to the fluid by wave generation, this would certainly affect the associated hydrodynamic mass of the body.

Others have pointed out the effect of frequency of oscillation on the virtual mass coefficient of a body moving normally to the water surface (see Korvin-Kroukovsky (13), Wendel (14), and Yu and Ursell (19)). There is probably an effect of frequency in these data, since the size of the wake of a body moving in a horizontal plane should be a function of frequency as well as the energy which goes into wave generation; however, the trend is not apparent. This also applies to the clearance and depth which Yu and Ursell (19) found to be important in defining the force on an oscillating cylinder in a free surface.

The values of the virtual mass coefficient obtained by Wilson (5) for a beam-length ratio of 0.25 are shown in Fig. 22 by arrows. These are reported by Wilson as values proposed by Wendel (14) and Browne et al (20) for the upper and lower values respectively. It is seen that these values correspond essentially to average values of the virtual mass coefficients determined in these experiments.

These data emphasize the need for a more thorough experimental study of this aspect of the problem. It would best be handled by studying the forces and the waves generated by the forced oscillations of such a body in a long wave tank having adequate absorbing materials at either end. This coupled with a theoretical study would allow the evaluation of force coefficients similar to those shown in Ref. 19. In other words

in order to accurately evaluate the virtual mass coefficient it should not be inferred, as was done here, from other system parameters, but it should be measured more directly through the evaluation of the forces involved. This type of study would also be of interest in determining in a detailed way the relationship between the time history of force on a body and the virtual mass defined through Eq. 24c.

The dissipative effects, i. e., the damping coefficients, β_x/ω, were determined from the logarithmic decay of the free oscillations of the body as shown in Fig. 23 and Eq. 42.

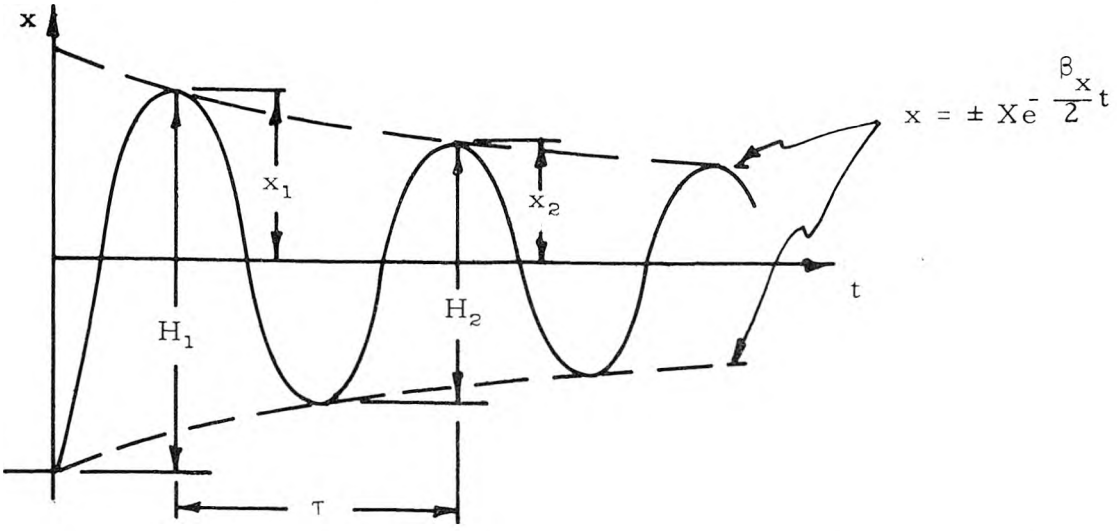

Fig. 23. Schematic Drawing of Damped Free Oscillations of Body

$$\ln\left[\frac{x_1}{x_2}\right] = \frac{\beta_x}{2} \quad \tau = \pi \frac{\beta_x}{\omega} \tag{42}$$

From Eq. 40 it is seen that β_x/ω is in reality a damping coefficient and if large enough the system will be overly damped with no apparent oscillation.

Experimentally the value of the damping coefficient was obtained from the normalized curves of H/H_1 vs t, such as those presented in

Fig. 24 for Run 6. Each point represents the normalized distance between maximum and minimum envelopes to the decay curves. It was established in another graph that the exponential decay of Eq. 40 also applied to the free oscillations in air. Due to the small degree of damping in this case a much longer sample record was taken to determine β_x/ω than for the damped oscillations in water. For this reason and because of the time scale of Fig. 25 only one point is presented here. Since the case of air damping also includes the attendent structural damping in the system, it is evident that the decay of the free oscillations in water is primarily due to viscous and free surface effects.

The values of β_x/ω are obtained from curves such as these after subtracting the value of the damping coefficient, for the free oscillations in air. These data are presented in Fig. 25 as a function of ωD, the product of circular natural frequency and draft. It may be considered better to use a type of Reynolds number as the abscissa, however, it was felt that this would tend to indicate a more general relationship than the data warranted. Since the body was initially displaced approximately the same distance for the data shown, the quantity ωD is essentially a Reynolds number to within a constant of proportionality, defining the Reynolds number as $R = \frac{\omega XD}{\nu}$. The quantity β_x/ω plotted as a function of ωD shows a general increase with increasing ωD.

It is instructive at this point to look closer at the definition of β_x/ω. From Eqs. 19 and 24b the damping coefficient for damped free oscillations can be expressed as:

$$\frac{\beta_x}{\omega} = \frac{C_{D_x}\,\dot{x}}{4C_M L\omega}$$

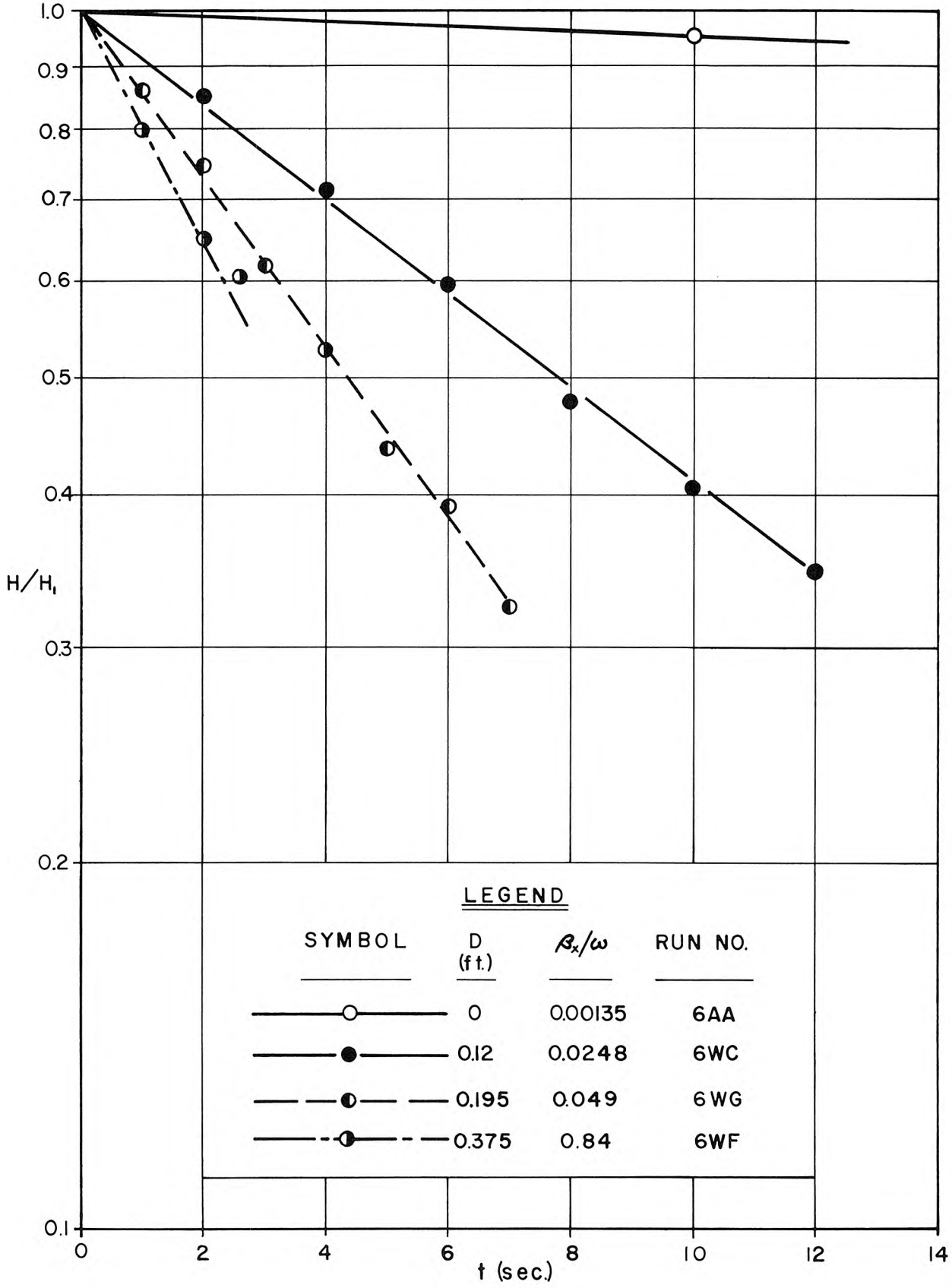

Fig. 24. Damped Free Oscillation of Body

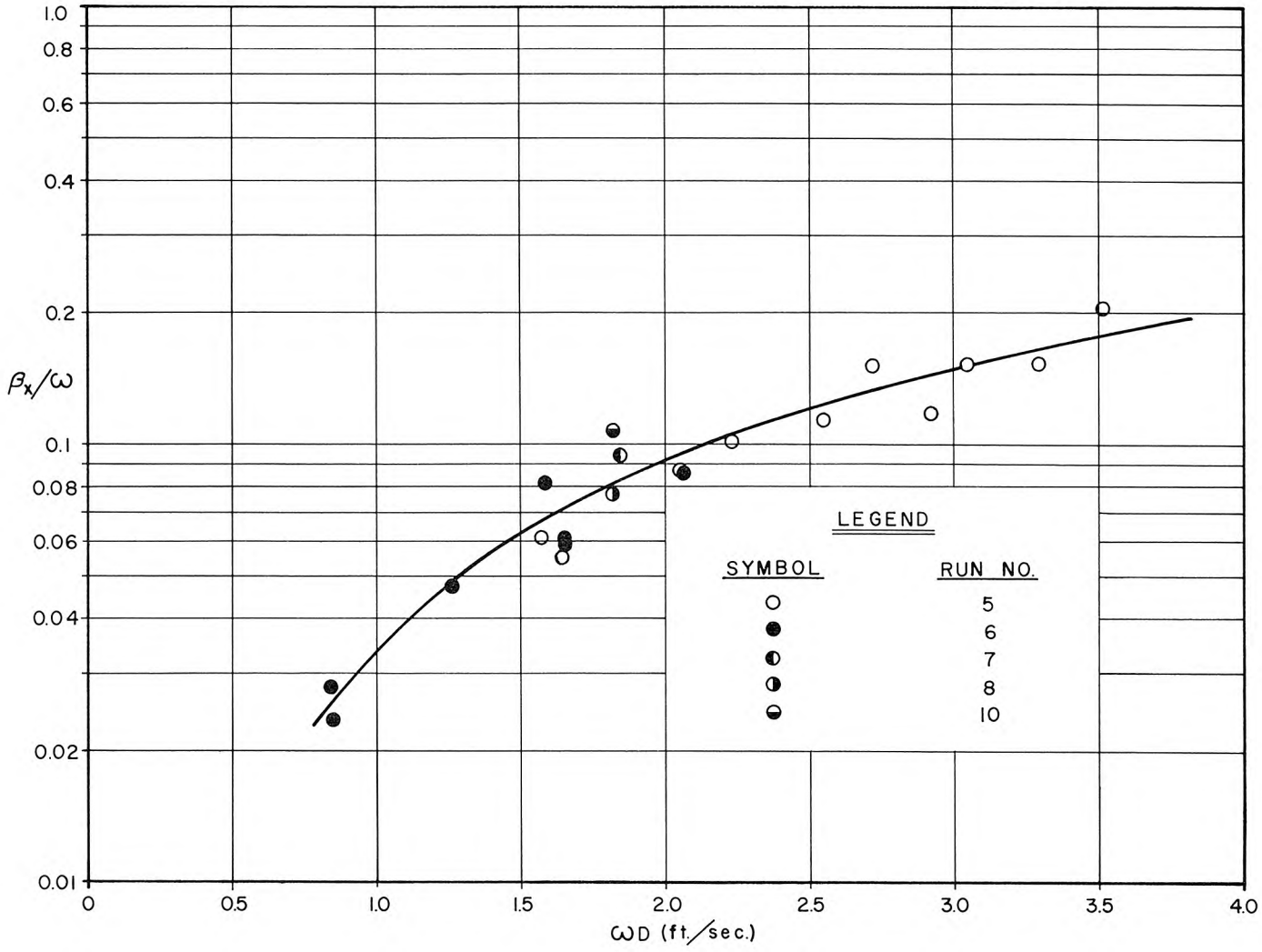

Fig. 25. Variation of Damping Coefficient β_x/ω with Product of Circular Frequency and Draft, ωD

If $\dot{x}$ is expressed as the maximum, ωX, (when $t = 0$ and $\varphi = 0$), then the damping coefficient becomes:

$$\frac{\beta_x}{\omega} \simeq \frac{C_{D_x} X}{4 C_M L}$$

An increase in $\frac{\beta_x}{\omega}$, as shown in Fig. 25, would then imply a corresponding increase in C_{D_x} for essentially the same initial body displacement, X, and virtual mass coefficient, C_M. For a shape such as this body, one would expect only a small variation of the drag coefficient with Reynolds Number. The explanation of the increase in $\frac{\beta_x}{\omega}$ with ωD perhaps lies in the effect of wave generation upon the quantity $\frac{\beta_x}{\omega}$.

From Eq. 40 it is seen that for the case of free oscillations all dissipative effects enter into the determination of the coefficient $\frac{\beta_x}{\omega}$. For a given amplitude of body motion, since the ends of the body act as wave generators, the wave amplitude generated and hence the energy dissipated by the body would increase with increasing frequency of oscillation. It appears that this is an important part of the dissipation associated with the body for this type of oscillation. Since the forced and free oscillations of the body are basically different insofar as wave generation is concerned, one would not expect the evaluation of the damping characteristics from free oscillations to give a realistic picture of the energy dissipation associated with the dynamics of moored bodies in waves. However, it will be shown that, for most of the experiments described herein, energy dissipation is relatively unimportant in describing the forced oscillations of the moored body in the laboratory system.

4.2 Characteristics of Wave Basin

Before discussing the response characteristics of a simply moored body in surge in a standing wave system, some comments should be made about the response of the basin alone. Consider a simple rectangular wave basin with a paddle wave generator, which is hinged at the bottom, at one end of the basin, parallel walls perpendicular to and at the ends of the paddle, and a perfectly reflecting wall parallel to and at a distance "a" from the paddle. It has been shown (see Ippen and Raichlen (17)) that variation of wave height at the reflecting surface with wave length for the inviscid case is approximately given by:

$$H = \frac{2\delta_o \, \lambda/\lambda_o}{\sin k\, a} \tag{43}$$

wherein δ_o is the amplitude of the paddle motion at the water surface and λ_o is the deep water wave length.

Eq. 43 says that one would expect infinite wave heights (resonance) at values of ka equal to integral multiples of π. For the fundamental mode this means that at resonance the wave length is one half the length of the basin. In other words when the paddle is passing through the zero motion point (the plane of the paddle is vertical) either a maximum or a minimum wave amplitude occurs at both the paddle and the end wall located a distance "a" from the paddle. Since in this position the paddle has attained the maximum velocity, this means that maximum kinetic energy is being added to the wave system when it possesses only potential energy. This addition of energy if not affected by viscous dissipation would cause infinite amplitudes in the basin.

The wave filter located in front of the wave generator and mentioned in Section 3.1 provides additional dissipation in the system and allows the wave period to be changed quickly compared to a system with low dissipation. The response of the basin with a wave filter is shown in Fig. 26 for wave periods slightly greater and slightly less than the 10th harmonic (T = 1.22 sec.). The wave heights presented were measured in a corner of the basin near the reflecting end. From a curve such as this it is possible to approximately determine the transmission coefficient of the wave filter (see Ippen, et al (21)) using the expression:

$$K_T^2 = \frac{H_R - H_A}{H_R + H_A} \tag{44}$$

where K_T is the ratio of the amplitude of the wave transmitted through the filter to that incident upon the filter, H_R is the wave height measured at the backwall at resonance, and H_A is the wave height measured at the backwall midway between resonant periods. Using Eq. 44 a transmission coefficient of approximately 78% is obtained. Ippen and Goda (22) show that the transmission coefficient of wave filters must be less than approximately 50% in order to adequately describe an open sea system. Therefore, the wave filter used in this study only provides sufficient dissipation so that it does not take a prohibitive amount of time for the wave system in the basin to come to a steady state after the wave period has been changed. The resonant periods of this basin for a 1 ft depth and a frictionless system are shown in Table 2. Since the wave period varies approximately as the square root of the wave length, as the wave period decreases the percentage difference between resonant periods decreases.

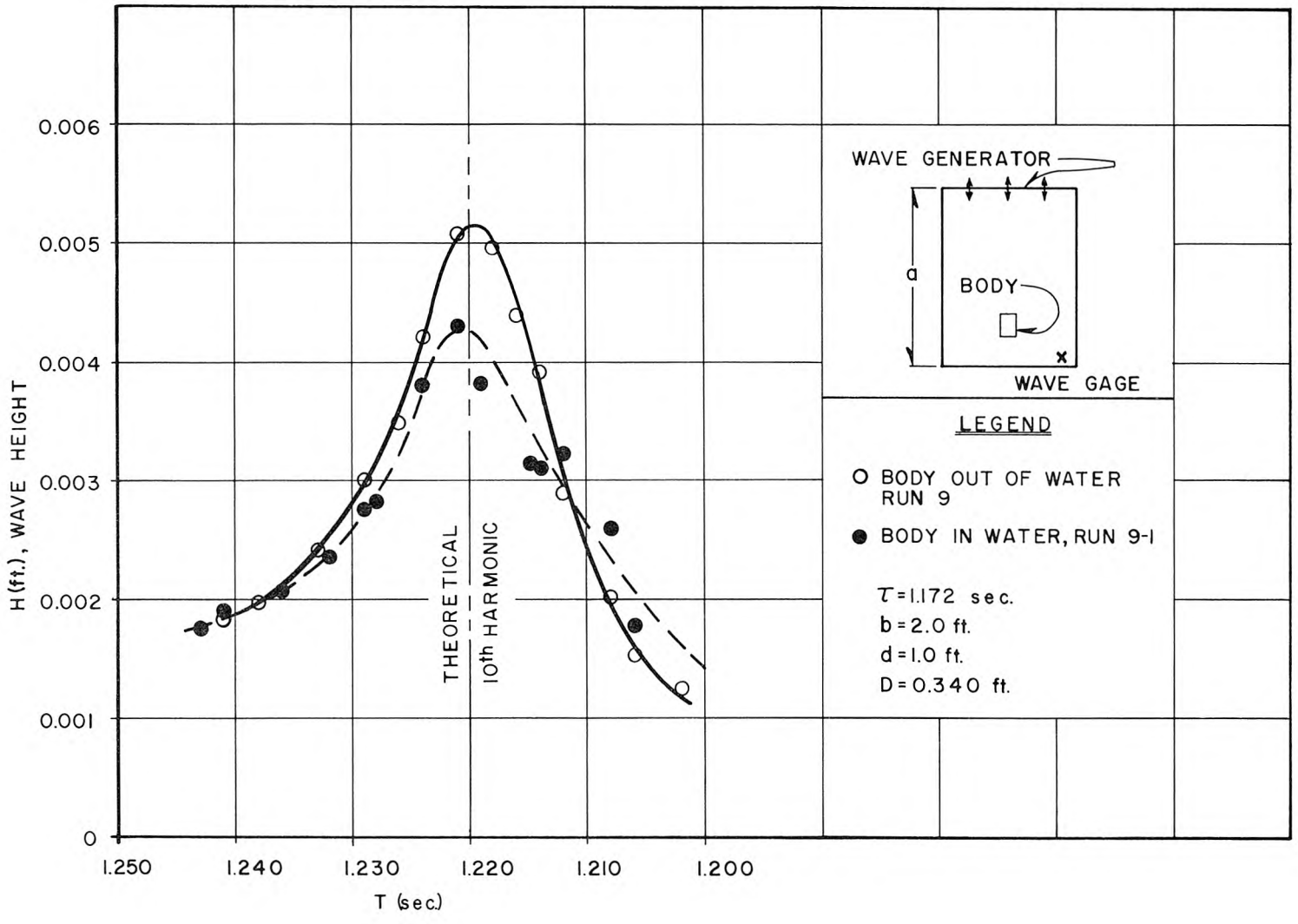

Fig. 26. Wave Basin Response with and without Body

Table 2. Resonant Periods for Closed Basin System

Harmonic	Wave Period (Sec.)
1	10.7
2	5.32
3	3.58
4	2.73
5	2.21
6	1.87
7	1.64
8	1.41
9	1.32
10	1.22
11	1.14
12	1.07
13	1.01
14	.97
15	.92
16	.89

Fig. 26 also shows the wave heights that were obtained with the moored rectangular body in the water and located with its centerline approximately 2 ft from the reflecting surface. The wave heights were measured in the same location as for the case without the body. This

shows some reduction in wave height near resonance due to the moored body, but away from resonance the wave height is essentially the same with the body in place as without the body. Therefore, one has some degree of confidence that away from resonance, measurements of the wave height with the body in the water at this location are equivalent to the wave heights with the body out of the water.

The two-dimensional nature of the wave system in the basin is shown in Figs. 27a and 27b. The ordinate of the figures is the wave height measured at three locations along the backwall of the basin, one at each corner of the basin (7 1/2 in. in from the sidewalls which are 12 ft apart), and one on the basin centerline at the backwall (all measured with the body in place). These locations are denoted in the figure as East, West, and Center. The ratio of the natural period of the moored body (τ = 1.305 sec) to the standing wave period is plotted as the abscissa. It is plotted this way so that this figure can be used in the discussion of the response curves. In Fig. 27a the wave generator was operated as a piston, and as a paddle in Fig. 27b moving at a somewhat smaller stroke. In both cases the centerline of the moored body was located 4 ft from the backwall. For the present discussion the wave heights measured on the basin centerline, directly behind the body, will be disregarded with attention given only to the data referring to the wave heights at the corners of the basin. The waves generated by the piston motion are generally higher for essentially the same stroke compared to the case of the generator moving as a paddle. For the data of Fig. 27a the difference between the wave heights at the two corners of the basin is less than 10%. The paddle generated waves, whose heights are presented in Fig. 27b, show more

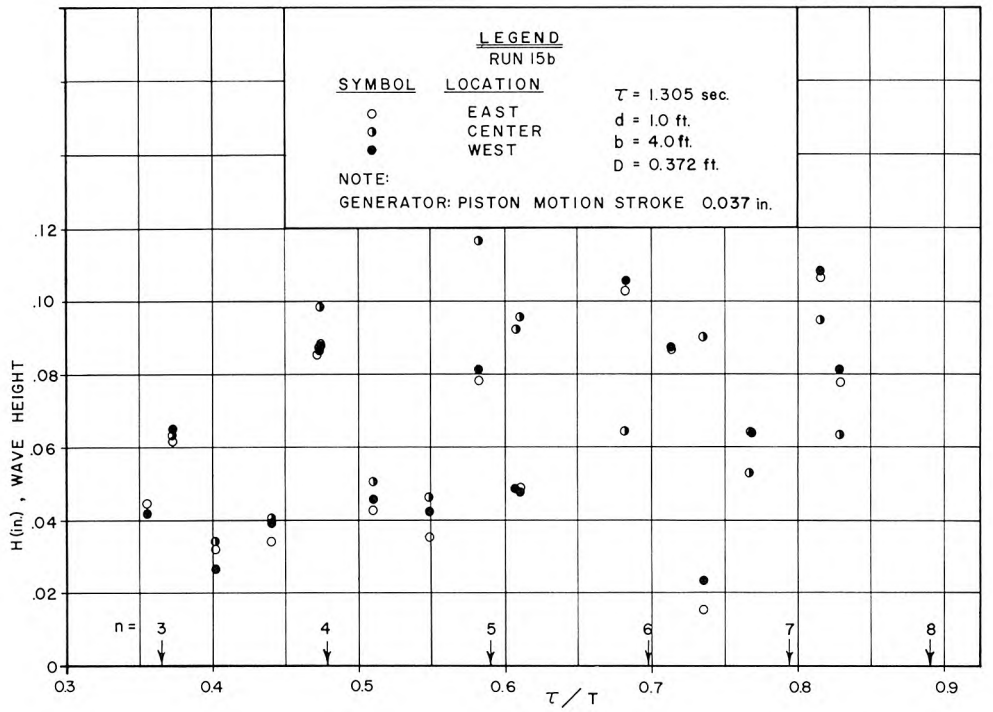

Fig. 27a. Wave Height Measured at Three Locations along Basin Backwall as a Function of Relative Period, ($.3 < \tau/T < .9$), Body in Place

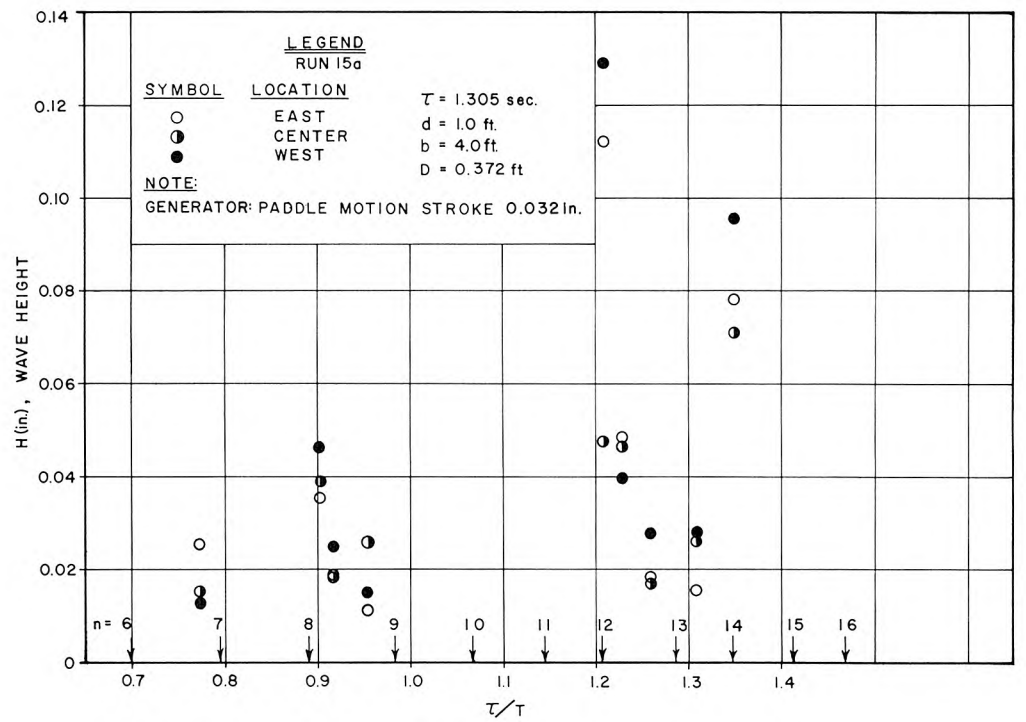

Fig. 27b. Wave Height Measured at Three Locations along Basin Backwall as a Function of Relative Period, ($.7 < \tau/T < 1.4$), Body in Place

scatter although the difference between the corners, except for very low wave heights, is approximately the same. The various basin harmonics are indicated along the abscissa by the arrows and the number of the harmonic written above. These values correspond fairly well to the maxima of the data presented.

4.3 Characteristics of Moored Body in Forced Oscillation

4.3.1 Linearity of System

Before discussing the general response characteristics of a simply moored body, it is of interest to investigate the linearity of the experimental system. This was accomplished by varying the stroke of the wave generator, and its mode of operation (piston or paddle motion) for the same wave periods and measuring the corresponding wave heights and body motions. If the system is linear, the response function $\frac{X}{A}$ should be independent of the stroke of the wave machine. The results of these experiments are shown in Fig. 28 where in the lower portion of the figure the wave amplitude and resulting body motions are plotted against the normalized wave period, $\frac{\tau}{T}$, and in the upper half of the figure the corresponding response function $\frac{X}{A}$ is presented.

The stroke of the wave generator was varied from 0.0207 to 0.0735 in. for the case where the generator was operating as a piston, and from 0.0435 in. to 0.064 in. when it was operating as a paddle. Hence, there was at most a three-fold variation in stroke. Therefore, there would be corresponding variations in the height of the generated wave for the same wave period. The wave heights denoted as 2A were measured in the two corners of the basin and on the basin centerline, the exact locations have been described previously. These locations are denoted in Fig. 28 as

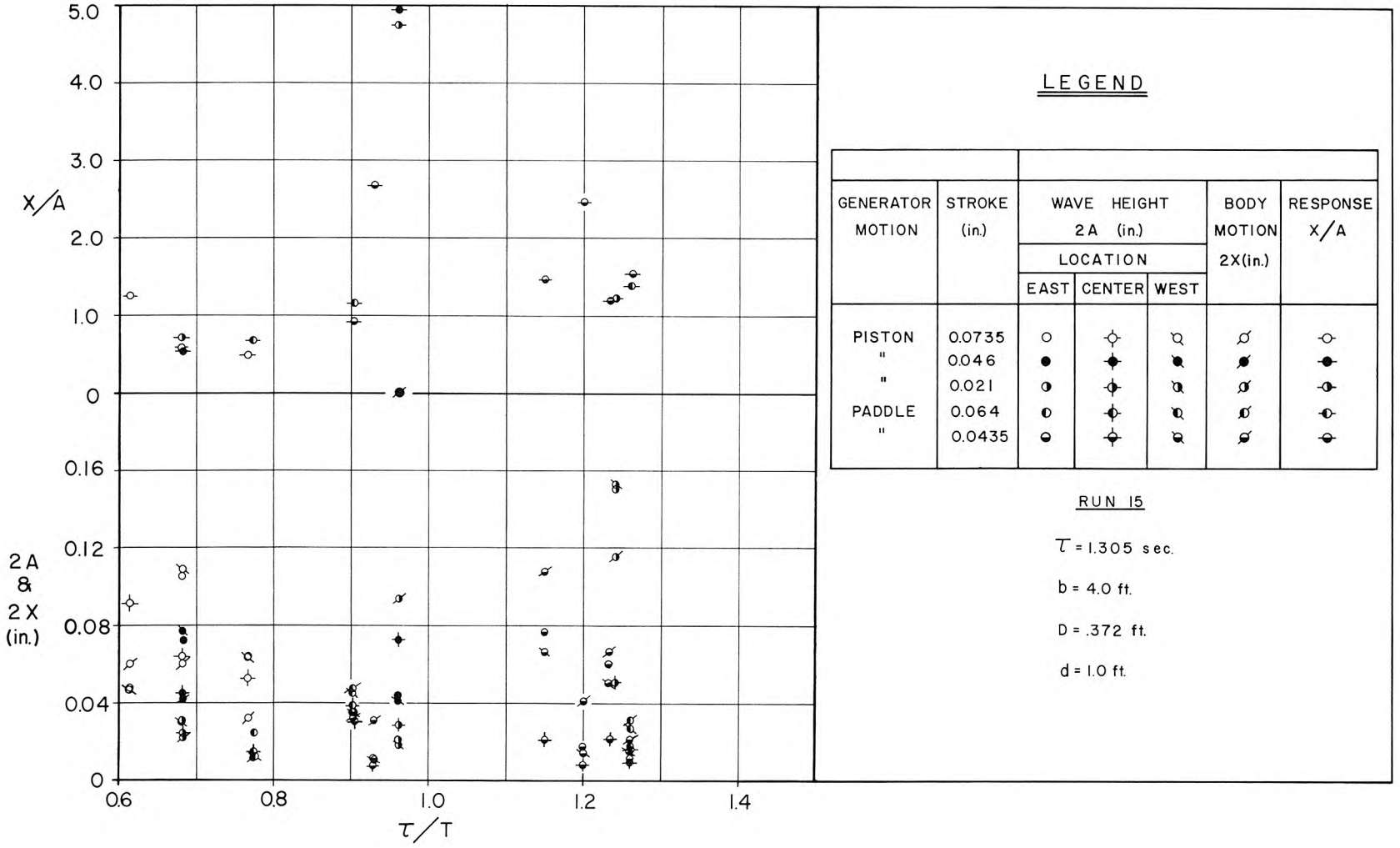

Fig. 28. The Effect of Wave Generator Stroke on Wave Height, Body Displacement, and Response Function

East, West, and Center. The maximum excursions of the body, 2X, are shown in the lower half of the figure. The centerline of the body was located 4 ft from the basin backwall for all data shown.

It is seen from this figure that the response characteristics of the body are reasonably independent of the height of the standing wave. (The normalizing wave height used in the experimental definition of the response function is the average of the wave heights measured in the two corners of the basin furthest from the wave machine. (The reason for this is discussed in Section 4.3.3.) For instance, at a value of $\frac{\tau}{T} = 0.96$ two waves were generated; one with an average height of 0.02 in. and one with an average height of 0.043 in. The corresponding amplification factors $\frac{X}{A}$ shown are 4.75 and 4.95. The discrepancies here and at other wave periods are probably due more to the difficulty of accurately measuring very small wave heights and body motions rather than to non-linearities of the system. From Fig. 28 it is felt that the general statement can be made that the moored body responds in a linear fashion to incident standing waves.

4.3.2 General Characteristics of Wave System

One of the objectives of this study was to investigate the forced oscillations of a simply moored body for a wave system ranging from deep-water waves to shallow-water waves. To accomplish this two natural periods (frequencies) of the body were chosen. For one case the natural period of the body was adjusted so that it corresponded to the average period of waves that were in the intermediate range between deep and shallow-water waves for the depth of water used. In the second case the natural period of the body was adjusted to be in the deep-water wave period region for this depth.

The range of periods used in the program is shown in Fig. 29 where the ratio of the wave length to the deep water wave length for that wave period is plotted as a function of the ratio of the natural period of the body to the wave period. This figure shows that for the body with the larger natural period the major portion of the testing program was over a range of wave lengths that was greater than 40% of the corresponding deep water wave length; whereas for the smaller natural period of the body the wave length over the major range of testing was greater than 75% of the corresponding deep-water wave length.

More general wave characteristics are shown in Figs. 30a and 30b for body natural periods of 1.305 sec and 0.664 sec respectively. In each of these figures the wave length, wave number, ratio of depth to wave length, and ratio of body length to wave length are plotted as functions of the ratio of the natural period of the body to the wave period. It is interesting to observe from these curves the ratio of the body length to the wave length near resonance ($\frac{\tau}{T} = 1$). For the case of the body with the larger natural period ($\tau = 1.305$ sec.) the wave length is approximately three times the body length near resonance, whereas for the body having a natural period of 0.664 sec. this ratio is approximately unity.

4.3.3 Response of Moored Body

Three response curves were obtained for each of the two natural periods of the body. Each set of curves is for a particular distance of the body from the backwall of the basin.

Figs. 31, 32, and 33 show theoretical response curves and corresponding experimental data for distances of 1.95 ft, 4.0 ft, and 6.0 ft respectively from the backwall of the basin to the center of the body for

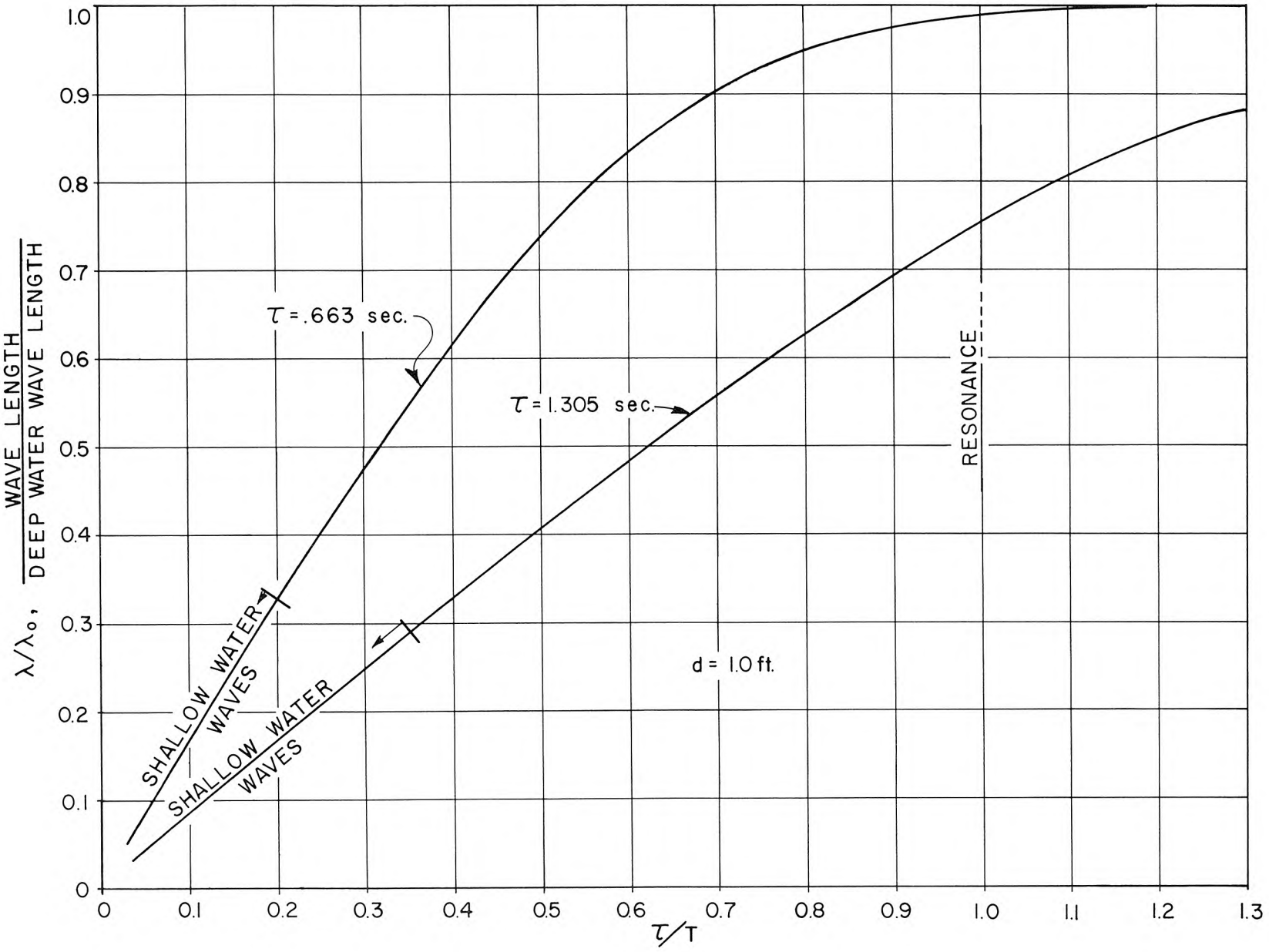

Fig. 29. Variation of Ratio of Wave Length to Deep-Water Wave Length, λ / λ_o, with Relative Period τ / T

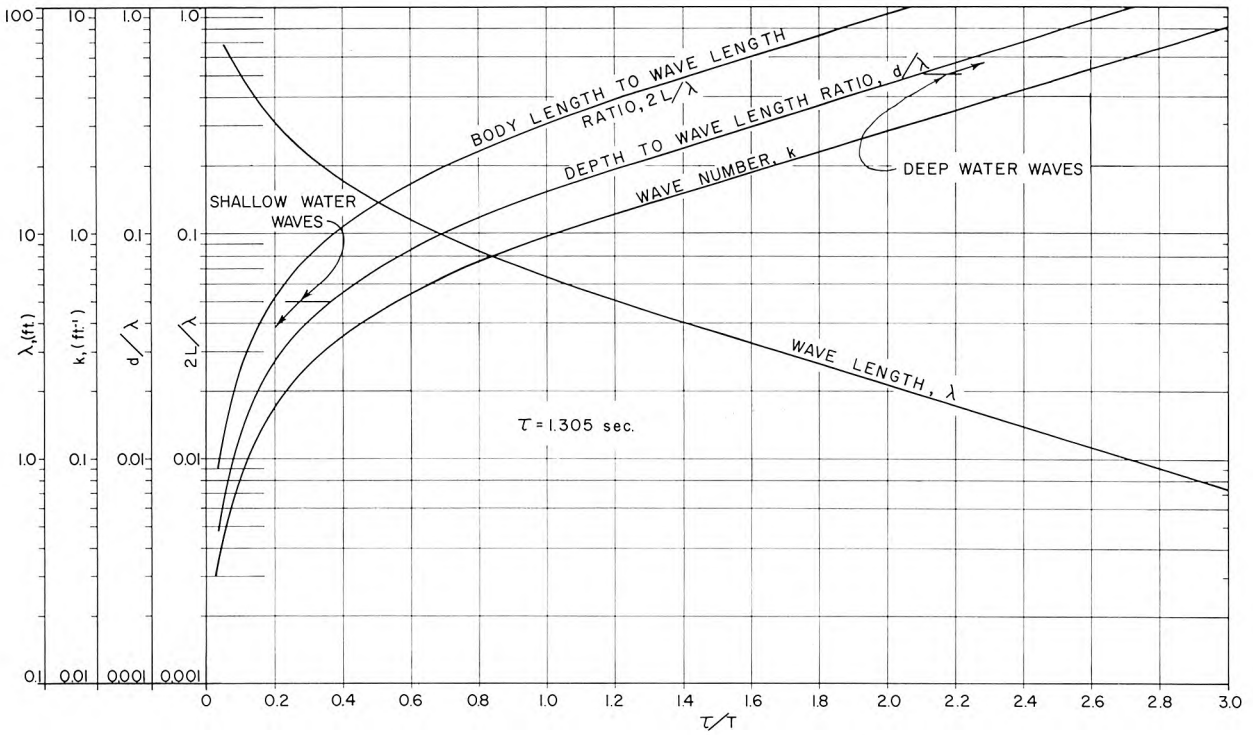

Fig. 30a. General Characteristics of Wave System (τ = 1.305 sec.)

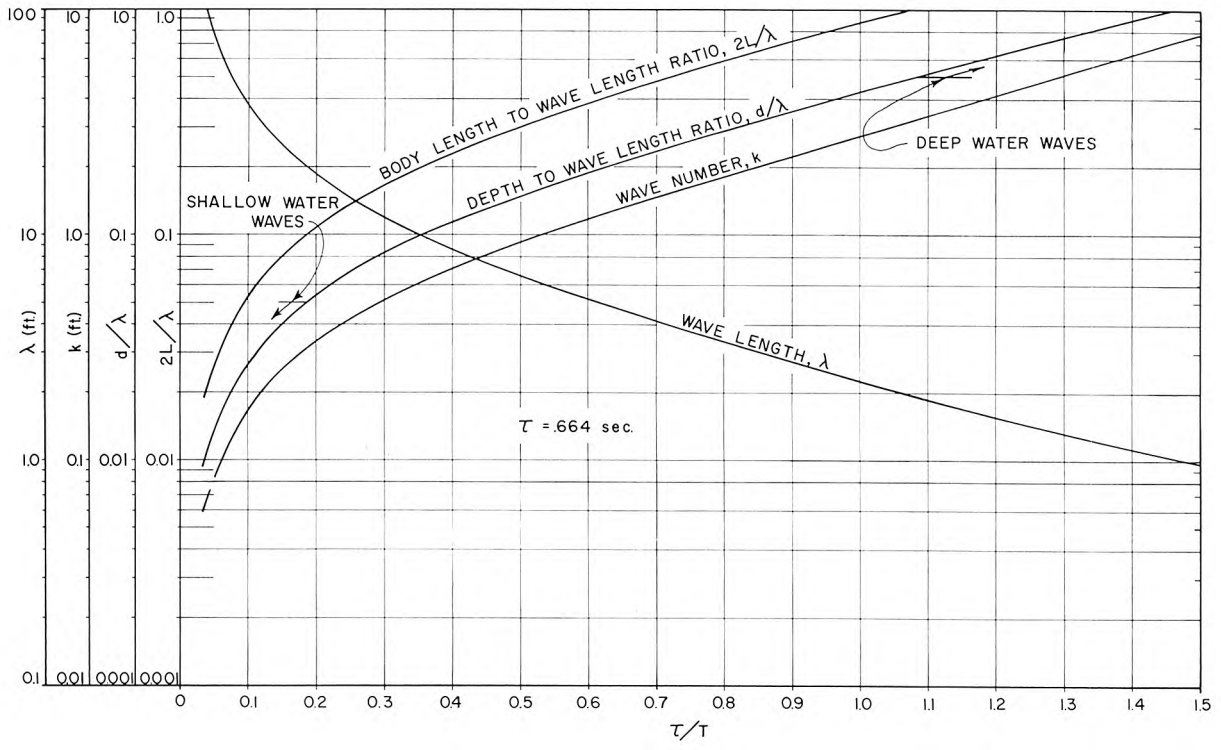

Fig. 30b. General Characteristics of Wave System (τ = 0.664 sec.)

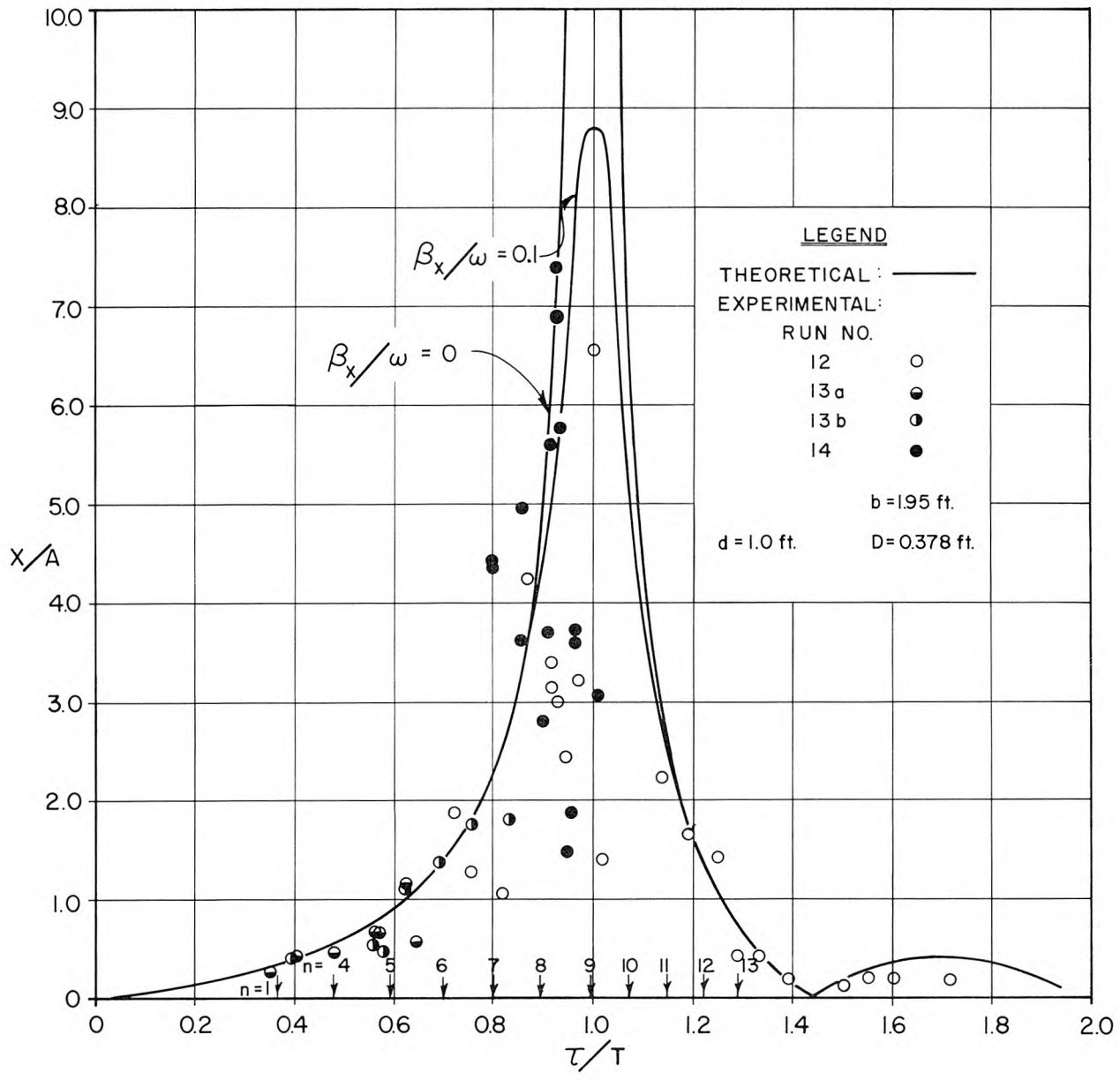

Fig. 31. Response Curve of Single Moored Body
(τ = 1.305 sec., b = 1.95 ft)

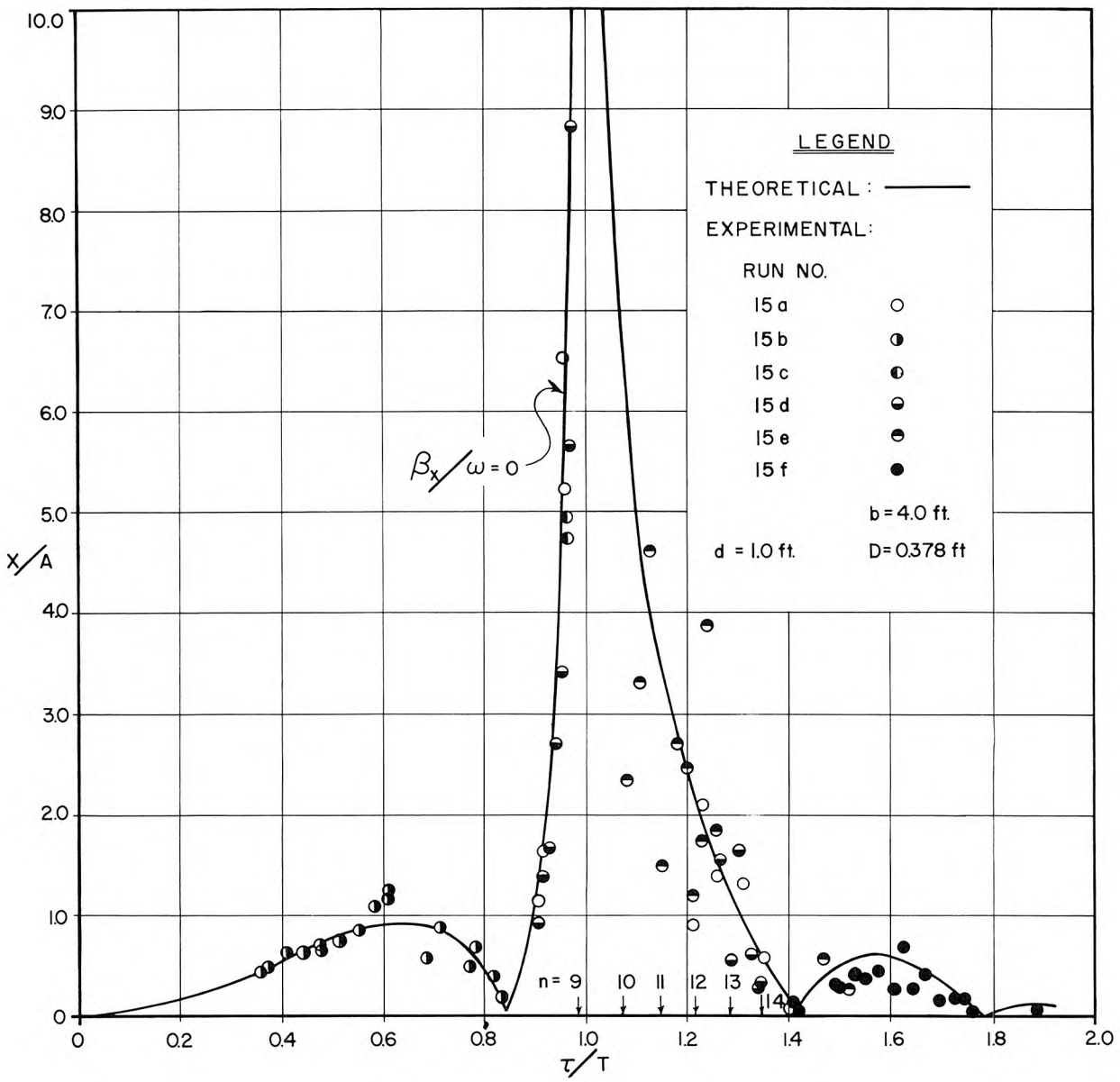

Fig. 32. Response Curve of Single Moored Body
(τ = 1.305 sec., b = 4.0 ft)

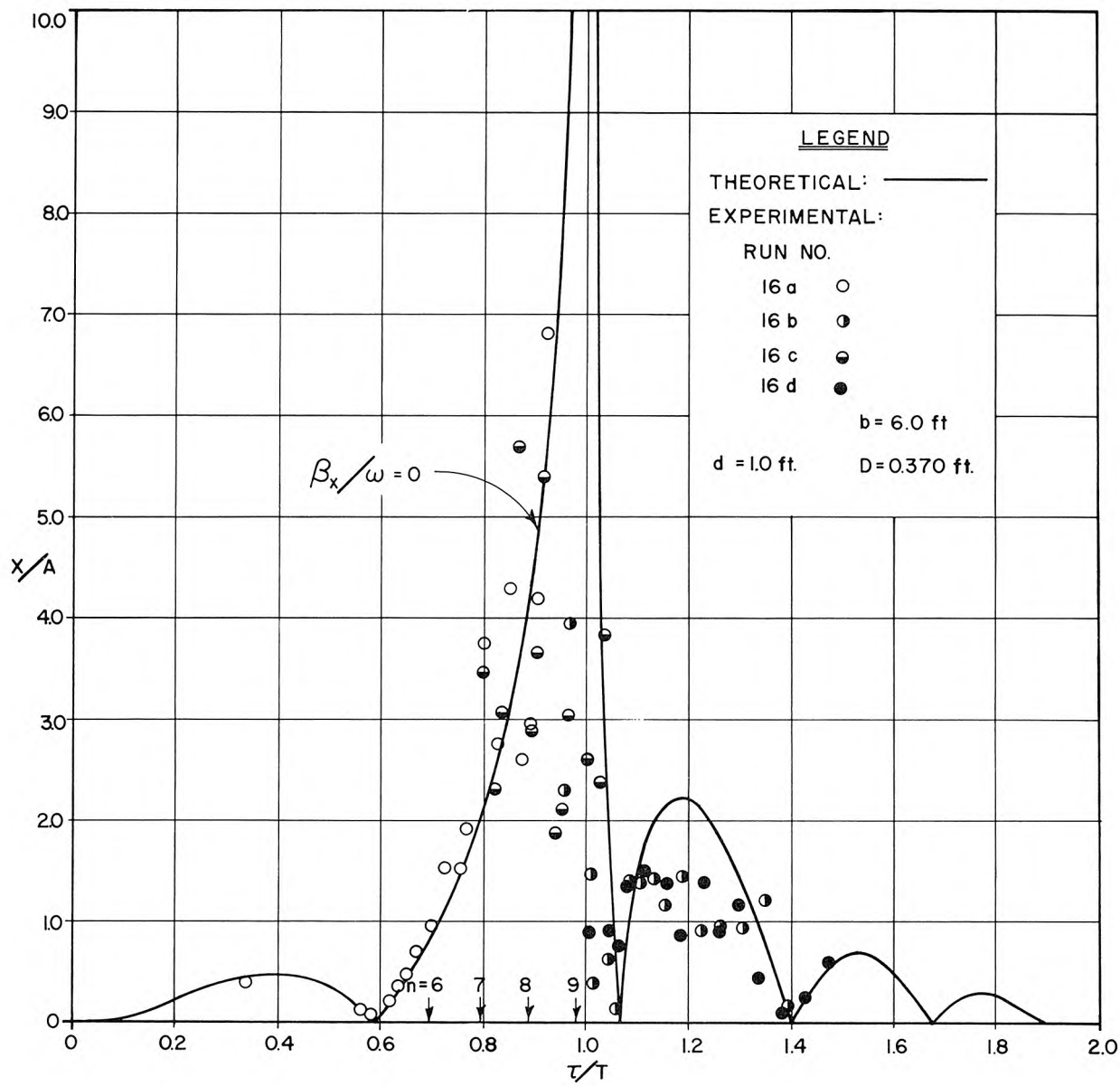

Fig. 33. Response Curve of Single Moored Body
(τ = 1.305 sec., b = 6.0 ft)

a natural period of the body of 1.305 sec. The weight of the body was adjusted so that for the depth of immersion chosen ($D \tilde{=} 0.375$ ft) the body was neutrally buoyant.

The results of four different experiments are shown in Fig. 31. The wave amplitudes used in normalizing the ordinates were obtained from the average of measurements taken near the two corners of the basin furthest from the wave machine (approximately 7 1/2 in. from the basin sidewalls and 1/2 in. from the backwall). Information on the stroke and configuration of the wave generator are presented in Table 3 for Runs 12 through 16 which are for the case of the body with the largest natural period ($T = 1.305$ sec.). Again it can be seen from the relatively good agreement among data with different wave generator settings but approximately the same wave period that, as shown in Fig. 29, the moored system responds linearly to the applied force. Considering the reproducibility of the data shown in Fig. 31 for values of τ/T less than unity the apparent scatter cannot be completely attributed to experimental error. It is interesting that the theoretical response curve for zero damping agrees well with the experimental data for small values of τ/T (less than 0.8) and for values of τ/T greater than unity. In fact it could be said that away from the neighborhood of resonance the average of the experimental data shown agrees fairly well with the theoretical curve for no damping.

The disagreement between theory and experiment over one range of wave periods and fairly good agreement over a different range of wave periods can probably be attributed to the waves which are generated by the oscillating body. The presence of a wave system caused by the

Table 3. Wave Generator Configuration and Stroke (τ = 1.305 sec.)

Run	Configuration	Total Stroke (in.)
12	Paddle	.064
13a	Piston	.134
13b	Piston	.060
14	Paddle	.0635
15a	Paddle	.064
15b	Piston	.074
15d	Paddle	.0435
15e	Paddle	.0435
15f	Paddle	.0435
16a	Paddle	.043
16b	Paddle	.043
16c	Paddle	.0672
16d	Paddle	.0672

motions of the body is apparent when the wave heights measured directly behind the body (near the backwall) are compared to the wave heights measured in the two corners of the basin. Unfortunately, for the data shown in Fig. 31, the centerline wave height was not measured; however, from Figs. 27 and 28 (corresponding to the response curve shown in Fig. 32) it can be postulated that there would also be a similar difference between the three wave heights for this case. If this assumption is correct, then it follows that any wave generated by the body will in turn

modify the net pressure force on the body thereby altering its motion and causing disagreement with a theoretical approach which neglects the wave-making ability of the body. To be consistent with the theory presented in Section 2.1, the wave height used to normalize the response function was always the average of the standing wave heights in the corners of the basin. Therefore, it seems reasonable to assume that where there is an apparent scatter of the data wave generation by the body is important (for $\tau/T < 1$ in Fig. 31); the converse being true for $\tau/T > 1$. This wave-generation effect will be discussed in more detail with reference to Fig. 32.

The values of the normalized period (τ/T) for the various modes of oscillation of the wave basin are indicated along the abscissa of Fig. 31 by arrows with the numbers above corresponding to the number of the harmonic. It is interesting to note that the maxima of the experimental data for values of $\tau/T < 1$ correspond relatively well to the harmonics of the basin. This indicates that when the body is acting as a wave generator the amplitude of the body motion and hence the wave generated is very much affected by the incident wave amplitude, i.e., the response characteristics of the wave basin.

A theoretical curve is included in Fig. 31 for the case with damping, $\beta_x/\omega = 0.1$. It is seen for this case that the effect of damping on the response curve is small except in the immediate vicinity of resonance where, due to finite amplitude effects, the applicability of this small amplitude theory would itself be in question. The value of the damping factor, β_x/ω, obtained for this configuration from the free oscillation of the moored body was 0.11. The question can rightly be asked: should the damping

factor for the free oscillation described by Eq. 40 be the same as that included in the solution for the forced oscillation, Eq. 27. The answer to this would, in all probability, have to be no. Since Fig. 25 indicates that the wave making contribution to energy dissipation in free oscillation may be quite large compared to viscous dissipation, one would not expect the wave making dissipation to be the same in both cases. However, it can be said with reference to the experimental data and the undamped theoretical response curve shown in Fig. 31 that in this case dissipative effects are small.

The effect upon the theoretical response curve of varying the natural frequency of the body was also investigated. If one assumes that the virtual mass (displaced mass + hydrodynamic added mass) could be in error by ±10% this would introduce an error of ±5% in the natural frequency. It was found that if this variation of the natural frequency was introduced into the expression describing the theoretical inviscid curve of Fig. 31, the variation from the curve shown was small; less than 3% away from the immediate vicinity of resonance.

Undamped response curves and corresponding experimental data are presented in Figs. 32 and 33 for a natural period of the body of 1.305 sec. and for two different locations of the body in the wave basin. In Fig. 32 the center of the body was located 4 ft from the backwall and in Fig. 33 this distance was increased to 6 ft. In both cases it is interesting to see that again there are distinct regions of τ/T where agreement between the small-amplitude theory and the experimental results is relatively good, and also regions where there is a significant scatter of experimental data about the theoretical curves. Typical wave amplitudes and body motions

that were used in defining the response function presented in Fig. 32 were presented in Fig. 28. From Fig. 28 it can be seen, in general, that where the scatter of the data in Fig. 32 is the greatest, there is a significant difference between the wave amplitudes measured in the two corners of the basin and that measured directly behind the body at the basin backwall. The converse is true in regions of τ/T where there is small scatter, e.g. $0.84 < \frac{\tau}{T} < 1.0$. Therefore, the wave-making characteristics of the body appear to be quite important in defining the response characteristics of a moored body.

It is interesting to view Figs. 31, 32 and 33 in an overall sense to see the effect of location of a moored body in a standing wave system. As mentioned previously, the wave function defined by Eq. 26c imposes a certain number of zero responses on the body characteristics which are a function of the range of wave periods under consideration. For a given range, as the distance of the body from the backwall increases, the number of zeroes increases. This in effect forces the response curve near resonance to become more peaked, or in other words, for the body response to become more selective in a periodwise sense.

This can be explained physically with the aid of Fig. 34. This descriptive figure shows the body located at two different distances from a reflecting surface in eight different standing wave systems with periods decreasing from T_1 to T_8. At the bottom of the figure qualitative response curves are shown for the corresponding body positions. These were drawn after letting the shortest period shown, T_8, correspond to the natural frequency of the body. If one assumes that the major force acting on the body is the net pressure force, then as the wave length decreases

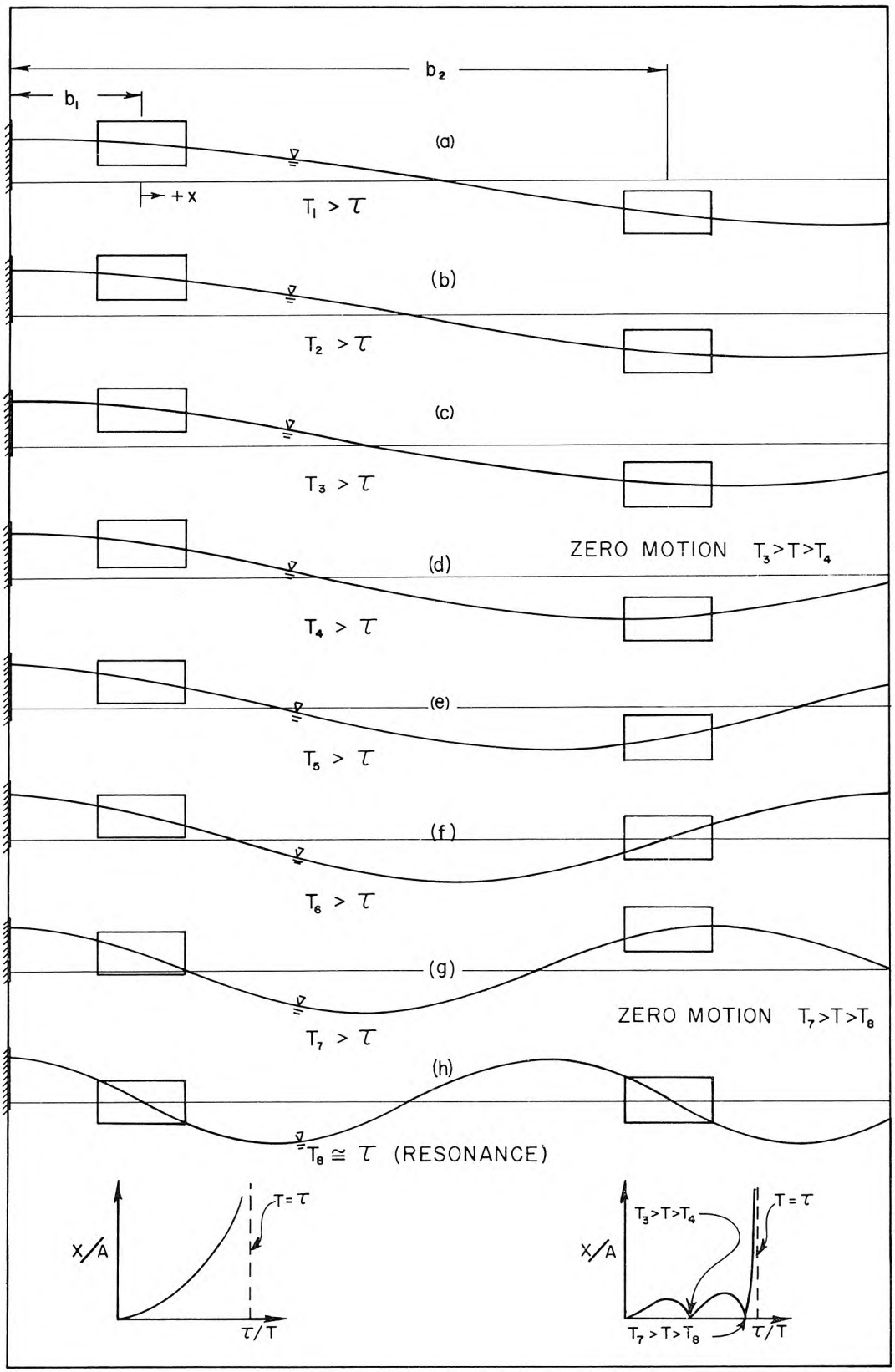

Fig. 34. Effect of Body Position and Wave Period on the Response Curve of a Body with a Given Natural Period

from T_1, for the body closest to the wall (distance b_1), the force continually increases. For a linear system the body motion will increase correspondingly. However, if the body is moved further from the wall to a distance b_2, it is seen that there will be two wave lengths in this group where an antinode of the standing wave coincides with the center of the body, i.e., between T_3 and T_4 and between T_7 and T_8. Since these are the wave lengths for zero net force, the body motion will be zero at these two wave periods. Hence, between wave periods T_3 and T_8 the body force goes from zero to a maximum and back to zero again with corresponding body motions as shown in the schematic response curve at the bottom of this portion of the figure. Therefore, it can be seen that a particular maximum amplitude of body motion can even be eliminated in this simple case by the proper location of the body in the standing wave system.

Theoretical and experimental response curves were also obtained for essentially the same conditions as those shown in Figs. 31, 32 and 33 except that the natural period of the body was reduced by nearly a factor of two to $\tau = 0.664$ sec. by increasing the spring constant. These results are presented in Figs. 35, 36, and 37 for distances from the center of the body to the reflecting surface of 2 ft, 4 ft, and 6 ft respectively. For all of the experiments which yielded the data presented in these figures the wave machine was set as a paddle with a total stroke of 0.067 in.

As before it can be seen that the number of zeroes of the response curve increase as the distance from a reflecting surface increases. This in turn causes the response curves to become more selective near

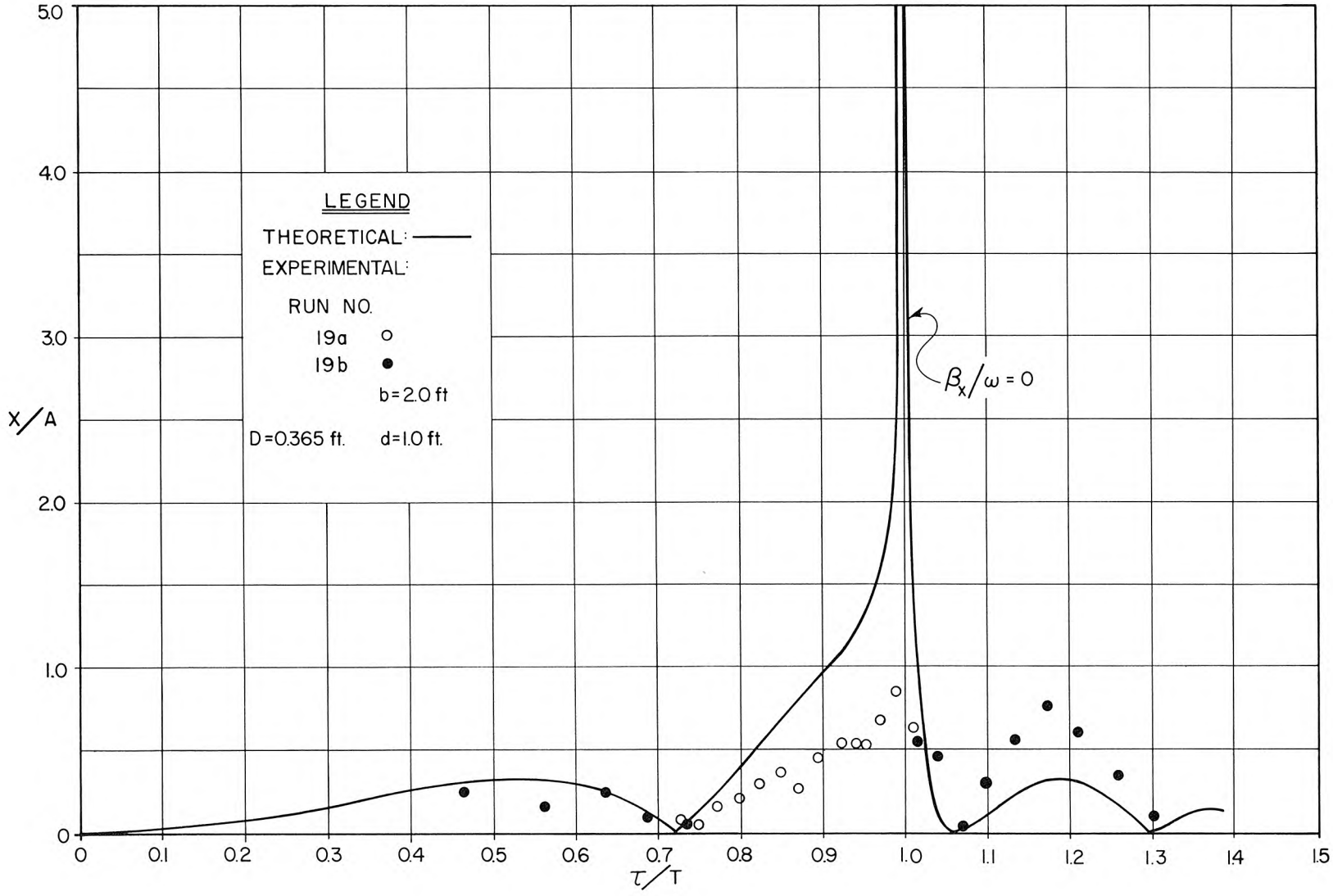

Fig. 35. Response Curve of Single Moored Body
(τ = 0.664 sec., b = 2.0 ft)

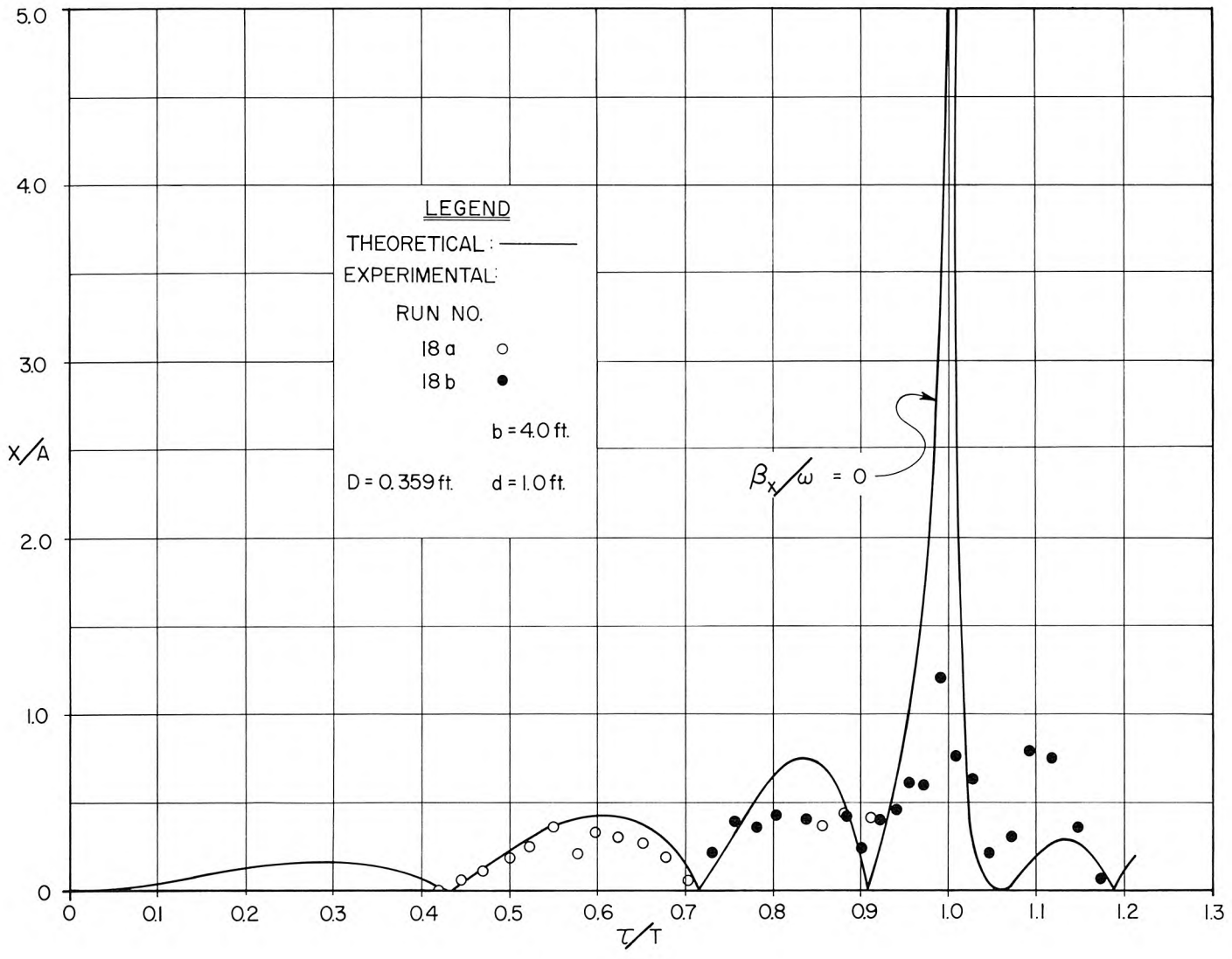

Fig. 36. Response Curve of Single Moored Body
(τ = 0.664 sec., b = 4.0 ft)

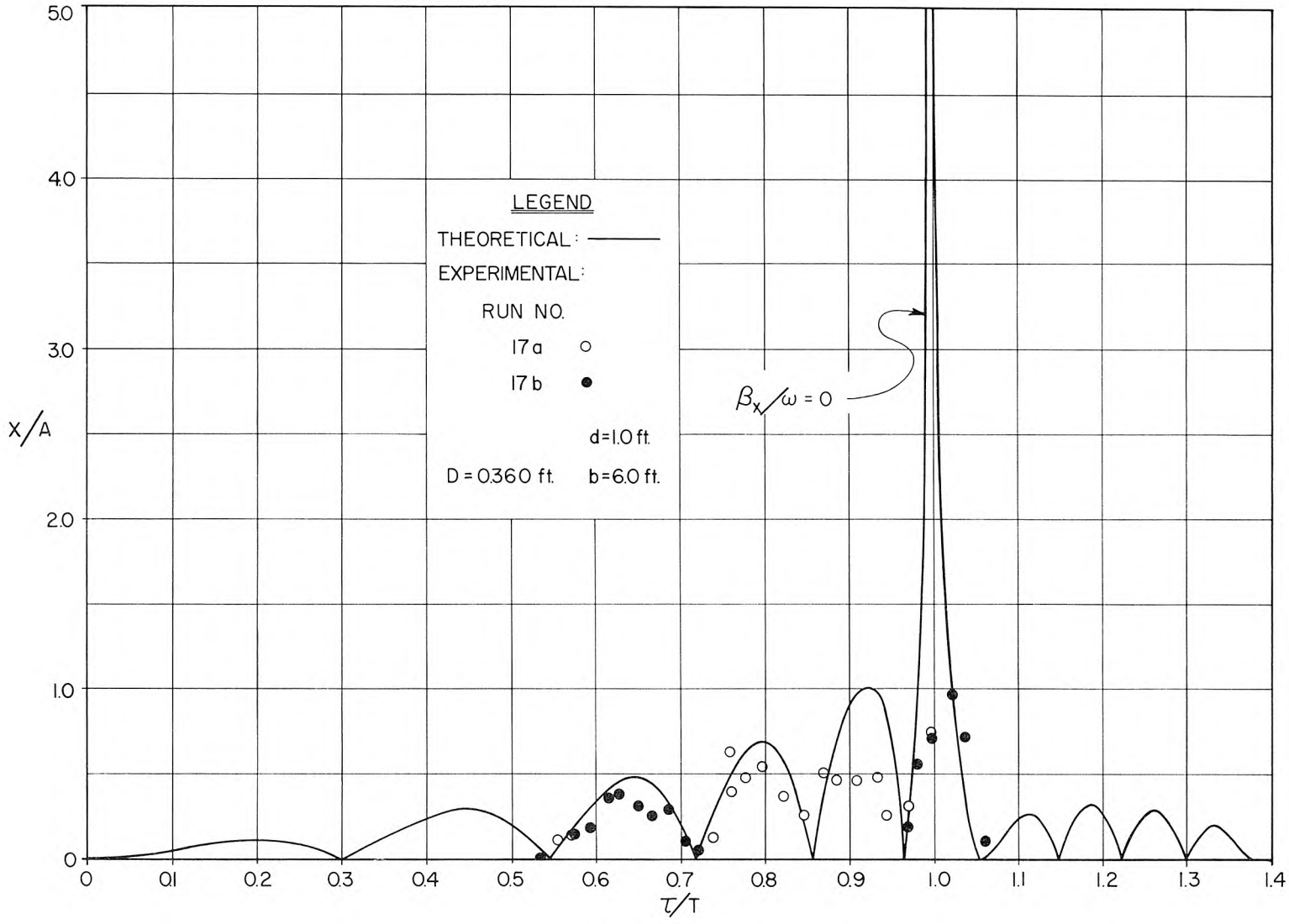

Fig. 37. Response Curve of Single Moored Body
(τ = 0.664 sec., b = 6.0 ft)

resonance as this distance increases. For instance, for a response X/A equal to unity and for the case where the center of the body is located 2 ft from the backwall, the bandwidth of the major peak ranges from $\tau/T = .91$ to $\tau/T = 1.015$ or a width of $\Delta(\tau/T) = 0.11$. When the distance increases to 6 ft the limits of the peak at a unit response are $\tau/T = 0.98$ to $\tau/T = 1.02$ or a width of $\Delta(\tau/T) = 0.04$. Since the major effect of damping is to reduce the body response at resonance it is possible that, due to the combined effects of energy dissipation and the narrowing of the response curve near resonance, an attenuated response always occurs, i.e., the response function X/A is always less than unity. In other words, due to a high body natural frequency, the response of the body in surge may be unimportant as far as gross movements are concerned.

The scatter of the data in Figs. 35, 36 and 37 is less than for the corresponding data obtained with moored body having a larger natural period ($\tau = 1.305$ sec.). This may be attributed to the smaller effect of wave generation in the case of the body with the smaller natural period. Since the natural period of the body was decreased by increasing the spring constant of the system, the restoring force was correspondingly increased and the body motions were reduced compared to the system with a larger natural period. Thus for the same period of oscillation the wave amplitude generated by the body would be smaller. This is supported to some extent by the fact that there is not as large a variation among the wave amplitudes measured at the three locations in the basin (the two corners and directly behind the body) for this case as there is for the body with the larger natural period and correspondingly larger body motions. This is not to say that energy dissipation is less

important here, actually it is the contrary. However, the effect of the basin responses on the body appears to be less. It is apparent from Figs. 35, 36 and 37 that resonance is not a significant problem for this moored system. In all three cases shown the body motion is attenuated compared to the wave amplitude instead of being amplified.

It is of interest to note the range of the ratio of body length to wave length represented by the two sets of response curves i.e Figs. 31, 32, and 33 for τ = 1.304 sec. and Figs. 35, 36 and 37 for τ = 0.664 sec. For the moored body having a natural period of τ = 1.305 sec. the ratio of body length to wave length varied from 0.1 to 0.8. This ratio varied from 0.25 to 1.5 for the moored body with the smaller natural period (τ = .664 sec.). Even for the latter case where the wave length is comparable to the body length, agreement with the small amplitude theory is fairly good. Therefore, it can be stated that the theory developed by Wilson applies reasonably well even when the wave length becomes small compared to the length of the body. Also, in addition to this, the theoretical approach is applicable over the full range of wave length to depth ratios, i.e., from shallow water waves through the intermediate region to deep water waves.

5. Conclusions and Recommendations

The conclusions which are drawn from this first phase of the investigation are divided into two parts; the first pertaining specifically to the laboratory study, and the second relating some of these conclusions to the small-craft mooring problem in marinas.

5.1 Conclusions Related to the Laboratory Investigation

1. In general it can be stated that the theory proposed by Wilson (5) and Kilner (7) adequately describes the surge motion of a body linearly moored in a standing wave system by elastic lines. The laboratory investigation reported herein was a more realistic representation of the physical system than that used by Kilner (7) and accordingly revealed certain features not reported previously.

2. The coefficient of virtual mass of the body (rectangular parallelpiped of aspect ratio 4:1) determined from simple free oscillations was found to correlate best with the ratio of draft to beam (D/B). For a variation of D/B from 0.25 to 0.95 the coefficient of virtual mass (C_M) varied from approximately 1.1 to 1.25. Due to the scatter of the experimental data, it is felt that this method of evaluation of the added mass is not completely satisfactory.

3. The damping coefficient, β_x/ω, obtained from the decay of the free oscillations of the body showed a definite tendency to increase with increasing ωD (the product of circular natural frequency of the moored body and draft). This is contrary to what one would expect for an oscillating body

in an infinite fluid, and indicates the effect of the energy that goes into waves generated by the body on the general dissipative qualities of the body. It should be realized that the dissipation associated with free oscillations is different from that associated with the wave induced oscillations of a body.

4. The body moored by a linear spring to a fixed support responds in a linear fashion even for relatively large body motions.

5. The experimental data obtained on the response characteristics of the body are in reasonably good agreement with the theory proposed by Wilson (5). The ratio of wave length to depth covered by this investigation varied from approximately the shallow water wave limit to the deep water wave limit. The ratio of body length to wave length varied from a value of 0.1 to 1.5.

6. It was found that a variation in the virtual mass coefficient, C_M, of ±10% which introduces a ±5% variation in the natural frequency of the body introduced a negligible variation in the theoretical response curve.

7. Agreement between the experimental data and the theoretical response curves is better for certain ranges of the ratio of the natural period of the body to the wave period, τ/T, than it is for others. This is attributed to the effect of wave generation by the body on its motion; the wave generation being more important at values of τ/T in the region of the maximum deviation of the experimental data from the theoretical curves.

8. The energy dissipation associated with the forced oscillation of the moored body is quite different for the two systems which were investigated. The body with the larger natural period exhibited very little energy dissipation, whereas the opposite is true for the body with the smaller natural period.

9. The response curves become more selective with respect to frequency as the distance of the body from a reflecting surface increases. It is possible to reduce the effect of resonance considerably, simply by choosing the proper body location for a particular natural frequency.

5.2 Conclusions and Recommendations Related to the Prototype System

1. The basin response is obviously of importance in determining the maximum amplitude of motion in surge of a moored body.

2. The location of a moored boat in a marina is important considering the effect of body location on the response curve. It may be feasible, for a given incident wave period, to locate boats of various sizes in different areas of the marina depending upon the natural frequency of the boat-mooring system. The preferred location would also be influenced by the response characteristics of the basin and the expected three-dimensional amplitude distribution within the basin.

3. Considering the effect of energy dissipation upon the response curve and the increase in selectivity of the response curve with increase in distance from a reflecting surface it appears that the further a body is from a reflecting surface the smaller the probability that there will be a significant response near resonance. It is possible that with a high natural frequency of the body coupled with the energy dissipation of the system the body response expressed as X/A could always be less than unity.

4. This initial study emphasizes the need for prototype information on small-craft motions, natural frequencies of a sizeable range of boat sizes, and damping information on these vessels.

ACKNOWLEDGEMENTS

The author would like to express his deep appreciation to Professor Vito A. Vanoni for his assistance and valuable criticism throughout the course of this investigation.

The construction and the maintenance of the wave basin and associated instrumentation was carried out by Elton Daly, Laboratory and Shop Supervisor and Robert Greenway, Laboratory Mechanic. A good deal of the system design can be attributed to the ingenuity of Elton Daly. The assistance of Carl Eastvedt, Senior Photographer and Robert W. Wilson, Laboratory Specialist, is appreciated. The drawings presented in this report were done by James Murray, Laboratory Technician. The writer wishes to thank Patricia Rankin for her assistance in typing and assembling this report.

Some of the initial experimental work on the virtual mass coefficient and the damping coefficient was done by Loh-Nien Fan, Research Assistant.

This project is supported by the U. S. Army Corps of Engineers under Contract DA-22-079-CIVENG-64-11.

APPENDIX A

Table A-1. System Characteristics for Determination of Damping Ciefficients and Virtual Mass Coefficients

Run No.	d (ft)	D (ft)	ω (rad/sec)	β_x (sec^{-1})	C (lb/ft)	W (lbs)	C_M	
5AA	---	---	11.28	.0362	61.2	15.54	---	Air
5WA	.538	.1645	10.0	.587	52.8	17.0	1.142	
5WB	.538	.2390	9.32	.978	47.0	17.48	1.130	
5WC	.538	.3560	8.55	1.34	42.3	18.65	1.140	
5WD	.538	.452	7.78	1.63	39.0	20.5	1.176	
5WE	.538	.4055	8.12	1.266	40.5	19.8	1.169	
5WF	.538	.8055	8.88	1.38	45.0	18.32	1.149	
5WG	.538	.1545	10.15	.661	51.6	16.2	1.07	
5WH	.538	.2140	9.56	.874	49.3	17.3	1.132	
5WI	.538	.2815	9.05	1.070	46.9	18.45	1.166	
5WJ	.538	.3355	8.71	1.162	45.0	19.10	1.171	
6AA	---	---	7.94	.0107	29.5	15.1	---	Air
6WA	1.102	.1175	7.15	.211	24.6	15.5	1.055	
6WB	1.102	.2775	5.95	.364	20.1	18.8	1.174	
6AB	---	---	7.94	.0102	30.0	15.3	---	Air
6WC	.966	.1200	7.14	.177	25.6	16.2	1.119	
6WD	.966	.2865	5.77	.366	18.7	18.1	1.157	
6WF	.966	.375	5.14	.432	17.3	21.1	1.248	
6WG	.966	.195	6.47	.316	22.7	17.5	1.182	
7	1.023	.35	5.32	.498	16.1	18.75	1.196	
8	1.016	.34	5.36	.413	17.7	19.85	1.205	
10	1.00	.378	4.82	.528	20.8	28.9	1.23	
14	1.00	.372	4.84	---	21.35	29.4	1.262	
15a	1.001	.372	4.82	---	21.4	29.7	1.275	
15b	1.002	.372	4.82	---	21.3	29.55	1.268	
16a	1.001	.370	4.85	---	21.3	29.15	1.252	
17a	1.00	.360	9.475	---	80.	28.7	1.228	
19a	1.003	.365	9.40	---	80.4	28.7	1.225	

REFERENCES

1. Lee, Charles E., "Small-Craft Harbor Problems", Journal of the Waterways and Harbors Division, ASCE, Aug. 1964.
2. Dunham, J. W., "Design Considerations for California Marinas", Trans. ASCE, Vol. 127, Part IV, 1962, pg. 131-162.
3. Wilson, B. W., "Ship Response to Range Action in Harbor Basins", Transactions ASCE, Vol. 116, 1951, pg. 1129-1157.
4. Abramson, H. N. and Wilson, B. W., "A Further Analysis of the Longitudinal Response of Moored Vessels to Sea Oscillations", Proceedings of the Joint Midwestern Conference on Solid and Fluid Mechanics, Purdue University, Indiana, Sept. 1955.
5. Wilson, B. W., "The Energy Problem in the Mooring of Ships Exposed to Waves", Proceedings of Princeton Conference on Berthing and Cargo Handling in Exposed Locations, Princeton University, New Jersey, Oct. 1958.
6. Wilson, B. W., "Case of the Critical Surging of a Moored Ship", Transactions ASCE, Vol. 126, Part IV, 1961.
7. Kilner, F. A., "Model Tests on the Motion of Moored Ships Placed in Long Waves", Proceedings of the Seventh Conference on Coastal Engineering, The Hague, 1960.
8. Russell, R. C. H., "A Study of the Movement of Moored Ships Subjected to Wave Action", Proceedings of the Institution of Civil Engineers, Vol. 12, April 1959.
9. Knapp, R. T., "Wave Produced Motion of Moored Ships", Proceedings of the Second Conference on Coastal Engineering, Houston, 1951.

10. O'Brien, J. T. and Kuchenreuther, D. I., "Forces Induced on a Large Vessel by Surge", Journal of the Waterways and Harbors Division, ASCE, Paper 1571, March 1958.

11. O'Brien, J. T. and Muga, B. J., "Sea Tests of a Spread-Moored Landing Craft", U. S. Naval Civil Engineering Laboratory, Technical Report R-268, June 1964.

12. Wiegel, R. L., Dilley, R. A., and Williams, J. B., "Model Study of Mooring Forces of Docked Ships", Journal of Waterways and Harbors Division, ASCE, Vol. 85, WW2, 1959.

13. Korvin-Kroukovsky, B. V., "Theory of Seakeeping", The Society of Naval Architects and Marine Engineers, New York, N. Y., 1961.

14. Wendel, K., "Hydrodynamic Masses and Hydrodynamic Moments of Inertia", The David Taylor Model Basin, Translation 260, July 1956.

15. Koch, J. J., "Eine experimentale Methode zur Bestimmung der reduzierten Masse des Mitschwingenden Wassers bei Schiffschwingsingen", Ingenieur-Archiv, band 4, heft 2, 1933, pp. 103-109.

16. Ransford, G. D., "A Wave Machine of Novel Type", Proceedings of Third Congress of International Association for Hydraulic Research, Grenoble, 1949.

17. Ippen, A. T. and Raichlen, F., "Wave Induced Oscillations in Harbors: The Problem of Coupling of Highly Reflective Basins", MIT Hydrodynamic Laboratory, Report No. 49, May 1962.

18. Goda, Y. and Ippen, A. T., "Theoretical and Experimental Wire Mesh Screens", MIT Hydrodynamics Laboratory Report No. 60, Aug. 1963.

19. Yu, Y. S. and Ursell, F., "Surface Waves Generated by an Oscillating Circular Cylinder on Water of Finite Depth: Theory and Experiment", Journal of Fluid Mechanics, Vol. 11, Part 4, 1961.

20. Browne, A. D., Moullin, E. B. and Perkins, A. J., "The Added Mass of Prisms Floating in Water", Proc. Cambr. Phil. Soc., v. 26, 1929-30, pp. 258-272.

21. Ippen, A. T., Raichlen, F., and Sullivan, R. K., Jr., "Wave Induced Oscillations in Harbors: Effect of Energy Dissipators in Coupled Basin Systems", MIT Hydrodynamics Laboratory Report No. 52, July 1962.

22. Ippen, A. T., and Goda, Y., "Wave Induced Oscillations in Harbors: The Solution for a Rectangular Harbor Connected to the Open Sea", MIT Hydrodynamics Laboratory Report No. 59, July 1963.

23. Chaney, C. A., "Marinas: Recommendations for Design, Construction and Maintenance", National Association of Engine and Boat Manufacturers, Inc., 1961.